

Lipid Regulation of Olfactory Cyclic Nucleotide-Gated Channels

By James D. Brady

A DISSERTATION

Presented to the Neuroscience Graduate Program and the Oregon Health &
Sciences University School of Medicine in partial fulfillment of the requirements
for the degree of Doctor of Philosophy

September 2006

School of Medicine
Oregon Health & Science University

CERTIFICATE OF APPROVAL

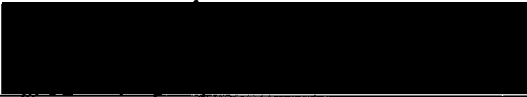
This is certify that the Ph.D. dissertation of

James D. Brady

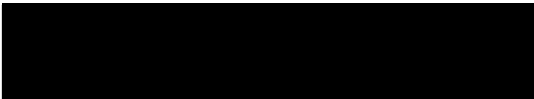
has been approved



H. Peter Larsson, Chair



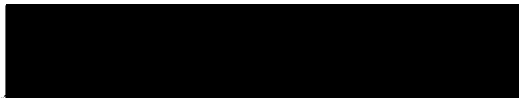
R. Lane Brown, Advisor



Jeffrey W. Karpen, Co-Advisor



Dennis R. Koop, Member



Show-Ling Shyng, Member



William Skach, Member

For my wife, without whom, for many reasons, this dissertation would not exist.

I am also grateful for the lessons learned from numerous colleagues; most notably the trio of advisors involved in my training throughout the work described

herein:

Dr. R. Lane Brown

Dr. Jeffrey W. Karpen

Dr. Jeffrey R. Martens

“The absurd has meaning only in so far as it is not agreed to”

Albert Camus, The Myth of Sisyphus

Table of Contents

CERTIFICATE OF APPROVAL	II
TABLE OF CONTENTS.....	IV
TABLE OF FIGURES.....	VI
ABSTRACT.....	IX
CHAPTER 1: INTRODUCTION.....	1
1.1 CNG CHANNELS	1
1.11 <i>Discovery and Physiological Role</i>	1
1.12 <i>Cloning and Molecular Structure</i>	8
1.12a Structural Features of the S4-S6 Region	9
1.12b Structure of the Cyclic Nucleotide Binding Domain and C-Linker.....	10
1.12c Quaternary Relationships	12
1.13 <i>Basic Functional Properties</i>	16
1.13a Permeant Block by Divalent Cations.....	16
1.13b: Cyclic Nucleotide Sensitivity and Selectivity.....	17
1.14 <i>The Channel Activation Process</i>	20
1.14a Role of the CNBD and the Pore in Channel Activation	21
1.14b Role of the C-Linker in the Activation Process.....	22
1.14c Role of the Amino Terminus in Channel Activation.....	23
1.15 <i>Kinetic Models of Channel Cooperativity</i>	25
1.15a The Hill and Sequential Models.....	26
1.15b Allosteric Models.....	27
1.16 <i>CNG Channel Modulation</i>	30
1.16a Phosphorylation	30
1.16b Calcium/Calmodulin Inhibition.....	31
1.16c Lipid Regulation of CNG Channels	33
1.16d PIP ₃ Regulation of Olfactory CNG Channels.....	36

1.17 <i>Compartmentation</i>	41
1.2 LIPID RAFTS AND ION CHANNELS	42
1.21 <i>Properties of Lipid Rafts</i>	42
1.22 <i>Identifying and Characterizing Biologically Relevant Lipid Rafts</i>	44
1.23 <i>Functional Relationships Between Ion Channels and Lipid Rafts</i>	47
CHAPTER 2: RESULTS	49
CHAPTER 2.1	50
FUNCTIONAL ROLE OF LIPID RAFT MICRODOMAINS IN CYCLIC NUCLEOTIDE-GATED CHANNEL ACTIVATION.....	50
CHAPTER 2.2	76
MBCD DOES NOT INHIBIT OLFACTORY CNG CHANNELS BY DISRUPTING LIPID RAFTS.....	76
CHAPTER 2.3	85
INTERPLAY BETWEEN PIP ₃ AND CALMODULIN REGULATION OF OLFACTORY CNG CHANNELS.	85
CHAPTER 3: SUMMARY AND DISCUSSION	107
3.1 RELATIONSHIP BETWEEN CNG CHANNELS AND LIPID RAFTS.....	108
3.2 MBCD INHIBITION OF CNGA2 CHANNELS.....	112
3.3 LIPID RAFTS AS ORGANIZERS OF cAMP SIGNALING COMPARTMENTS	118
3.4 MECHANISM OF PIP ₃ INHIBITION OF OLFACTORY CNG CHANNELS.....	120
3.5 INTERPLAY BETWEEN PIP ₃ AND CALMODULIN INHIBITION.....	128
3.6 PHYSIOLOGICAL IMPLICATIONS OF PIP ₃ INHIBITION.....	129
CHAPTER 4: CONCLUSIONS	133
CHAPTER 5: MATERIALS AND METHODS	134
APPENDIX: SUPPLEMENTAL FIGURES	144
REFERENCES	148

Table of Figures

FIGURE 1: CNG CHANNEL PHYSIOLOGY	6
FIGURE 2: CNG CHANNEL STRUCTURE	14
FIGURE 3: CNG CHANNEL ACTIVATION CURVES	19
FIGURE 4: CALMODULIN REGULATION OF OLFACTORY CNG CHANNELS	39
FIGURE 5. CNGA2 LOCALIZES TO LIPID RAFTS IN HETEROLOGOUS EXPRESSION SYSTEMS.....	66
FIGURE 6. GLYCOSYLATED CNGA2 LOCALIZES TO LIPID RAFTS IN MEMBRANES FROM RAT OLFACTORY TISSUE.	68
FIGURE 7. CNGA2 DOES NOT DIRECTLY BIND CAVEOLIN AND IS ONLY PARTIALLY COLOCALIZED WITH CAVEOLIN AT THE SURFACE OF HEK-293 CELLS.	70
FIGURE 8. CHOLESTEROL DEPLETION INCREASES THE DENSITY OF CNGA2-CONTAINING LIPID RAFT MEMBRANES.....	72
FIGURE 9. CHOLESTEROL DEPLETION ABOLISHES PGE1-STIMULATED CNGA2 CHANNEL ACTIVITY IN INTACT CELLS.	73
FIGURE 10. CHOLESTEROL DEPLETION REDUCES THE APPARENT CAMP BINDING AFFINITY OF CNGA2 CHANNELS IN ISOLATED PATCHES.....	75
FIGURE 11: CNGA3 RAFT PREPARATION	81
FIGURE 12: CNGA2 vs. CNGA3 ACTIVATION CURVES FOLLOWING MBCD TREATMENT	82
FIGURE 13: EFFECT OF DIFFERENT MBCD TREATMENT CONDITIONS ON CNGA2 CHANNELS	83
FIGURE 14: CHOLESTEROL EXTRACTION DATA	84
FIGURE 15: PIP3 INHIBITS CNGA2 CHANNELS, BUT NOT CNGA3 CHANNELS.....	98
FIGURE 16: EFFECTS OF PIP3 ANALOGS ON CNGA2	100
FIGURE 17: THE N-TERMINUS OF CNGA2 CONFERS PIP3 SENSITIVITY TO CNGA3 CHANNELS.....	101
FIGURE 18: PIP3 INHIBITS OLFACTORY CNG CHANNELS THROUGH A DIRECT INTERACTION WITH THE N- TERMINUS OF CNGA2.....	103
FIGURE 19: PIP3 PREVENTS CALMODULIN REGULATION OF OLFACTORY CNG CHANNELS.	105

FIGURE 20: CALMODULIN VS. PIP3 INHIBITION OF OLFACTORY CNG CHANNELS	126
SUPPLEMENTAL FIGURE 1: CNGA2 DOES NOT DIRECTLY BIND OR COLOCALIZE WITH FLOTILLIN 1 OR 2. ...	144
SUPPLEMENTAL FIGURE 2: CYCLODEXTRIN REDUCES PGE1- AND FORSKOLIN-STIMULATED WHOLE-CELL CAMP PRODUCTION.	146
SUPPLEMENTAL FIGURE 3: PIP2 INHIBITS CNGA2 CHANNELS.	147

Major Abbreviations Used

Ca²⁺/CaM = calcium-calmodulin, CAP = catabolite activator protein, CFP = Cyan Fluorescent Protein, CNBD = cyclic nucleotide-binding domain, CNG = cyclic nucleotide-gated, DAG = diacylglycerol, HCN = hyperpolarization-activated, cyclic nucleotide-regulated, MBCD = methyl- β -cyclodextrin, OSN = olfactory sensory neuron, PGE₁ = prostaglandin E₁, PIP₂ = phosphatidylinositol-4,5-bisphosphate, PIP₃ = phosphatidylinositol-3,4,5-trisphosphate, PKA = protein kinase A, YFP = Yellow Fluorescent Protein

Abstract

Cyclic nucleotide-gated (CNG) channels are non-selective cation channels directly activated by cyclic nucleotide binding. They play a vital role in the signal transduction cascades that detect and respond to light and odorants, therefore molecules that regulate their activity can have a profound impact on the processing of visual and olfactory sensory input. The work described in this dissertation seeks to provide molecular explanations for two newly discovered forms of olfactory CNG channel regulation, by cholesterol and phosphoinositide-3,4,5-trisphosphate (PIP₃).

We discovered a potential functional relationship between membrane cholesterol and olfactory CNG channels during experiments designed to understand the molecular basis for compartmentation of cyclic nucleotide signaling at the membrane. Following exposure of HEK-293 cells to the hormone prostaglandin E₁ (PGE₁), heterologously expressed olfactory CNG channels generate a rapid and dramatic rise in calcium influx as a result of increased cAMP production near the membrane. We found that pretreating cells with the compound methyl- β -cyclodextrin (MBCD) at 37°C, to extract plasma membrane cholesterol, impaired PGE₁-stimulated calcium influx. Patch clamp analysis revealed that part of this effect could be explained by an average 3-fold decrease in the cyclic nucleotide sensitivity of olfactory CNG channels following MBCD treatment. Sucrose gradient fractionation of detergent-solubilized cells suggested that the channels resided in cholesterol-rich, highly ordered membrane microdomains, called lipid rafts. Together, these results implied that an association between olfactory CNG channels and cholesterol-rich membrane microdomains was important for maintaining high cyclic nucleotide sensitivity. However, further experimental analysis demonstrated that the

change in CNG channel sensitivity following MBCD treatment did not correlate with the amount of cholesterol removed, or the ability of channels to associate with lipid rafts. Therefore, it appears that MBCD alters CNG channel function through non-specific extraction of membrane lipids other than cholesterol, or by changing the concentrations of regulatory molecules.

The membrane lipid, PIP₃, has previously been shown to inhibit native olfactory CNG channels and the response of olfactory sensory neurons (OSNs) to complex odorants. We attempted to define the molecular determinants of PIP₃ inhibition, in part to assess the role of PIP₃ regulation in the MBCD-induced decrease in channel function. Heterotetrameric olfactory CNG channels, containing CNGA2, A4, and B1b subunits, as well as homomeric channels containing only CNGA2 subunits, are dramatically inhibited by PIP₃. In contrast, we found that homomeric channels containing CNGA3 subunits, from cone photoreceptor CNG channels, were insensitive to PIP₃. Patch clamp analysis of channels containing CNGA2/A3 chimeric subunits and CNGA2 subunits with small deletions demonstrated that a 30 amino acid stretch of the N-terminus of CNGA2 was required for PIP₃ inhibition of both homomeric and heteromeric olfactory channels. Ca²⁺/CaM binding to this same region of CNGA2 can also inhibit homomeric channel activity. For heteromeric channels, however, Ca²⁺/CaM causes inhibition by binding to CNGA4 and CNGB1b subunits. We found that PIP₃ could occlude Ca²⁺/CaM inhibition of both homomeric and heteromeric olfactory CNG channels by interacting with different sites in each subunit, even in mutant channels that were not inhibited by PIP₃. Our results provide evidence that PIP₃ disrupts intersubunit interactions in homomeric channels, and

may block intersubunit interactions from forming during Ca^{2+} /CaM binding to heteromeric channels.

Chapter 1: Introduction

1.1 CNG Channels

1.11 Discovery and Physiological Role

The existence of ion channels activated by the direct binding of cytoplasmic cGMP and cAMP, called cyclic nucleotide-gated (CNG) channels, was originally revealed during attempts to understand how photoreceptor cells of the retina transduce light into physiologically useful electrical signals. Concurrently, researchers studying olfaction realized that odorants could depolarize the membrane potential of olfactory sensory neurons through changes in cAMP, and they eventually learned that the channels mediating this effect were closely related to those discovered in photoreceptors. The ideas and experiments leading to the discovery of CNG channels form a rather classic tale of neuroscience history, involving talented investigators employing innovative electrophysiological techniques in their search for the molecular basis of sensation. This history is well documented in a number of reviews¹⁻⁶, but a very short account is presented below to provide a general framework for understanding the physiological significance of the experiments described in later chapters.

By 1970, it was well recognized that light striking the pigment-rich outer segments of vertebrate rod and cone photoreceptors hyperpolarizes the plasma membrane and reduces the release of neurotransmitter onto secondary neurons. Strangely, the light-evoked hyperpolarization was accompanied by an increase in membrane resistance, which hinted at the existence of ion channels that remain open in the dark, and close in response to light. Hagins and colleagues⁷ analyzed current sources and sinks along the

length of rat photoreceptors to help establish that the light-induced rise in membrane resistance was due to the reduction of a steady, inward, sodium rich 'dark current'. Based on the non-linear relationship between light intensity and the change in outer segment membrane conductance, Baylor and Fuortes⁸ proposed the existence of an amplification mechanism involving a diffusible signal that could close the channels responsible for generating the dark current. While calcium was favored by many as a candidate for the proposed diffusible messenger¹, biochemical experiments and data from intracellular recordings suggested that a decrease in cGMP concentration might be responsible for the photoresponse⁹⁻¹⁸. This idea received strong support with the development of the patch clamp technique and its application to the study of photoreceptor physiology, when Fesenko and colleagues successfully recorded cGMP-activated currents from inside-out membrane patches of amphibian rod outer segments¹⁹. Others later demonstrated that the cGMP-activated conductance and the photosensitive conductance were identical²⁰⁻²². More recently, the requirement for CNG channels in this process is supported by loss of function channel mutations in patients with certain inherited forms of blindness²³⁻²⁶.

These reports and others helped establish that the ongoing dark current in the outer segments of both rods and cones results from the steady synthesis of cGMP by guanylyl cyclase, which persistently activates sodium and calcium entry through a small percentage of CNG channels. Light striking the outer segments activates visual pigment proteins by converting covalently attached 11-*cis*-retinal moieties into all-*trans* isomers. When the trimeric G-protein, called transducin, interacts with an activated pigment protein, it exchanges bound GDP for GTP, and stimulates phosphodiesterase activity^{17,18}. The dramatic reduction in cGMP concentration that follows leads to CNG channel

closure and decreased glutamate release onto second order neurons. The light response can be rapidly terminated through phosphorylation of activated visual pigments by opsin kinase, and subsequent interaction with the protein arrestin. The hydrolysis of GTP to GDP by transducin and the spontaneous release of all-*trans* retinal from visual pigments also lead to slower restoration of the dark current. During adaptation to constant light stimulation, dark current is also partially restored when decreased calcium influx releases the calcium-dependent inhibition of guanylate cyclase and activation of phosphodiesterase, leading to slightly elevated cGMP levels (see Figure 1A)²⁷.

Concurrent with the later work on photoreceptors, researchers studying chemosensory neurons of the olfactory epithelium were learning that odorants trigger cAMP synthesis²⁸⁻³⁰, followed by membrane depolarization and a decrease in input resistance^{31,32}. These processes were thought to occur in the long, thin dendritic cilia extending from the soma of the sensory neurons. But investigators could not accurately determine exactly how cAMP caused membrane depolarization, and the small size of the cilia made it technically difficult to electrophysiologically isolate the channels responsible for the change in membrane potential. The idea that odorants activated ciliary channels through a phosphorylation mechanism involving a cAMP-sensitive protein kinase was considered⁵, but had no direct support. Finally, in 1987, Nakamura and Gold accomplished the difficult task of recording cAMP-activated currents in patches of ciliary membrane with solutions lacking ATP and GTP, eliminating the possibility of channel phosphorylation³³.

Further voltage-clamp experiments comparing the properties of odorant-evoked channel currents to those recorded in isolated patches³⁴⁻³⁹ helped establish that

chemosensation occurs through what is now considered a typical stimulatory G-protein reaction scheme. Airborne odorants bind to specific G-protein coupled receptors in the ciliary membrane and promote the exchange of GDP for GTP on the trimeric G-protein, G_{olf} . This leads to allosteric stimulation of type III adenylyl cyclase and activation of CNG channels through direct interaction with newly synthesized cAMP. The calcium that enters through open CNG channels then activates chloride channels, which allow chloride ions to exit the cilia, thereby depolarizing the membrane and increasing transmitter release onto second order neurons⁴⁰. As in photoreceptors, elevated intraciliary calcium levels also play a role in adaptation of the odorant response, in this case by stimulating calmodulin-mediated inhibition of CNG channels and adenylyl cyclases⁴¹. The absolutely essential role played by CNG channels in this process is best demonstrated by reports on mice lacking specific channel subunits (see Figure 1B)^{42,43}.

Since their discovery in photoreceptor outer segments and OSN cilia, CNG channel mRNA and proteins have been detected in a variety of neuronal and non-neuronal tissues, such as cortex, lung, kidney, and testis⁴⁴. However, many of these reports have not been confirmed, and the physiological role of CNG channels in these tissues remains unclear for several reasons. One major hindrance is the lack of specific pharmacological agents that block or alter native CNG channel function⁴⁵. Whole-cell patch clamp studies are also difficult since intracellularly applied or membrane-permeant cyclic nucleotides can induce a number of responses unrelated to channel activity. Also, while experiments with outer segments and olfactory cilia benefit from the advantage of channel abundance, CNG channels in other cells are likely not as densely expressed, and

may in addition be specifically localized to discrete subcellular regions that may not be amenable to direct study.

Despite these issues, a few potentially novel roles for CNG channels are worth mentioning. Accumulating evidence from a number of labs suggests possible functional roles for CNG channels in hippocampal pyramidal cells. For example, CNG channel subunit mRNAs and proteins have been detected in hippocampal neurons, and mice lacking CNGA2 subunits exhibit disrupted hippocampal long term potentiation with theta burst induction protocols⁴⁶. Also, prolonged depolarization of hippocampal neurons following coincident spiking and muscarinic activation, called plateau potentials, rely on a cGMP-sensitive conductance that can be blocked by two non-specific CNG channel blockers⁴⁷. These plateau potentials may play a role in seizure spread. Finally, CNG channels have been implicated in stimulating neurotransmitter release in cones in response to retrograde nitric oxide signaling⁴⁸.

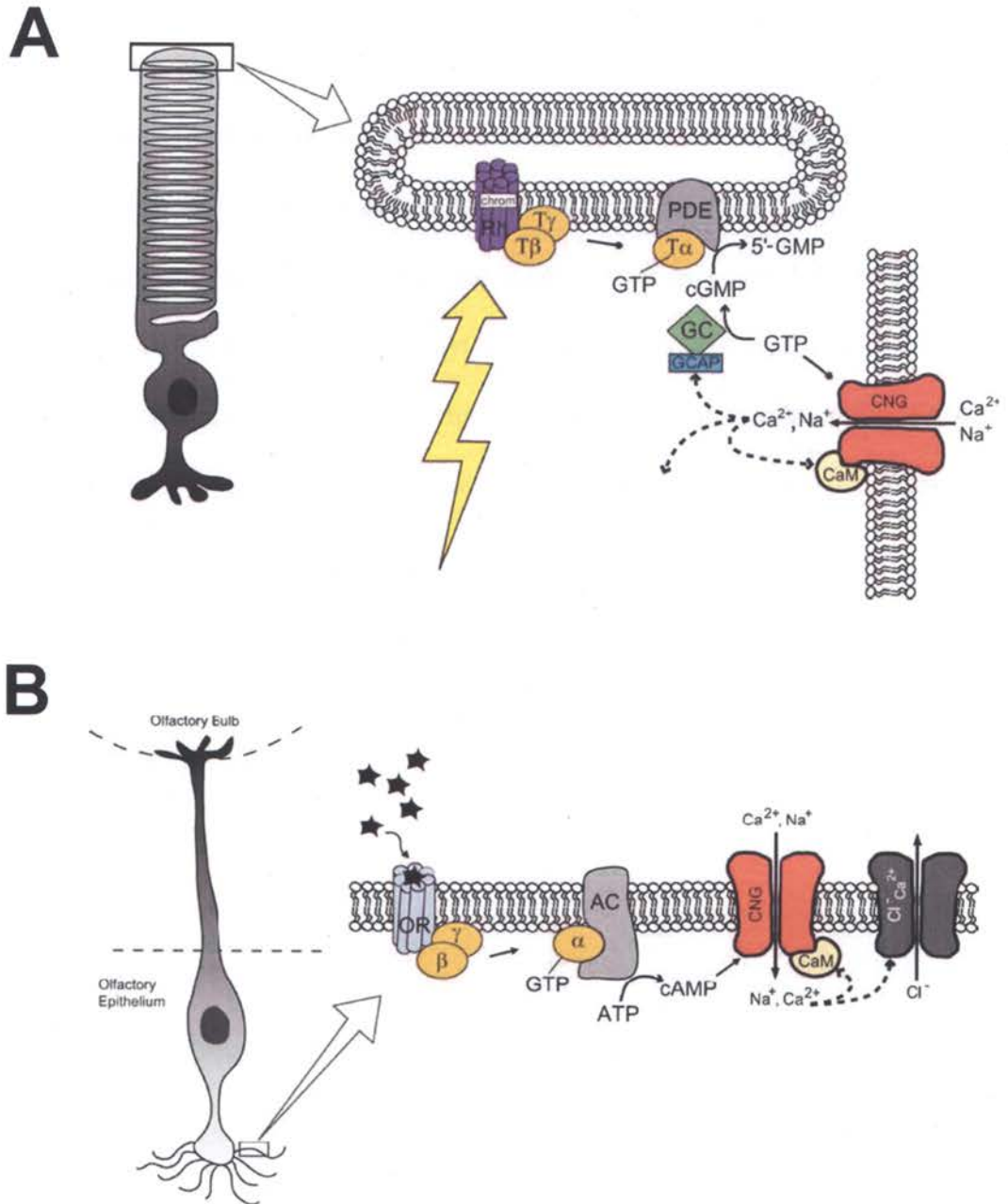


Figure 1: CNG Channel Physiology (A) Phototransduction cascade in rod photoreceptor. Rod photoreceptor (*left*) with phototransduction cascade on rod disc membrane and rod outer segment (*right*). A photon activates rhodopsin (Rh), which in turn activates the heterotrimeric G protein transducin (T), whose α subunit activates a phosphodiesterase (PDE). A CNG channel is shown in the outer segment membrane, and

the downstream effects of Ca^{2+} influx [calmodulin (CaM) binding, activation of guanylyl cyclase (GC) by guanylyl cyclase-activating protein (GCAP), and other effects] are shown with dotted arrows. **(B)** Olfactory transduction cascade in olfactory epithelium. Olfactory receptor cell (*left*) with olfactory transduction cascade in cilia (*right*). Odorants bind to and activate the olfactory receptor (OR), which activates a heterotrimeric G-protein, whose α subunit activates adenylyl cyclase (AC). AC produces cAMP, which activates CNG channels. Downstream effects of Ca^{2+} [binding of calmodulin (CaM) and activating of a Ca^{2+} -sensitive Cl^- channel] are shown by dotted arrows. Figures and legends from reference 90.

1.12 Cloning and Molecular Structure

The high density of CNG channels expressed in rod outer segments facilitated their purification from bovine retina⁴⁹. Based on a partial amino acid sequence of one of the purified proteins, a cDNA clone was then isolated⁵⁰. Using probes based on this initial clone, 6 different mammalian CNG channel genes were gradually discovered⁵¹⁻⁵⁸. Sequence comparisons place the genes into two different subfamilies, referred to as A and B.

Each gene has been expressed in both *X. laevis* oocytes and cultured mammalian cells, and the resulting channels have been studied intensively. Functional comparisons between native and heterologously expressed channels support the idea that each native channel is a heteromeric assembly of at least 2 different subunits, and subunit stoichiometries have been investigated using a variety of approaches (Figure 2B). The CNG channels of rod outer segments are complexes of three A1 subunits with one B1 subunit⁵⁹⁻⁶¹, while cone photoreceptor channels contain two A3 subunits and two B3 subunits⁶². Channels of olfactory cilia contain two copies of CNGA2, one copy of CNGA4, and one copy of CNGB1b, which is an alternatively spliced variant of B1⁶³⁻⁶⁵. Human orthologues have been identified⁶⁶⁻⁶⁸, and the genomes of *D. melanogaster* and *C. elegans* also contain CNG channel genes homologous to those found in mammals⁴⁴.

Primary sequence analysis places CNG channels within the superfamily of voltage-gated cation channels, which includes K⁺, Na⁺, and Ca²⁺ channels. The current model for the transmembrane topology of CNG channel subunits resembles that proposed for the cation channel superfamily⁶⁹. The CNG channel model is based largely on amino acid hydrophobicity profiles, but has also received support from antibody labeling and a

gene fusion approach using an enzyme reporter expressed at different locations within the A1 subunit⁷⁰⁻⁷². According to this model, each subunit consists of 6 transmembrane segments (S1-S6) surrounding a central pore and flanked by cytoplasmic C- and N-termini. The greatest diversity between subunits exists within the amino terminals, for which little structural information is available, as well as within the small loops connecting transmembrane segments (refer to Figure 2A for general topological features).

1.12a Structural Features of the S4-S6 Region

The S4 segments are modeled as helices with 3 or 4 positively charged residues along one face, an unusually large number of charges for a helix spanning the hydrophobic bilayer. This is reminiscent of the S4 regions of voltage-gated cation channels, which contain even more positive charges and act as major component of the voltage-sensing mechanism⁷³. The open probability of rod channels, and to a lesser extent olfactory channels, is mildly voltage dependent, leading to mild outward rectification. While the S4 region has not been directly implicated in this voltage dependence, the S4 from the CNGA2 subunit can support voltage-dependent activation in the context of an ether-a-go-go channel⁷⁴. Therefore, while CNG channels cannot be directly activated by voltage changes alone, the S4 segment may impart some voltage-dependence by altering the conformation of the pore.

The S5 and S6 segments, which are linked by an extracellular loop that partially enters the plane of the membrane, comprise the highly conserved pore domain. The crystal structure of a bacterial potassium channel, KcsA, which consists solely of a pore domain with sequence similarity to the pore of voltage-gated cation channels⁷⁵, provided

a template for predicting the pore structure in CNG channels, and now several lines of evidence support this comparison⁷⁶. These data imply that the small S5-S6 linker loop, called the P loop, leaves the top of S5 and enters the membrane plane as a small alpha helix, then it curls back out of the plane of the membrane as a coiled strand, eventually connecting to the top of S6. The P loop has received much attention since its residues are critical members of the 'selectivity filter' that determines which ions pass through the pore of cation channels⁷⁷. Mutagenesis studies support the role of the P loop in controlling CNG channel ion selectivity as well⁷⁸⁻⁸². Recently, Qu *et al* demonstrated that reversing the charge of a single P loop glutamate residue produces anion-selective CNGA2 channels⁸³. Accessibility studies also show that many P-loop residues move during channel gating, and some evidence suggests that this region may actually serve as the primary gate for CNG channels^{76,84-86}.

1.12b Structure of the Cyclic Nucleotide Binding Domain and C-Linker

One of the most defining, but certainly not unique, structural and functional domains of CNG channels is the cyclic nucleotide binding domain (CNBD) within the C-terminal region of every subunit. Intense investigation of this domain has provided a significant amount of structural information, as well as great insight into the conformational changes that may occur following cyclic nucleotide binding. Each of these domains is approximately 80-100 residues in length, and the sequences strongly resemble those of functionally related domains in other cyclic nucleotide binding proteins, such as protein kinase A (PKA), protein kinase G, the bacterial catabolite

activator protein (CAP), and the CNBD of the HCN2 channel (see Figure 2C). The crystal structures for three of these CNBDs – those from PKA, CAP, and HCN2 - have been solved with bound cyclic nucleotides, and the structural homology between the three proteins from different species is remarkable⁸⁷⁻⁹⁰. Based on these results, CNG channel CNBDs are thought to be formed by a flattened beta-roll structure connected to alpha helices at both ends (Figure 2C). This model has proven extremely reliable for predicting residues critical for ligand binding and selectivity (see section 1.13b).

In the crystal structure for the CNBD of HCN2, the sequence linking the CNBD to the pore, called the C-linker, was also resolved as a series of 6 alpha helices of varying length connected by short loops⁸⁹. For both HCN and CNG channels, the C-linker plays a critical role in transferring the energy of cyclic nucleotide binding into conformational changes that favor opening of the pore (see section 1.14b). Mutagenesis studies with CNGA1 suggest that the C-linkers of CNG channels share structural homology with the x-ray structure of HCN2⁹¹. Based on the HCN2 crystal structure, as well as electron microscopy and mutagenesis data^{92,93}, it appears that the CNBDs and C-linker regions of each of the four CNG channel subunits in a tetramer interact to form a quaternary ‘hanging donut’ feature. According to this model, a tunnel formed at the intersubunit interface between CNBDs runs perpendicular to the face of the membrane and operates as a ‘gating ring’; ions may flow through a gap between the hanging CNBDs and the membrane surface.

1.12c Quaternary Relationships

Significant details about the quaternary structure of CNG channels have recently emerged. The idea that functional CNG channels are oligomeric assemblies was originally inferred from the cooperativity of homomeric channels; single subunits contain only one CNBD sequence, but dose-response relations suggested cooperative activation by at least 2-3 ligands. Work with the related voltage-gated potassium channels pointed to a tetrameric arrangement⁹⁴, but data specific to CNG channels was first provided by Steven Siegelbaum and colleagues in 1996⁹⁵. Their work relied on coexpressing individual or linked dimer constructs of wild type A1 subunits with mutant subunits containing the CNGA2 P-loop, which altered the single-channel conductance. The results of this study not only strongly supported a tetrameric arrangement for CNG subunits, but showed that the precise location of individual subunits in relation to each other could influence pore properties. Subsequent work has established that when two or more different subunits are coexpressed, they preferentially assemble into heterotetramers with characteristic stoichiometries⁵⁹⁻⁶³.

Specific residues responsible for tetramerization have not yet been defined. The structural data discussed above, in addition to cysteine cross-linking and nickel interaction studies, suggest that the C-linkers and CNBDs of adjacent subunits are in very close proximity⁹⁶⁻⁹⁸. Other work shows that the amino- and carboxy-terminal domains can interact with each other⁹⁹⁻¹⁰¹. However, mutating amino acids in either the amino terminus or the C-linker, or removing the distal half of the amino terminus of CNGA1 and CNGA2, disrupts activation without eliminating channel conductance. Thus tetramerization is likely governed by residues elsewhere in the subunits. It is worth noting

that a mutant CNGA2 subunit lacking approximately 30 amino acids in the amino terminus just before S1 does not form functional channels¹⁰². The location of these residues and the functional results following removal are somewhat reminiscent of the T1 domain identified as important for tetramerization of voltage-gated potassium channels¹⁰³.

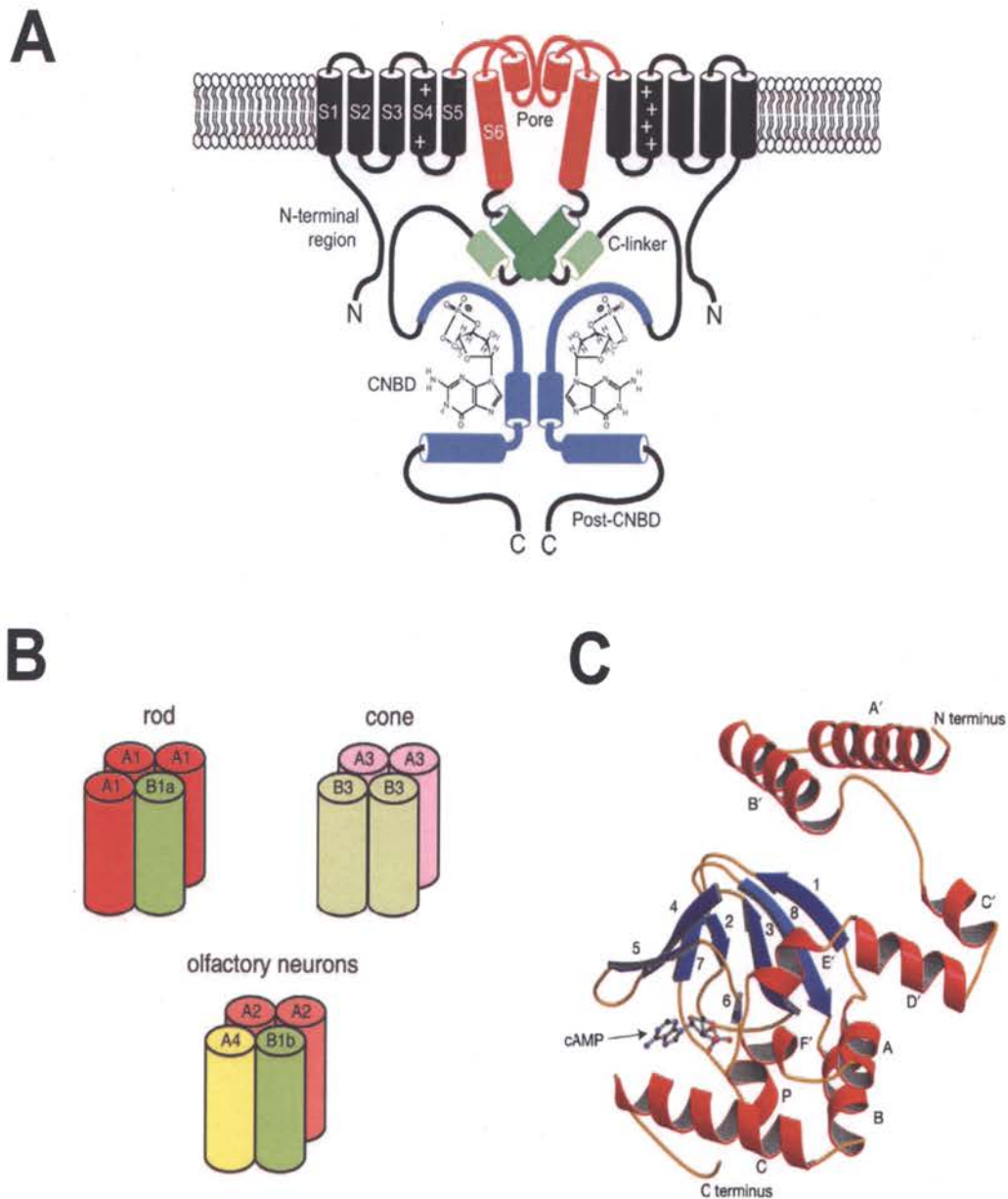


Figure 2: CNG Channel Structure (A) Predicted topology of a pair of CNGA2 channel subunits. See text for detailed description. Modified from reference 90. (B) Reported stoichiometry for the three known types of native CNG channels. For olfactory channels, the exact spatial arrangement of the subunits is not known. Modified from reference 44. (C) Ribbon diagram of the HCN2 C-terminus crystal structure. The N-terminus in the diagram connects to the cytoplasmic end of S6. cAMP is shown in its binding pocket.

Numbers refer to β -sheets while letters refer to α -helices. Helices A' through F' make up the C-linker. Modified from reference 89.

1.13 Basic Functional Properties

Only the A1-A3 subunits form functional homomeric channels when heterologously expressed, but these channels do not recapitulate all properties of native channels. Now it is clear that channels in photoreceptors and OSNs are heterotetrameric complexes of 2 or 3 different subunits, and the subunit composition and arrangement have a pronounced effect on various channel properties. All homomeric and heteromeric channels are non-selective cation channels with qualitatively similar selectivities for monovalent cations⁴⁴. However other properties, especially calcium permeability and ligand sensitivity, differ significantly across channel subtypes, and the molecular elements underlying these differences have received intense study over the past two decades.

1.13a Permeant Block by Divalent Cations

All CNG channels exhibit a voltage-dependent block of monovalent current by extracellular divalent cations¹⁰⁴⁻¹⁰⁹. The voltage-dependence of divalent block is somewhat complex, with permeation occurring at positive and strongly negative membrane potentials. This behavior was taken as evidence that divalent cations act as permeant blockers by moving through the channel pore in single file with long transit times, due to high affinity interactions with pore residues. Work with mutant alpha subunits led to the identification of a single glutamate residue in the P loop as the sole binding site for extracellular divalent cations^{79,80,110}. While this residue is critical for divalent block, residues within S5 and S6 and the extracellular loops connecting these segments to the pore loop can influence blocking characteristics^{78,109,111}. Beta subunits

carry a glycine rather than a glutamate, and thus contribute to decreased divalent block when present in heteromeric channels. The decreased affinity of heteromeric channels results in flickery single channel behavior in the presence of divalents, reflecting the fact that divalent ions rapidly enter and leave the extracellular region of the pore^{104,105}. The voltage-dependent calcium permeability of native CNG channels plays an extremely important physiological role. For example, partial calcium block of native rod CNG channels contributes to reduced noise and increased sensitivity during rapid illumination changes. Calcium also influences the activity of multiple enzymes in the photosensitive transduction cascade. In OSNs, small amounts of calcium entering through ciliary CNG channels trigger large changes in membrane potential by opening calcium-activated chloride channels⁴⁰. Also, as discussed further in the next section, calcium can act through calmodulin to shift the cyclic nucleotide sensitivity of CNG channels and inhibit adenylyl cyclases, two processes involved in sensory adaptation.

1.13b: Cyclic Nucleotide Sensitivity and Selectivity

Perhaps the most salient distinguishing feature across CNG channel subtypes is their relative sensitivities to cGMP and cAMP. Two features are typically used to characterize cyclic nucleotide sensitivity, maximum current and the $K_{1/2}$, which is the concentration required for activation of half the maximal current produced by the same agonist. For heteromeric olfactory channels, the $K_{1/2}$ for cGMP is only slightly less than that for cAMP, and saturating amounts of both agonists generate the same maximum current. Rod and cone channels, however, exhibit only partial activation by cAMP, less than half the current activated by cGMP, and the $K_{1/2}$ for cAMP is orders of magnitude

greater than for cGMP. Thus cAMP is considered a partial agonist for these channels (see Figure 3). The cyclic nucleotide selectivity of A1-A3 homomeric channels is qualitatively similar to that seen in native or heterologously expressed heteromeric channels. In general, the inclusion of beta subunits confers greater overall sensitivity. Homomeric CNGA2 channels, for example, have a $K_{1/2}$ for cAMP that is about 30 times greater than that for cGMP. Heteromeric CNGA2/A4/B1b channels, though, exhibit only a 2-fold difference in $K_{1/2}$ values for cAMP and cGMP.

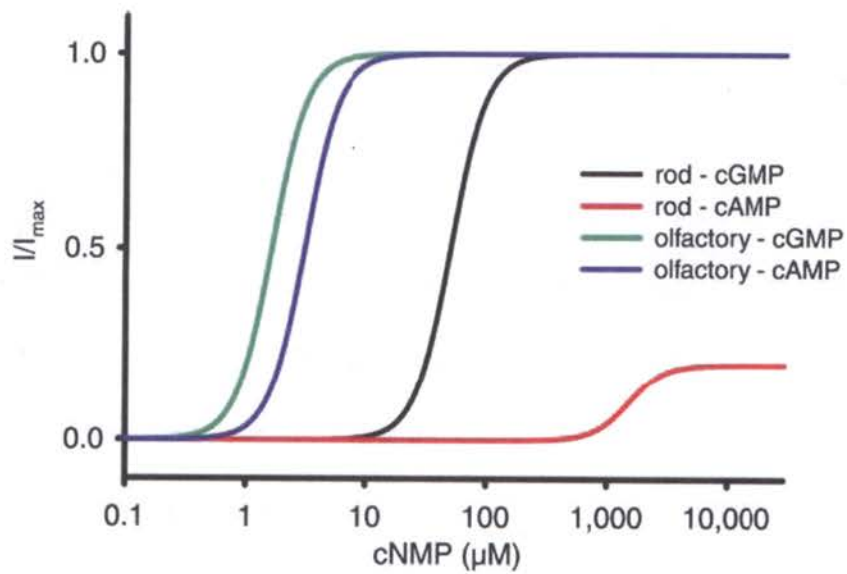


Figure 3: CNG Channel Activation Curves Simulated cyclic nucleotide activation curves for native rod and olfactory CNG channels. While cGMP and cAMP are both strong activators of olfactory channels, cAMP serves as only a partial agonist for rod channels. Figure modified from reference 44.

1.14 The Channel Activation Process

Two conceptually distinct events underlie channel activation by cyclic nucleotides: binding and the subsequent conformational changes that lead to opening of the pore, referred to as the gating process. Thus cyclic nucleotide sensitivity is determined both by the affinity of the ligand for its binding site and the ability of the ligand-binding event to alter the conformation of the gate. In practice, these two events are difficult to independently measure, and the cyclic nucleotide binding affinity has not been directly determined for any CNG channel. For this reason, the term apparent affinity is used to describe the response of channels to cyclic nucleotides. However, state models of CNG channel kinetic behavior have facilitated mathematical estimations of the relative contributions that binding affinity and gating make to sensitivity¹¹². With such models (discussed in more detail in section 1.15), most researchers have concluded that cGMP is a much stronger channel activator than cAMP by virtue of its gating efficacy alone, and that the two ligands exhibit similar binding affinities. Also, different sensitivities across channel subtypes are thought to result almost entirely from changes in gating efficacy. Gordon and Zagotta have suggested that the cGMP/cAMP gating efficacy ratio is roughly the same across channel subtypes, and only the strength of the common gating mechanism changes¹¹³. According to this idea, cGMP and cAMP are both effective agonists for olfactory channels because the resistance toward common conformational changes following binding is low. Yet in photoreceptor channels the resistance to opening is much higher, so although the relative cGMP/cAMP gating efficacy is identical to that in olfactory channels, the absolute efficacy is shifted such that cAMP acts as a partial agonist.

The molecular mechanisms underlying cyclic nucleotide sensitivity and selectivity have received much attention. With the aid of simple mutagenesis studies, cysteine crosslinking and modification, and the construction of chimeric channels, numerous regions of the channel are now known to affect either the binding of cyclic nucleotides or the gating mechanism. Four different subunit regions are especially important: the cyclic nucleotide binding domain (CNBD), the linker between the CNBD and S6 (C-linker), the P-loop, and the amino terminus.

1.14a Role of the CNBD and the Pore in Channel Activation

The high degree of sequence similarity between the CNBDs of CNG channels and those of other proteins (CAP, PKA, HCN2) has greatly facilitated studies on the control of ligand sensitivity and discrimination by this region, especially since crystal structures with bound nucleotides have been generated. Based on this information, at least two residues have been identified within the β -roll region of the CNBD that, when mutated, dramatically reduce cGMP sensitivity either without affecting cAMP sensitivity or increasing it¹¹⁴⁻¹¹⁶. One of these residues, D604 of the rod channel and E583 of the olfactory channel, appears to make an unfavorable interaction with cAMP that inhibits conformational changes following binding¹¹⁵. The state dependence of cysteine accessibility for residues in the β -roll suggests that a large portion of this domain undergoes structural rearrangements after ligand binding that may be necessary for initiating pore opening¹¹⁷.

Not surprisingly, and as predicted by the principle of detailed balances as applied to closed loop reaction schemes, pore opening leads to enhanced agonist affinity at the

CNBD¹¹⁸. Other mutagenesis studies strongly suggest that the pore environment influences gating efficacy^{79,110,119}. Again, these findings are perhaps not too surprising since opening of the pore is the final step in the gating process, and any change in the resistance to opening will alter cyclic nucleotide dose-response relations.

1.14b Role of the C-Linker in the Activation Process

The transfer of ligand binding energy into pore opening appears to involve rearrangements of the C-linker connecting the CNBD to S6. The first indication of this behavior came from attempts to understand how divalent transition metal ions, especially nickel, alter cyclic nucleotide sensitivity. Nickel applied to the cytoplasmic surface of homomeric A1 channels potentiates activation by both cGMP and cAMP, while CNGA2 channels are inhibited^{85,113,120}. Sequence comparisons led to targeted mutagenesis experiments, and single histidine residues in the C-linkers were identified as necessary for nickel regulation^{113,120}. Subsequent studies with chimeric channels led to the discovery of an additional 3 residues in the C-linker that controlled cyclic nucleotide sensitivity^{121,122}. Substituting histidines along the C-linker and analyzing nickel regulation suggested that a large portion rotates during activation⁹⁷. Covalent modification of a naturally occurring cysteine residue in the C-linker of A1 dramatically alters cyclic nucleotide sensitivity and displays a state-dependent difference in the rate of covalent modification, further supporting movement during activation¹²³. The HCN2 C-terminal crystal structure showed intrasubunit salt bridges between the C-linker and the CNBD, as well as intersubunit salt bridges between adjacent C-linkers. Mutagenesis

studies now show that these salt bridges stabilize the closed state of the channel, and disrupting them greatly facilitates channel opening⁹¹.

1.14c Role of the Amino Terminus in Channel Activation

Quite unexpectedly, the N-terminus of CNG channel subunits also dramatically affects channel gating through interactions with regions of the C-terminus. In fact, for CNGA2 channels, interactions involving the N-terminals appear to contribute significantly to increased cyclic nucleotide sensitivity relative to A1 and A3 channels. Studies with chimeras show that when the N-terminus of A1 is replaced with that from CNGA2, the cAMP efficacy vastly increases. Including the S1 domain through the S2-S3 linker from CNGA2 converts cAMP from a partial agonist to nearly a full agonist¹¹⁸. Similar results are observed with CNGA2/A3 chimeras¹²⁴. Also, deletion of a 30 amino acid region from the amino terminus of CNGA2 increases both the cGMP and cAMP $K_{1/2}$ values, and converts cAMP into a partial agonist¹⁰⁰. Through gel overlay and fluorescence resonance energy transfer (FRET) experiments, it now appears that the N-terminus of CNGA2 enhances gating transitions through an interaction with the β -roll of the CNBD^{100,101}. This interaction is referred to as autoexcitatory, since it lowers the free energy required for the gating process¹²⁵. In the HCN2 C-terminal crystal structure, some of the regions of the CNBD reportedly involved in the N-terminal interaction are slightly buried by the adjacent subunit. Thus, the N-terminus may distort the shape of the CNBD to enhance cyclic nucleotide sensitivity. Though a similar interaction reportedly exists in rod channels, it does not seem to play a significant role in gating⁹⁹. An intersubunit interaction between the N-terminus of CNGB1 and the C-terminus of CNGA1 has also

been identified, but this interaction facilitates trafficking rather than gating¹²⁶. No studies have directly examined interactions involving the N-terminus of cone channels.

1.15 Kinetic Models of Channel Cooperativity

Most of the experiments described thus far have employed steady-state analysis of wild-type and mutant CNG channel behavior. While such studies have helped define multiple subunit regions that play a role in channel activation, steady-state analysis alone provides only limited information about the sequence of molecular events leading from cyclic nucleotide binding to pore opening. Furthermore, the results of steady-state experiments performed at saturating ligand concentrations may have little physiological relevance, since ligand concentrations in native cells responding to natural stimuli are generally much more dynamic and well below the concentrations required to saturate CNG channel activity.

Another important aspect of the CNG channel gating process that is difficult to study under steady-state conditions with saturating ligand concentrations is cooperativity. With the first recordings from patches containing different CNG channel types^{19,33}, researchers recognized that the sigmoidal shape of dose response relationships indicated that multiple ligands bind in a cooperative fashion to promote channel activation. Thus, the binding of ligand at one CNBD can facilitate binding at other subunits, resulting in a steep cyclic nucleotide dependence. Although CNG channels function as tetramers, the slope of dose response relationships suggests that at least 2 or 3 ligands must bind for significant activation.

To better understand the CNG channel gating mechanism and its inherent cooperative nature, researchers have directly studied the kinetics of channel behavior using a variety of approaches, including recording from single channels, covalently

tethering ligands to channels, and rapidly presenting ligands by photoactivation. Kinetic analysis has led to the development of models that attempt to describe the steps leading to activation by defining the relationships between short- and long-lifetime channel states. Early models based primarily on steady-state data, such as the Hill and sequential models described below, inadequately explain CNG channel behavior. Through kinetic analysis, more accurate models have been generated, which may provide a core set of relationships upon which further research can build.

1.15a The Hill and Sequential Models

The simplest model first employed to describe CNG channel data is the Hill model^{104,105}. This is essentially a sequential cooperative model involving only two states, open and closed, and the binding of all ligands is assumed to occur all at once. While somewhat unrealistic, this model does roughly fit macroscopic dose-response data, and provides a lower limit for the number of ligands involved in channel activation. Today, the most commonly used method for quantitatively comparing the cyclic nucleotide dependence of different channels or the effects of modulation relies on the equation derived from this model, called the Hill equation: $I/I_{\max} = [\text{ligand}]^n / ((K_{1/2})^n + [\text{ligand}]^n)$, where I/I_{\max} represents the relative activation at a given cyclic nucleotide concentration, and n is the function of the slope, referred to as the cooperativity constant. Values of 1.5 to 3 are typically seen for different CNG channels, where a value of 1 represents the absence of cooperativity. Ruiz *et al* found that the Hill coefficient of macroscopic currents is generally lower than that of single channels due to variation in single channel $K_{1/2}$ values, perhaps as a result of varying degrees of channel modulation¹²⁷.

More detailed sequential models have been tried that maintain a single closed to open transition, but propose that the channel can exist in multiple closed states depending on the number of ligands bound. Such models are similar to those employed by Hodgkin and Huxley to describe the voltage dependence of the action potential. Models requiring as many as 3 binding steps before opening, or as few as 2, and even one, have been developed^{120,128,129}. These models have been applied to homomeric A1 channels to determine the basis for the vast difference in cAMP and cGMP sensitivity. One group proposed that the difference could primarily be accounted for by approximately a 1000-fold difference in the equilibrium constant of the final closed to open transition, since changes in binding affinity alone could not account for the partial agonist effect of cAMP¹¹³. Li and Lester, however, propose a 30-fold difference in the dissociation constants for the two nucleotides, with only a 3-fold difference in the closed to open transition¹²⁹. The disagreement may represent the fact that one group relied on macroscopic data¹¹³, while the other used single channel data¹²⁹. But it also illustrates the inadequacy of sequential models for describing all aspects of CNG channel behavior. Sequential models do not allow spontaneous channel opening in the absence of ligand or the presence of multiple open states with different conductances, though both of these phenomena have been observed for CNG channels^{104,105,119,125,128,130-134}.

1.15b Allosteric Models

To account for spontaneous channel opening and subconductance states, cyclic allosteric models based on the Monod, Wyman, and Changeux (MWC) model have been developed^{125,135,136}. In these models, channel openings can occur with any number of

bound ligands, though some states are rarely observed. When one subunit transitions into an open conformation, all other subunits follow suit. This concerted transition means that for each bound ligand, there is still only one closed state, and one open state. Ligands can also bind to either closed or open channel conformations. A modified version of the cyclic allosteric model, called the coupled dimer model, proposes that two adjacent subunits act essentially as a single allosteric unit with 2 binding sites, and only the conversion of a single dimer into the open configuration is required for channel opening¹³⁷. In general, MWC-type allosteric models provide more accurate descriptions of CNG channel behavior.

A greatly expanded general allosteric model was proposed by Ruiz and Karpen to explain their data involving A1 channels locked in different ligand-bound states¹³¹. Using an analogue of cGMP that, upon photoactivation, covalently tethers to channel binding sites, they observed numerous distinct subconductance states in single channel recordings. The ability to covalently lock a specific number of ligands to the channel largely avoids the need to consider changes in binding affinity when modeling kinetic behavior. Their model, which they call a connected state model, allows for a much wider range of structural flexibility. Unlike an MWC-type model, the connected state model allows each subunit to independently assume one of 2 or more possible conformations, either spontaneously or upon ligand binding. Ligand binding of course favors one conformation over others. Further, the conformation of one subunit affects the probability that nearby subunits undergo a state transition. According to this model, the size of the channel conductance is in general influenced by the number of subunits in a given

conformation, while the lifetime of a state is determined by the spatial relationship, diagonal or adjacent, of other subunits in given states.

Finally, a recent study has proposed that olfactory CNG channels function through a non-cyclic and non-sequential allosteric model¹³⁸. Their kinetic data comes from macroscopic patch clamp recordings where channels are activated by derivatives of cyclic nucleotides that do not bind to the channels until activated by a light flash. These derivatives allow the patch to be bathed in ligand for an extended period before channel binding, which eliminates any errors that diffusion or other steric hindrances may provide. With this method, the activation timecourse primarily represents the kinetics of binding and gating. The authors say that their data does not fit with previously proposed models, and propose their own model with channel open states occurring with none, one, two, or three bound ligands. Transitions from one open state to another are only possible by first returning to a closed state followed by binding to another ligand. This interesting model has not received further testing, and inadequately deals with the existence of multiple subconductance states.

While no single model perhaps perfectly describes all aspects of CNG channel behavior, each model has its particular merits and uses. The Hill model, for example, provides a simple method for fitting macroscopic dose-response data, and determining the degree of cooperativity under different conditions. Sequential models can provide low-end estimates of the number of ligands necessary for full channel activation, and these models can also be used to qualify whether changes in channel sensitivity due to experimental manipulations or modulation, can be explained entirely by changes in gating or binding affinity. The models that best fit macroscopic and single channel

behavior, however, are the allosteric models, which propose that ligand binding at one subunit pressures other subunits into assuming a configuration that favors channel opening. These models are much more mathematically complicated, but they may ultimately be useful and necessary for understanding the molecular determinants of cooperativity as well as for describing specific biophysical mechanisms underlying channel regulation.

1.16 CNG Channel Modulation

Since CNG channels mediate the initial electrical response to light and odorants, modulation of their activity can have a dramatic impact on initial sensory sensitivity and further processing. In isolated patches, all CNG channel subtypes can be modulated by divalent cations, phosphorylation and calmodulin, as well as by certain physiologically relevant lipid molecules. However, the effects of each regulator can vary widely across different channel subtypes. Furthermore, the physiological significance of the different forms of modulation is unclear, with the exception of calmodulin inhibition of olfactory channels.

1.16a Phosphorylation

Phosphorylation has been reported to inhibit both rod and cone CNG channels, and potentiate olfactory channels. Channels in patches pulled from rod outer segment membranes show a gradual increase in their cGMP sensitivity over a period of minutes. This behavior is blocked by the presence of compounds that inhibit serine/threonine phosphatases. However no specific residues have been identified as important, thus it is

unclear if this behavior is due to direct or indirect effects¹³⁹. Both native and heterologously expressed rod CNG channels can be inhibited by activators of tyrosine kinases¹⁴⁰. A tyrosine in the CNBD of A1 is required for this regulation, and addition of a tyrosine to CNGA2 at this location confers sensitivity to tyrosine phosphorylation¹⁴¹. Interestingly, A1 channels lacking this tyrosine can still be inhibited to a similar extent by the tyrosine phosphatase inhibitor, genistein^{142,143}. Regions in and near the cytoplasmic end of S6 are important for this effect, and may be involved in directly binding genistein to stabilize channel closed states¹⁴⁴. A3 channels are reportedly inhibited by phosphorylation at two specific serines, but the importance of this form of modulation has not been studied with native channels⁴⁴. The apparent affinity of CNGA2 channels is increased by an order of magnitude by phosphorylation of a serine in the amino terminus, just downstream of the calmodulin binding site¹⁴⁵. The mechanism of this effect is unclear, but it does not appear to influence regulation by calmodulin. No such modulation by phosphorylation is observed with native or heterologously expressed heteromeric olfactory channels. And, if you've read this far I applaud your stamina.

1.16b Calcium/Calmodulin Inhibition

Compared to phosphorylation, much more is known about the molecular mechanisms underlying CNG channel regulation by the calcium binding protein, calmodulin. For all heteromeric channels, calcium-bound calmodulin ($\text{Ca}^{2+}/\text{CaM}$) interacts with sequences in beta subunits and appears to influence the gating process¹⁴⁶. B1 subunits of rod channels have a calmodulin binding site in the distal N-terminus¹⁴⁷⁻¹⁴⁹, a region that is also capable of interacting with the distal C-terminus of A1 subunits¹²⁶.

Disruption of the intersubunit interaction is thought to be responsible for the mild, approximately 2-fold decrease in apparent affinity upon $\text{Ca}^{2+}/\text{CaM}$ binding^{150,151}. Cone channels also exhibit a mild decrease in apparent affinity with $\text{Ca}^{2+}/\text{CaM}$ binding, and sequences in both the N- and C-termini of B3 are necessary for this effect¹⁵². Homomeric A3 channels are insensitive to regulation by $\text{Ca}^{2+}/\text{CaM}$, although a region in the N-terminus is capable of binding $\text{Ca}^{2+}/\text{CaM}$ ¹²⁴. Despite an understanding of the molecular details of calmodulin regulation of the rod and cone CNG channels, a role for calmodulin regulation in adjusting the light response has not yet been established^{113,153-156}.

In contrast, calmodulin plays a central role in olfaction, where it is critical for adaptation to the persistent presence of background odors¹⁵⁷⁻¹⁵⁹. This occurs rapidly, as calcium enters channels activated by the background odorant and binds to calmodulin. Early experiments observed that native and CNGA2 homomeric channels were inhibited up to 20-fold by nanomolar amounts of $\text{Ca}^{2+}/\text{CaM}$ (Figure 4A)^{102,160}. Subsequently, a domain within the N-terminus of CNGA2 necessary for $\text{Ca}^{2+}/\text{CaM}$ regulation was discovered^{100,102,124}. This domain resembles the 14-3-3 class of calmodulin binding motifs, which consists of basic and hydrophobic residues on opposite faces of a short alpha helix¹⁶¹. Removal of this region from CNGA2 subunits produces channels with severely decreased cyclic nucleotide sensitivity, and the shift in sensitivity is identical to that seen in wild type channels following $\text{Ca}^{2+}/\text{CaM}$ exposure^{100,102}. This observation contributed to the now well supported idea that in homomeric CNGA2 channels, the 14-3-3 motif of one subunit interacts with the CNBD of another subunit, which facilitates gating to produce an autostimulatory effect on cyclic nucleotide sensitivity. $\text{Ca}^{2+}/\text{CaM}$ lowers channel sensitivity by disrupting this interaction (Figure 4B)^{100,101}.

Interestingly, removal of the 14-3-3 motif from CNGA2 subunits does not affect Ca^{2+} /CaM regulation of heteromeric channels. Instead, domains in the C-linker region of CNGA4 and the N-terminus of CNGB1b are both necessary for Ca^{2+} /CaM regulation of heteromeric channels (Figure 4C-E)^{162,163}. These domains resemble typical IQ motifs, which begin with an I, L, or V residue followed immediately by a Q, then by a short sequence of interspersed hydrophobic and basic residues. In other channels, these sequences bind tightly to the calcium-free form of calmodulin, called apocalmodulin. The IQ domains of CNGA4 and CNGB1b also appear to bind tightly to apocalmodulin¹⁶², which likely leads to the faster kinetics of calmodulin regulation for heteromeric versus homomeric channels¹⁶³. A severe defect in olfactory adaptation behavior is observed in CNGA4 knockout mice, due to the lack of Ca^{2+} /CaM-mediated feedback inhibition^{65,164}. In contrast to our understanding of the mechanism of Ca^{2+} /CaM inhibition of CNGA2 channels, it is still unclear how Ca^{2+} /CaM alters the ligand sensitivity of native heteromeric channels.

1.16c Lipid Regulation of CNG Channels

During the last decade, interest in the regulation of CNG channels by lipids has increased. Rod CNG channels are inhibited by supposedly physiological levels (low micromolar) of all-trans-retinal, which dissociates from opsin after light induced isomerization of 11-*cis*-retinal¹⁶⁵. The effect of all-*trans* retinal is more pronounced at subsaturating cyclic nucleotide concentrations, suggesting a greater interaction with closed states¹⁶⁶. No specific channel regions have been implicated in this form of regulation, but studies with various retinoid analogues place certain spatial constraints on

the locus of action¹⁶⁷. Although 11-cis-retinal can also inhibit channel function, much higher concentrations are required, and this opsin-bound isomer would not likely have access to channels in outer segment membranes. The authors of these studies argue that all-*trans* retinal may contribute to decreased channel activity during bright light exposure, but this remains to be demonstrated.

CNG channels can also be inhibited by the phosphoinositides, phosphatidylinositol-4,5-bisphosphate (PIP₂) and phosphatidylinositol -3,4,5-triphosphate (PIP₃), as well as by analogues of one of the major metabolites of these lipids, diacylglycerol (DAG). Together, PIP₂ and PIP₃ are estimated to make up approximately 1% of the total plasma membrane content¹⁶⁸. They appear to regulate a variety of cellular functions, with PIP₂ playing a major role in cytoskeletal dynamics, and PIP₃ operating in signaling cascades important for cell growth and death¹⁶⁸⁻¹⁷⁰. Using GFP-tagged pleckstrin homology domains that specifically interact with either PIP₂ or PIP₃, it has been shown that PIP₂ levels at the plasma membrane are generally more stable than PIP₃ levels^{168,171}. Stimulation by hormones often results in a decrease in plasma membrane PIP₂, either through phospholipase C (PLC)-mediated cleavage into soluble inositol trisphosphate (IP₃) and membrane embedded DAG, or through the phosphoinositide-3-kinase (PI3K)-mediated synthesis of PIP₃. However, PIP₂ levels can also increase, following EGF stimulation for example. It has also been proposed that particular membrane associated proteins can sequester PIP₂, until a higher affinity ligand, calmodulin for example, binds to a nearby or overlapping site, thereby releasing PIP₂ and increasing its local concentration¹⁷². Proteins like RGS4, MARCKS, and Myosin 1C exhibit behavior that may serve this proposed function¹⁷²⁻¹⁷⁴. In contrast to PIP₂, plasma

membrane PIP₃ levels are very low under basal conditions, but can increase rapidly and dramatically following hormone stimulation¹⁷⁵. High levels of plasma membrane PIP₃ are not maintained for long, however, due to the action of phosphatase enzymes, such as PTEN and SHIP. In general, data collected from multiple cell types suggests that a relatively constant level and homogenous distribution of PIP₂ serves to stabilize membrane proteins and act as a marker that distinguishes the plasma membrane from other intracellular membranes. PIP₃ and DAG, on the other hand, behave more like true second messenger signaling molecules, exhibiting dynamic and restricted changes in concentration following stimulation¹⁷¹.

Channels in inside-out patches from rod outer segments can be inhibited by micromolar amounts of cytoplasmic diacylglycerol (DAG) analogues with short, 8-carbon acyl groups¹⁷⁶. Subsequent studies found that DAG inhibits A1 channels to the same extent as native rod channels, but CNGA2 channels are only mildly affected¹⁷⁷. Work with chimeras between CNGA1 & CNGA2 suggests that the transmembrane segments and interconnecting loops are important for DAG regulation, and mutating a single glycine in the cytoplasmic S2-S3 loop alters DAG sensitivity^{177,178}. DAG appears to act by stabilizing channel closed states, and Hill coefficients of DAG dose-response relationships imply that more than one DAG molecule is involved. It is unclear whether the DAG effect involves direct interactions with the channel, or indirect effects on membrane structure. Interestingly, one report found no change, or a slight potentiation effect, in rod CNG channel activity following exposure to physiologically relevant forms of DAG containing longer acyl chains¹⁷⁹.

More recent studies show that PIP₂ can also impact the cyclic nucleotide sensitivity of rod CNG channels. In patches from rod outer segments, exposure to an anti-PIP₂ antibody increased channel sensitivity, while exposure to PIP₂ lowered sensitivity¹⁷⁹. These studies were complicated by the fact that PIP₂ also modulated PDE activity in the patches. Still, similar effects were observed with A1 homomeric channels expressed in oocytes, suggesting that A1 subunits harbor PIP₂ responsive elements.

1.16d PIP₃ Regulation of Olfactory CNG Channels

Recently, PIP₃ inhibition of olfactory CNG channels has been implicated in regulating the response of OSNs to complex odorants. Blocking PI3K enhances the response of isolated olfactory sensory neurons to complex odorants, in some cases unmasking a previously undetectable response¹⁸⁰. CNG channels in patches pulled from isolated OSNs are dramatically inhibited by exposure to micromolar amounts of exogenous PIP₃, and inhibited to a smaller degree by PIP₂¹⁸¹. Heterologously expressed CNGA2 channels are also sensitive to PIP₃ but insensitive to PIP₂, suggesting that the effect of PIP₃ on native channels may be due to specific interactions with the CNGA2 subunit.

Following PIP₃ exposure, the efficacy of cAMP is markedly reduced without a change in the single channel conductance, implying that PIP₃ modulates the gating process. It is interesting that while the PIP₃-induced shift in the cyclic nucleotide sensitivity of native channels is smaller than that seen following Ca²⁺/CaM exposure, PIP₃ dramatically reduces the efficacy of cAMP while Ca²⁺/CaM causes no change. These differences point to fundamentally distinct mechanisms for regulation by the two

different molecules, and may allow for a potent combined effect in OSNs. Thus, inhibition by PIP₃ could have a profound and complicated impact on the odorant response, but the true physiological relevance is currently unknown. One long term goal of some of the studies described in this dissertation is to facilitate investigation into the role of PIP₃ regulation in OSNs.

Demonstrating the physiological relevance of phosphoinositide regulation of CNG channels is challenging for a few reasons. First, changing lipid levels in native tissues or cells is difficult, and may induce changes in sensory signaling networks beyond just altering channel activity. The physiologically relevant stimulus for phosphoinositide metabolism is also unclear. Second, all forms of lipid regulation studied so far appear to involve sequence elements present in alpha subunits, thus it is not possible to remove lipid regulation in native cells through subunit knockouts without losing channel function altogether. Ultimately, perhaps the best approach for defining the physiological contributions of phosphoinositide regulation involves defining the sequence elements necessary for modulation, and producing transgenic animals carrying mutations in these sequences.

Defining the sequence elements involved in PIP₃ regulation of olfactory CNG channels may benefit from work with other ion channels, where specific sequences important for phosphoinositide regulation have already been identified. Unlike the larger phosphoinositide binding domains found in many cytoplasmic proteins, such as pleckstrin homology and FYVE domains¹⁷⁰, in most cases, the defined phosphoinositide interaction regions of ion channels are short sequences loosely consisting of basic amino acid clusters separated by hydrophobic residues. This arrangement is thought to favor

relatively non-specific electrostatic interactions with multiple phosphates on the headgroups. For example, binding of PIP₂ to a number of K_{ir} channel subtypes promotes channel activation by stabilizing the open state, and hydrophobic and basic residues in the carboxy terminal are known to be important¹⁸²⁻¹⁹⁰. PIP₂ activates KCNQ and mechanosensitive TREK-1 channels, but inhibits TRPV1 channels, through similar interactions with basic amino acids¹⁹¹⁻¹⁹³. Finally, evidence suggests that PIP₂ can remove N-type inactivation in some Kv channels by interacting with the basic residues in the amino-terminal inactivation ball, which normally plugs the pore following channel opening¹⁹⁴. Less is known about specific PIP₃ interactions with ion channels, but at least one PIP₃-ion channel interaction has been examined in detail, and again basic residues in cytoplasmic domains are involved¹⁹⁵. Many of these phosphoinositide sequences are relatively non-specific, that is other phosphoinositides like PIP and PIP₂ can produce similar changes in channel function. However, they generally show little or no interaction with other types of phospholipids or with the phosphorylated inositol headgroups alone, suggesting that both the lipid and headgroup portions are important determinants of binding. Interestingly, some of these small phosphoinositide interaction sequences resemble Ca²⁺/CaM binding motifs that also contain basic residues flanked by hydrophobic amino acids¹⁹⁶. Based on all the evidence from work with other ion channels, the calmodulin binding domain in the amino terminus of the CNGA2 subunit is a likely candidate for the PIP₃ interaction site. I've got to remember to eat sometime today.

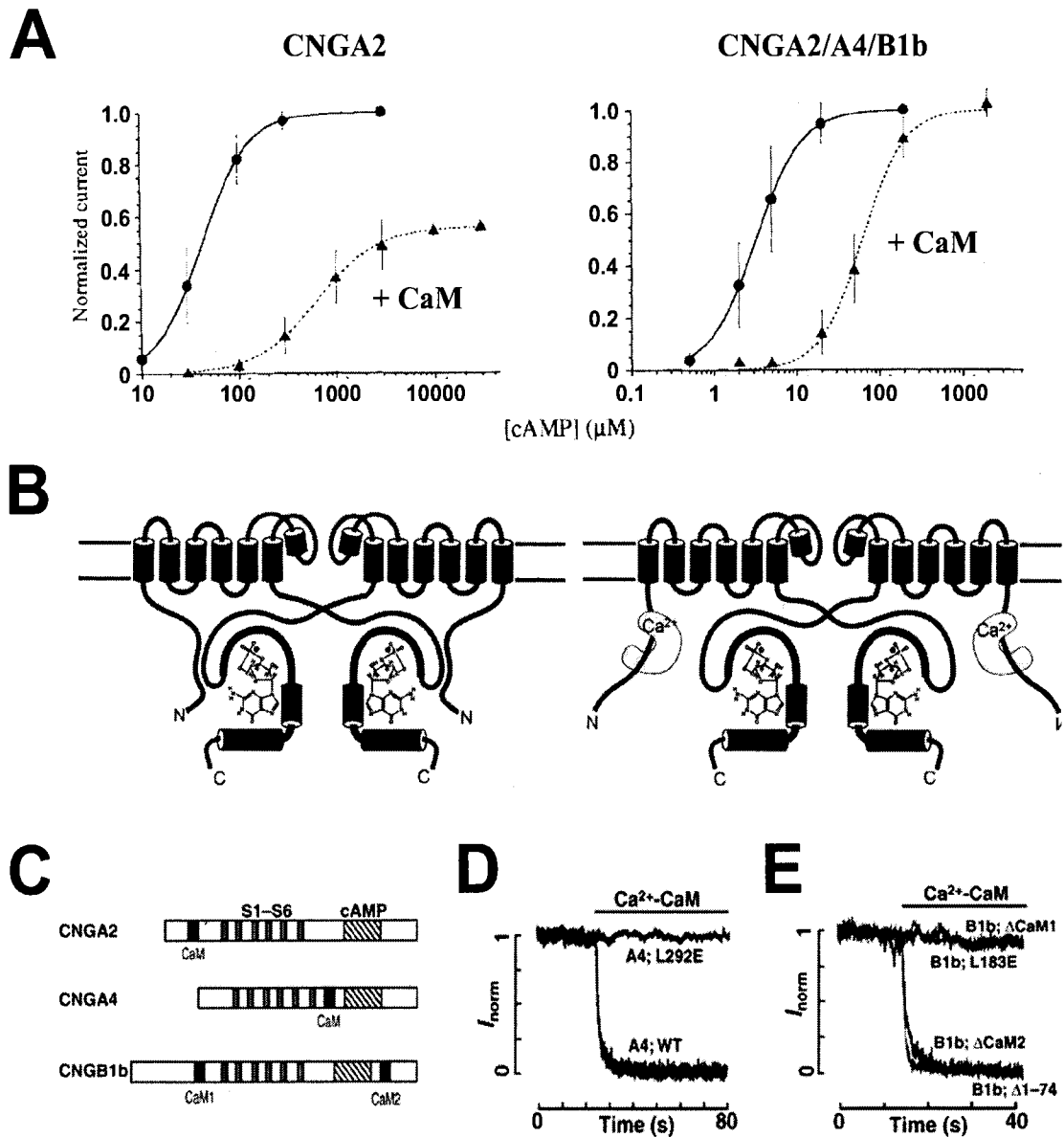


Figure 4: Calmodulin Regulation of Olfactory CNG Channels (A) Average activation curves in the presence of calcium before (Ctrl) and after calmodulin exposure (+CaM). Shown are data for heterologously-expressed CNGA2 channels and native channels in OSN membrane patches. (CNGA2/A4/B1b). Solid lines are fits to Hill equations using the following parameters ($K_{1/2}$ in μM , n): CNGA2 control = 43.4, 1.8, +CaM = 645, 1.4; CNGA2/A4/B1b control = 3.2, 1.6, +CaM = 63, 1.7. Modified from reference 161. (B)

Model proposed for mechanism of $\text{Ca}^{2+}/\text{CaM}$ inhibition of CNGA2 channels. The N-terminus of one subunit normally interacts with the C-linker and CNBD of another subunit to enhance cyclic nucleotide sensitivity. $\text{Ca}^{2+}/\text{CaM}$ binding to the N-terminus disrupts this autoexcitatory interaction. Modified from reference 101. **(C)** Linear representations of olfactory CNG channel subunit proteins. $\text{Ca}^{2+}/\text{CaM}$ binding motifs are shown in black, Grey rectangles denote the S1-S6 transmembrane segments, and the hashed boxes represent the CNBD. **(D)** Inside-out patch clamp recordings of heteromeric olfactory CNG channels containing wild type A4 subunits or subunits that lack the CaM-binding motif in their C-linker. Wild-type channels are dramatically inhibited by $\text{Ca}^{2+}/\text{CaM}$ while those containing mutant CNGA4 are not affected. **(E)** Heteromeric channels containing CNGB1b subunits that lack the CaM-binding motif in their N-terminus are not inhibited by $\text{Ca}^{2+}/\text{CaM}$, but those lacking the CaM-binding motif in the C-terminus are still inhibited. Panels C, D, & E modified from reference 163.

1.17 Compartmentation

In order for CNG channels to contribute to cellular activity, stimulus-induced cyclic nucleotide synthesis must occur in close proximity to channel binding sites, otherwise diffusion and the action of phosphodiesterases would rapidly reduce the cyclic nucleotide concentration below that needed to effectively activate channels. This requires that CNG channels be localized with the signaling cascades responsible for cyclic nucleotide synthesis. Such colocalization, or compartmentation, is evident in the photoreceptor outer segments and the cilia of OSNs, where channels and members of the G-protein signaling cascades gather densely. Based on these ideas and observations, it has been postulated that CNG channels contain sequence elements that somehow mandate close relationships with cyclase enzymes and associated signaling molecules.

Evidence for this idea was discovered during attempts to use CNG channels as sensors of membrane-localized cAMP levels. In initial whole-cell patch clamp experiments, stimulation of membrane resident adenylyl cyclases by forskolin significantly activated CNGA2 channels, even when the bulk cytosol was dialyzed with cAMP-free solution¹⁹⁷. Accurate quantitative modeling of this behavior relied on the existence of a compartment near the membrane surface where newly synthesized cAMP accumulated without diffusing into the bulk cytosol. To investigate this possibility, mutations of CNGA2 were made to remove calmodulin regulation ($\Delta 61-90$), and increase cAMP sensitivity while decreasing cGMP sensitivity (C460W/E583M)^{116,198}. In cells expressing these mutated channels, the timecourse of calcium influx following exposure to an extracellular stimulus accurately reflects changes in membrane-localized cAMP levels. Work with these modified channels lead to two important discoveries. First, the

hormone prostaglandin E₁ (PGE₁) stimulated a rapid but transient rise in calcium influx that represented an increase in cAMP synthesis followed by phosphodiesterase-mediated hydrolysis^{116,199,200}. Second, the PGE₁-stimulated increase in bulk cytosolic cAMP was much smaller and more stable than that observed at the membrane²⁰⁰. These results imply that CNGA2 channels reside in very close proximity to adenylyl cyclases, and quantitative considerations suggest that the diffusion of cAMP away from the channels must be limited to produce the levels of channel activity observed. While this might result from the homogenous distribution of large numbers of overexpressed channels, it may instead reflect the fact that channels preferentially colocalize with members of G-protein signaling cascades. Beta subunits of CNG channels have been shown to be important for outer segment and ciliary targeting^{201,202}, but the data collected with CNGA2 channels suggests that alpha subunits alone may contain sequence elements that participate in colocalization with signaling partners. Protein-protein interactions may be involved, but, as discussed further in the next section, protein-lipid interactions can also facilitate the assembly of different proteins into organized signaling compartments. This idea served as the foundation for the experiments described in this dissertation.

1.2 Lipid Rafts and Ion Channels

1.21 Properties of Lipid Rafts

Beginning with work by Jeffrey Martens on voltage-gated potassium channels in 2000, interest in the regulation of ion channels by a specific type of membrane microdomain, called lipid rafts, has steadily increased²⁰³. Lipid rafts are operationally defined as membrane microdomains that resist solubilization by Triton X-100 detergent

at low temperatures^{204,205}. In artificial systems, membranes that resist Triton X-100 solubilization exist in a liquid-crystalline phase²⁰⁶⁻²⁰⁹. These phases typically form when sphingolipids and other membrane lipids containing saturated acyl chains pack tightly together in the presence of biologically relevant concentrations of cholesterol^{204,209-211}. The liquid-crystalline, like the crystalline phase, is highly ordered, that is the acyl chains exhibit limited flexibility. Like the fluid phase, though, the lipids in liquid-crystalline phases are laterally mobile within the bilayer. It is expected, though not entirely established, that proteins within liquid-crystalline phases experience greater resistance toward large scale conformational changes, which may stimulate or inhibit their function.

Biologically relevant lipid rafts were first identified in polarized epithelial cells, during experiments to understand the sorting process that selectively concentrates proteins carrying glycosylphosphatidylinositol (GPI) anchors within the detergent-insoluble apical membrane²¹²⁻²¹⁴. Since then, evidence for the existence of small cholesterol-rich microdomains in other cell types has accumulated, and lipid rafts have been implicated in regulating vital cellular processes such as protein sorting, the organization of signaling events at the membrane, and nerve growth cone development^{215,216}. However, except in a few unique systems, the existence of lipid rafts in biological membranes remains controversial, and the methods used to show functional relevance are considered by some to be inadequate²¹⁷.

1.22 Identifying and Characterizing Biologically Relevant Lipid Rafts

Much of the controversy centers around potential problems associated with the standard technique used to isolate lipid rafts: sucrose gradient fractionation of Triton X-100 solubilized cellular membranes. Because cells are generally cooled to 4°C before mechanical lysis in detergent, liquid crystalline phases may form unnaturally. Additionally, the detergent itself can induce the formation of non-native ordered phases²¹⁸. Finally, it has been proposed that during lysis and initial loading on the sucrose gradient, membranes may remix according to their biophysical properties, producing liposomes and lipid sheets that do not resemble the original membrane form.

Despite these concerns, a few striking observations provide a compelling case for the existence of functionally relevant lipid rafts in at least some biological membranes. First, detergent-resistant model membranes and biological membranes exhibit similar lipid compositions, and proteins that sort to detergent-resistant membranes in biological preparations also do so in artificial systems²⁰⁴. Second, not all membrane proteins are found in detergent-resistant membranes, and some proteins change their solubility properties following particular modifications or cellular events, such as movement out of the endoplasmic reticulum (ER) and into the Golgi^{213,219}. These and other observations during the past decade support the generally accepted idea that proteins are localized in discrete domains of the plasma membrane, and this localization depends on the presence of cholesterol and sphingolipids. Much of the debate about lipid rafts now centers on the molecular basis for the cholesterol and sphingolipid requirement²¹⁷. It is still largely unclear whether the ability of these lipids to form liquid-crystalline phases is important,

or whether more specific interactions with membrane proteins or more general effects on membrane structure are involved.

To demonstrate that lipid rafts play a role in the function of a particular protein or signaling system, researchers have relied on two primary techniques. The most common technique involves removing cellular cholesterol, typically by using the compound methyl- β -cyclodextrin (MBCD). This large tubular-shaped oligosaccharide selectively binds cholesterol, is fast-acting, and does not imbed into or cross the plasma membrane, unlike other cholesterol depleting agents such as the pore-forming antibiotic filipin and the enzyme cholesterol oxidase²²⁰⁻²²⁴. Thus, it is regarded as an effective tool for rapidly removing cholesterol specifically from the plasma membrane, while leaving the concentrations of other lipids largely unchanged. Treating resting mammalian cells with MBCD can cause a variety of effects, including ligand-independent activation of EGF receptors, reduced clathrin-coated pit formation, rearrangement or stiffening of the cytoskeleton, loss of GPI-anchored proteins from the extracellular surface, membrane leakage, and non-specific extraction of phospholipids^{217,223,225-229}. Some of these effects, membrane leakage and non-specific phospholipids extraction for example, critically depend on the MBCD concentration and treatment time. The role that liquid-crystalline domains play in these more general effects of MBCD treatment is unknown.

In addition to effects on resting cells, MBCD treatment can alter the cellular response to a variety of stimuli, which has led to the idea that lipid raft microdomains serve as platforms that help organize signaling events at the plasma membrane. The polarization of T-cells following chemoattractant exposure and the formation of a T-cell signaling complex following antigen presentation are two notable examples of systems

where lipid rafts are thought to be important, and where MBCD treatment disrupts function^{219,230}. However, evidence suggests that at least part of the effect of MBCD treatment may be due to non-specific effects on internal calcium stores and membrane integrity, thus the role of lipid rafts in T-cell signaling remains controversial²³¹. Cyclic nucleotide signaling following hormone stimulation of G-protein coupled receptors is also dramatically altered by MBCD treatment, which correlates with the detergent resistance of many of the proteins involved²³²⁻²³⁷. But it has not yet been definitively shown that the mechanism by which MBCD treatment alters cyclic nucleotide signaling specifically involves disruption of liquid-crystalline domains.

A second method used to study the functional importance of lipid rafts relies on mutant proteins that mistarget either into or out of lipid raft domains, as assessed by their detergent-resistance. In general, the molecular determinants of lipid raft association are not well understood^{215,238-240}. For some proteins, lipid raft association is regulated by co-translational covalent modifications, such as the addition of sugars, lipid moieties, or glycosphosphoinositide anchors^{241,242}. The kinase protein Lck in T-cells, for example, is normally both myristoylated and palmitoylated, which targets the protein to detergent-resistant membranes. Removing the sequences that govern lipidation and attaching a transmembrane protein anchor to Lck, which targets the kinase out of detergent-resistant membranes, results in disrupted T-cell signaling. Proteins may also associate with lipid raft microdomains by interacting with other raft-associated proteins, like the strongly raft-associated protein, caveolin²⁴³. For example, the predominant G-proteins and adenylyl cyclase present in olfactory cilia all exhibit detergent-resistance and also coimmunoprecipitate with caveolin²⁴⁴. The presence of anti-caveolin antibodies during

odorant stimulation inhibits cAMP synthesis, which may result from the migration of the G-proteins and adenylyl cyclase out of lipid rafts, thereby decreasing their functional interactions. Finally, it has been proposed that specific amino acid sequences buried within the bilayer or resting near the membrane surface impart an affinity for specific lipids or for particular physical states of the lipid bilayer^{245,246}. Further characterization of specific sequences that control lipid raft association would help assess the hotly debated physiological relevance of these membrane microdomains²¹⁷

1.23 Functional Relationships Between Ion Channels and Lipid Rafts

A number of ion channels associate with biochemically isolated lipid raft membranes, and some show functional changes following cholesterol extraction. For example, K_v2.1 channels were the first voltage-gated ion channels localized to lipid raft membranes, and cholesterol depletion dramatically shifts their voltage dependence of inactivation²⁰³. K_v1.5 channels also localize to biochemically isolated rafts, and the voltage dependence of both activation and inactivation are shifted following cholesterol depletion²⁴⁷. In aortic endothelial cells, changes in the membrane cholesterol concentration can alter the level of Kir2.1 surface expression²⁴⁸. Other ion channels, such as Trp1, L-type Ca²⁺, and voltage-gated Na⁺ channels, as well as nicotinic acetylcholine receptors, and AMPA receptors, have been localized to lipid raft microdomains, but no direct functional relationship has yet been established²³⁸.

In general, the molecular mechanisms underlying changes in channel activity following cholesterol depletion are poorly understood. To more specifically address this

issue a few interesting techniques have been employed. Irena Levitan and colleagues have used an approach involving the replacement of membrane cholesterol with analogues that vary in their ability to form direct interactions with proteins and promote liquid-ordered phases. Their work has found evidence for two separate mechanisms underlying the cholesterol sensitivity of two different channels in the same cell type. For inward rectifier potassium channels in endothelial cells, specific protein-cholesterol interactions may be involved in regulating current density by changing surface expression levels²⁴⁸. Yet in the same cell type, changes in the volume-regulated anion current following MBCD treatment could be reversed only by replacing cholesterol with analogues that support liquid-crystalline phase formation²⁴⁹. Olaf Andersen and colleagues have tried a different approach, relying on the well characterized ability of gramicidin channels to change their conductance state as a property of bilayer elasticity. By adding various amphiphiles to HEK-293 cells heterologously expressing skeletal muscle sodium channels, these researchers found that changes in sodium channel function correlated with changes in elasticity, as reported by gramicidin channel activity²⁵⁰. The results from all of these studies clearly demonstrate that cholesterol can alter channel activity in a variety of ways, and that no general mechanism applies to all ion channels subtypes.

Chapter 2: Results

The following sections describe the results from experiments exploring the molecular basis for cholesterol and PIP₃ regulation of olfactory CNG channels. Most of these results have been published or accepted for publication, and the modified manuscripts are reproduced without the methods in sections 2.1 and 2.3^{251,252}. The results described in section 2.2 have not been prepared for publication. Figures are located at the end of each section, and a detailed description of methods can be found in chapter 5.

CHAPTER 2.1

Functional Role of Lipid Raft Microdomains in Cyclic
Nucleotide-Gated Channel Activation.

Functional Role of Lipid Raft Microdomains in Cyclic Nucleotide-Gated Channel Activation*

James D. Brady[‡], Thomas C. Rich[§], Xuan Le[‡], Kimberlee Stafford[‡], Cedar J. Fowler[‡],
Leatha Lynch[¶], Jeffrey W. Karpen[‡], R. Lane Brown[¶], Jeffrey R. Martens[‡]

[‡]Department of Physiology & Pharmacology, Oregon Health & Science University, 3181
S.W. Sam Jackson Park Road, Portland, Oregon 97239; [§]Department of Integrative
Biology and Pharmacology, University of Texas Health Science Center at Houston, 6431
Fannin, MSB 4.108 Houston, TX 77030; [¶]Neurological Sciences Institute, Oregon Health
& Science University, 505 N.W. 185th Avenue, Beaverton, OR, 97006

* This work was supported by National Eye Institute Grants EY09275 (to J.W.K.) and
EY12837 (to R.L.B.), and a National Heart, Lung, and Blood Institute Grant HL070973
(to J.R.M.).

Cyclic nucleotide-gated (CNG) channels are the primary targets of light- and odorant-induced signaling in photoreceptors and olfactory sensory neurons (OSNs). Compartmentized cyclic nucleotide signaling is necessary to ensure rapid and efficient activation of these non-selective cation channels. However, relatively little is known about the subcellular localization of CNG channels or the mechanisms of their membrane partitioning. Lipid raft domains are specialized membrane microdomains rich in cholesterol and sphingolipids that have been implicated in the organization of many membrane-associated signaling pathways. Here we report that the alpha subunit of the olfactory CNG channel, CNGA2, associates with lipid rafts in heterologous expression systems and in rat olfactory epithelium. However, CNGA2 does not directly bind caveolin, and its membrane localization only slightly overlaps with that of caveolin at the surface of HEK-293 cells. To test for a possible functional role of lipid raft association, we treated HEK-293 cells with the cholesterol-depleting agent, methyl- β -cyclodextrin. Cholesterol depletion abolished prostaglandin E₁-stimulated CNGA2 channel activity in intact cells. Recordings from membrane patches excised from CNGA2-expressing HEK-293 cells revealed that cholesterol depletion dramatically reduced the apparent affinity of homomeric CNGA2 channels for cAMP while only slightly reducing the maximal current. Our results show that olfactory CNG channels target to lipid rafts and that disruption of lipid raft microdomains dramatically alters the function of CNGA2 channels.

Introduction

Cyclic nucleotide-gated (CNG) ion channels were first discovered in retinal photoreceptors and olfactory neurons where they modulate the membrane potential in response to stimulus-induced changes in the intracellular concentrations of cyclic nucleotides^{19,33,35}. Although CNG channels have now been found in many other neuronal and non-neuronal cells, their physiological roles in non-sensory tissues remain obscure²⁵³. Over the past several years, however, we have learned much about the structure and functional properties of these non-selective cation channels⁴⁴. To date, six CNG channel subunits have been cloned, including both α (CNGA1-4) and β (CNGB1 & 3) subunits. Although many of the α -subunits can be functionally expressed as homomultimers, co-expression of the β -subunits is known to confer distinct functional properties, in terms of ion permeation, ligand sensitivity, gating mechanisms, and regulation. Recent evidence suggests that the stoichiometry of the native rod photoreceptor channel is 3 CNGA1 to 1 CNGB1⁵⁹⁻⁶¹. The native olfactory channel is thought to contain three subunit types, including CNGA2, CNGA4, and CNGB1.3, although the stoichiometry remains unknown^{53,57,58,64}.

Despite a relative wealth of knowledge about CNG channel structure and function, very little is known about the mechanisms responsible for their targeting and subcellular localization. Since a growing number of channel-linked genetic diseases involve the failure of channels to reach the cell surface²⁵⁴, the general mechanisms of ion channel targeting are of considerable interest. The importance of CNG channel targeting is illustrated by a recent report showing that the trafficking of rod CNG channels to the plasma membrane is disrupted in an inherited form of blindness¹²⁶. In photoreceptors and

OSNs, the targeting of CNG channels to very specific regions of the plasma membrane rich in sensory signaling molecules allows for efficient and spatially confined responses to sensory stimuli^{33,35,48,255}.

Recently, it was shown that several proteins involved in sensory signaling in photoreceptors and OSNs reside in specialized plasma membrane subdomains called lipid rafts^{244,256}. These physically distinct membrane regions are rich in particular lipids, especially sphingolipids and cholesterol, and they concentrate certain membrane proteins, including signal transduction enzymes, membrane receptors, and ion channels^{203,257,258}. Lipid rafts are thought to facilitate the lateral assembly of signaling cascades²¹⁵, while depletion of raft lipids is known to disrupt a number of signaling events, such as T-cell activation²⁵⁹ and β -adrenergic signaling²³².

Here we report for the first time that the primary subunit of the olfactory CNG channel, CNGA2, is localized to lipid rafts in both heterologous expression systems and in native olfactory tissue. Depleting membrane cholesterol to perturb lipid rafts dramatically altered the function of homomeric CNGA2 channels in intact cells and isolated patches. Our results show that the integrity of the cholesterol-rich lipid environment is an important modulator of raft-localized CNGA2 channel function. Furthermore, these results support the idea that local membrane environment is important for maintaining protein-lipid interactions necessary for transmembrane signaling.

Results

CNGA2 Associates with Lipid Rafts in Heterologous Expression Systems and Olfactory Tissue. Lipid rafts are experimentally characterized by their resistance to

solubilization by non-ionic detergents, such as Triton X-100, and a low buoyant density²⁵⁸. We first examined the detergent insolubility of CNGA2 in a heterologous expression system. HEK-293 cells were transiently transfected with a CNGA2 construct tagged at the N-terminus with the 3XFLAG epitope. When transfected cells were extracted at 4°C with buffer containing 1% Triton X-100, FLAG-CNGA2 was found primarily in the detergent-insoluble pellet (Fig. 5A). Detergent insolubility can arise from associations with detergent-resistant membranes, such as lipid rafts, or through interactions with large protein complexes, such as the cytoskeleton. To investigate the possibility of a cytoskeletal interaction, we treated cell homogenates with high salt (0.6 M potassium iodide) to disrupt protein-protein interactions. Treatment of the Triton X-100 cell extracts with potassium iodide did not solubilize CNGA2 (Fig. 5A), suggesting that CNGA2 was associated with detergent-resistant membranes.

To determine if CNGA2 partitions into lipid raft microdomains, we examined the density of the insoluble membrane fragments containing CNGA2. HEK-293 cells expressing FLAG-CNGA2 were extracted with 1% Triton X-100 at 4°C, and the resulting extracts were layered on the bottom of a discontinuous sucrose gradient and subjected to equilibrium density centrifugation. Immunoblotting of gradient fractions revealed two peaks of CNGA2 immunoreactivity (Fig. 5B). A significant percentage of FLAG-CNGA2 was found in buoyant detergent-insoluble fractions at the interface between the 5% and 30% sucrose layers. Under these conditions, the CNGA2 subunit co-migrated with the raft marker proteins caveolin²⁶⁰ and flotillin 1 in the low-density fractions (Fig. 5B). FLAG-CNGA2 protein was also present in the high-density, detergent-soluble fractions at the bottom of the gradient, which is most likely due to the

intracellular accumulation of overexpressed protein²⁰³. Similar results were obtained with COS-1 cells (Fig. 5C), indicating that raft association was independent of the cell type chosen for heterologous expression.

When assessing raft affinity using detergents, it is critical to choose a detergent concentration that effectively separates detergent-insoluble membranes from detergent-soluble membranes and proteins. To ensure against incomplete solubilization of non-raft proteins, the transferrin receptor, which is not associated with lipid rafts^{205,261,262}, was used as a marker for Triton X-100 soluble membranes in each experiment (Fig. 5B). The effects of Triton X-100 concentration on detergent-resistant membrane (DRM) recovery in our system was determined by comparing extraction at several different concentrations of detergent (Fig. 5D). With 1% Triton X-100 in the homogenization buffer, approximately 80% of cellular caveolin and 25% of CNGA2 channel protein was detected in raft fractions whereas endogenous transferrin receptor was completely solubilized. Importantly, lowering the Triton X-100 concentration to 0.1% resulted in undersolubilization of cellular membranes, and approximately 50% of the transferrin receptor was now detected in the low-density fractions along with caveolin and CNGA2. Increasing the detergent concentration to 3% or 5% significantly solubilized caveolin. These results demonstrate that 1% Triton X-100 effectively separated DRMs from detergent soluble membranes in our preparation. In addition, at this detergent concentration a very small amount of total cellular protein (approximately 4%) was recovered in the DRMs whereas these fractions contain the majority (approximately 70%) of cellular cholesterol (Fig. 5E). While it is important to note that this assay is only a qualitative measure of a proteins DRM affinity and not quantitative measure of raft

association²⁰⁵, together these experiments show that heterologously expressed CNGA2 associates with cholesterol-rich, detergent resistant membranes.

In OSNs, CNG channels containing the CNGA2 subunit are concentrated in the dendritic cilia where they generate an electrical signal in response to odorant-stimulated production of cAMP³³. To determine if endogenous CNGA2 was associated with lipid rafts, we used an antibody against the wild type subunit (kind gift of Dr. U. Benjamin Kaupp). To confirm specificity, we probed Western blots containing membranes from untransfected HEK-293 cells or cells transiently expressing wtCNGA2, FLAG-CNGA2 or CFP-CNGA2. The results indicate that the anti-wtCNGA2 antibody recognizes both the wild type and epitope-tagged forms of the CNGA2 subunit with very little background staining (Fig. 6A). In OSNs, CNGA2 predominately exists in a highly glycosylated form, and the carbohydrate moiety can be removed by enzymatic digestion⁶⁴, as illustrated in Fig. 6B. Western blot analysis of sucrose gradient fractions from detergent-extracted rat nasal membranes revealed that the glycosylated form of CNGA2 was present in buoyant lipid raft fractions (Fig. 6C). Again, these buoyant fractions were rich in caveolin but contained no transferrin receptor. These results indicate that a portion of native olfactory CNG channels associates with lipid rafts in olfactory membranes. The sizeable percentage of CNG channel found at the bottom of the gradient may reflect the existence of multiple channel populations (see Fig. 5C) or the expression of CNG channels in different cell types. Again, it should be noted, however, that the biochemical isolation of DRMs is useful as a qualitative, not a quantitative, measure of protein affinity for raft domains^{205,263}. Importantly, these results indicate that CNGA2/raft association is not an artifact of heterologous expression. Although only the

glycosylated form of CNGA2 was detected in the detergent resistant gradient fractions, our data in heterologous expression systems suggest that glycosylation is not necessary for the association of CNGA2 with raft domains. This idea is consistent with previous work demonstrating that glycosylation is not a signal for raft association^{264,265}.

CNGA2 Associates with Predominately Non-Caveolar Lipid Rafts in Heterologous Expression Systems. Previous work implicates caveolin in the regulation of odorant signaling²⁴⁴, and caveolar and non-caveolar raft domains are known to play different roles in the regulation of membrane signaling²⁶⁶. The biochemical isolation of lipid rafts does not, however, distinguish between caveolar and non-caveolar lipid raft membranes. Therefore we performed additional experiments to determine whether CNGA2 associates with caveolae in native membranes and heterologous expression systems.

Although CNGA2 cofractionates with caveolin in detergent-resistant sucrose gradient fractions, immunoprecipitation experiments gave no evidence that CNGA2 and caveolin directly interact in either HEK-293 cells (Fig. 7A) or in olfactory membranes (Fig. 7B). In addition, fluorescence microscopy revealed incomplete colocalization of the two proteins at the cell surface (Fig. 7C-E). Similar results were obtained for flotillin 1 and 2 (Supplemental Figure 1). Based on these results, we conclude that CNGA2 is found in predominately non-caveolar lipid raft domains at the plasma membrane.

Cholesterol Depletion Disrupts the Association of CNGA2 with Lipid Rafts and Alters Channel Function. Given that lipid rafts are enriched in cholesterol and sphingolipids, their integrity is sensitive to exogenously applied lipid-depleting agents²⁵⁸.

Prior to detergent extraction, we treated HEK-293 cells expressing FLAG-CNGA2, for 1 hour with the membrane-impermeant cholesterol-binding agent methyl- β -cyclodextrin (CD). This treatment is commonly used to disrupt lipid raft integrity²¹⁵. Gas chromatography and mass spectrometry analysis demonstrated that 2% CD pretreatment of HEK-293 cells for 1 hour produced a 90% decrease in total cellular cholesterol (see Figure 14). Western blot analysis of sucrose gradient fractions from CD pretreated cells demonstrated that cholesterol depletion reduced the buoyancy of CNGA2 lipid raft membranes (Fig. 8). The peak of buoyant CNGA2 immunoreactivity was shifted down the gradient and increased levels of CNGA2 were found in higher density fractions. This pattern was characteristic of all cyclodextrin experiments (n=3). A similar gradient pattern was observed for caveolin, consistent with previous reports^{266,267}. These results indicate that CD pretreatment significantly depletes cellular cholesterol and perturbs the integrity of CNGA2-rich lipid raft membranes.

We next examined the functional significance of raft association by measuring prostaglandin E₁ (PGE₁)-stimulated CNGA2 channel activity before and after cholesterol depletion. The fluorescent indicator fura-2 was used to monitor channel-mediated Ca²⁺ influx in HEK-293 cell populations expressing a modified CNGA2 channel with increased sensitivity to cAMP^{116,200}. Stimulation of cells with PGE₁ (100 nM) resulted in a rapid rise in intracellular calcium followed by a slower decline to a steady state (Fig. 9A). Several lines of evidence indicate that this response is due to a rise and fall in cAMP near the membrane²⁰⁰. For example, cells not expressing CNGA2 showed no significant PGE₁-stimulated increase in intracellular calcium. Surprisingly, pretreatment of cells with 2% CD nearly abolished the PGE₁-stimulated increase in CNGA2 channel

activity (Fig. 9A & E) without affecting basal calcium levels. These results are summarized in figure 9E, in which the rate of calcium influx was calculated as the slope of the rising phase and plotted for each condition. When cells were pretreated with both 2% CD and 1 mM cholesterol, no loss of PGE₁-stimulated calcium influx was observed (Fig. 9B). This suggests that the loss of PGE₁-stimulated channel activity following CD pretreatment is due specifically to the depletion of cholesterol.

The dramatic loss of PGE₁-stimulated CNGA2 channel activity after cholesterol depletion could reflect a decrease in cAMP accumulation. Therefore we measured whole-cell cAMP levels following cholesterol depletion using an enzyme immunoassay (Amersham). Although 5 μM forskolin produced a measurable rise in whole-cell cAMP, 100 nM PGE₁ produced no detectable increase in whole-cell cAMP (Supplemental Figure 2). The finding that 100 nM PGE₁ generated a robust increase in Ca²⁺ influx without altering whole-cell cAMP levels reflects the fact that cAMP accumulates to higher concentrations in diffusionally-restricted microdomains near the surface membrane, and that CNG channels monitor cAMP levels in this pool^{197,200}. Thus, conventional cAMP assays do not have the sensitivity to determine whether cAMP accumulation was significantly affected.

Alternatively, a decrease in channel expression or function may contribute to the dramatic loss of PGE₁-stimulated CNGA2 channel activity after cholesterol depletion. Treatment of CNGA2-expressing cells with a membrane permeant form of cGMP (CPT-cGMP) produced a sustained increase in calcium influx that was not significantly reduced by a 1 h pretreatment with 2% CD (Fig. 9C & E). Similar treatment of uninfected cells produced no significant rise in intracellular calcium levels (Fig. 9D). These data indicate

that the expression of CNGA2 channels at the cell surface and the maximal conductance were largely unaffected by cholesterol depletion. Since the maximal current is a product of the number of channels, the single channel open probability, and the maximal single channel current ($I=Np_o i$), we set out to determine if CD altered CNGA2 channel activity evoked by subsaturating cAMP concentrations. We therefore measured the dose-response relations of homomeric CNGA2 channels for cAMP in inside-out patches pulled from HEK-293 cells expressing wtCNGA2. Without CD pretreatment, CNGA2 channels exhibited an average $K_{1/2}$ for cAMP of 39 μ M, and a saturating concentration of cAMP elicited the same maximal current as a saturating concentration of cGMP (1 mM). Pretreatment with 2% CD profoundly decreased the apparent affinity for cAMP ($K_{1/2}$ = 123 μ M) while only slightly reducing the maximal current in saturating cAMP by approximately 20% (c.f. saturating cGMP, Fig. 10). If the $K_{1/2}$ values for individual patches are calculated and then averaged such that each patch is weighted equally, the difference is even greater (control, $K_{1/2}$ = 42 ± 6 μ M; cyclodextrin, $K_{1/2}$ = 173 ± 36 μ M). Interestingly, there was high variability in this effect across patches, with some patches showing very little effect and others showing a large shift in the dose-response relation. While this variability may be a result of non-uniform cholesterol extraction between cells, it may also reflect the existence of multiple channel populations. The extremes of this variation are represented in the inset of Fig. 10.

Discussion

The results presented in this manuscript demonstrate for the first time that an alpha subunit of the olfactory CNG channel, CNGA2, associates with lipid rafts in both

heterologous expression systems and membranes from rat nasal tissue. This association does not appear to involve caveolin but does rely on the presence of membrane cholesterol. In biochemical preparations, cholesterol depletion reduced the buoyancy of membrane fractions containing CNGA2. Depletion of plasma membrane cholesterol also dramatically reduced PGE₁-stimulated channel activity in intact cells, in part by causing a 3-fold decrease in the apparent affinity of CNGA2 channels for cAMP. At low, physiologically relevant cAMP concentrations, the 3-fold shift in the average apparent affinity could result in roughly a 9-fold change in CNG channel activity due to the cooperative nature of channel gating. This effect might be even greater given that these numbers reflect the average change, and some experiments showed a much greater shift in apparent affinity. Together, our results indicate that the local lipid environment of the CNGA2 channel profoundly impacts its participation in cyclic nucleotide signaling by regulating channel function.

Though the effect of cholesterol depletion on the apparent affinity of CNGA2 channels for cAMP was variable, in most patches the effect was quite remarkable, with a greater than 10-fold shift in affinity in some recordings. Further experiments are required to establish whether cholesterol depletion affects the intrinsic affinity for cAMP or the allosteric conformational changes involved in channel opening. Cholesterol depletion almost certainly disrupts interactions between the channel and the lipid bilayer, either in the form of specific protein-lipid interactions or through changes in the physical properties of the bilayer itself²⁶⁸. For example, a recent report suggests that interactions between membrane lipids and the hydrophobic transmembrane helices of ion channels directly influence channel properties²⁶⁹. There is also precedence for a role of lipid

signaling molecules such as DAG and all-*trans* retinal in the modulation of CNG channel function^{165,177}.

It is also likely that the functional significance of lipid raft localization includes the compartmentation of ion channels with regulatory proteins²¹⁵. Serine phosphorylation of the CNGA2 subunit near the calmodulin binding site on the carboxy terminus increases the sensitivity of CNGA2 channels to cyclic nucleotides¹⁴⁵. Lipid raft perturbation may destroy an association between CNGA2 channels and raft-associated kinases or other proteins to lower the apparent cAMP affinity²⁷⁰.

It is clear that the spatial and temporal confinement of signaling proteins is a general mechanism for coordinating cellular function by preventing cross-talk between competing pathways. Compartmentized cyclic nucleotide signaling in three-dimensions is necessary to explain differential regulation of cellular targets by cAMP and to ensure rapid and efficient activation of CNG channels^{197,200}. It is tempting to hypothesize a role for lipid rafts in the establishment and/or maintenance of these restricted microdomains. Certainly, there is increasing evidence that rafts organize cAMP signaling proteins. For instance, many of the components involved in cAMP-mediated signaling, including G protein coupled receptors, certain G-protein isoforms, and some adenylyl cyclases, associate with lipid rafts in a diverse number of cell types^{232,236,242,271-273}. In addition, some reports suggest that lipid raft perturbation disrupts G-protein mediated cAMP accumulation^{232,234,274}. Therefore, association of CNGA2 with lipid rafts may be a mechanism for ensuring proximity to effector molecules within restricted plasma membrane microdomains. Our finding that CNGA2 channel activation following PGE₁-stimulation is disrupted by cholesterol depletion suggests that prostaglandin receptors and

CNGA2 channels exist together within a cholesterol-rich membrane microdomain. If so, we predict that specific prostaglandin receptor subtypes also associate with biochemically-isolated lipid rafts and that they reside in close proximity to CNGA2 channels at the plasma membrane. Further work is necessary to test these predictions.

Though our data strongly support the idea that the integrity of cholesterol-rich raft membranes is important for CNGA2 channel function, it is possible that not all CNGA2 channels are localized to lipid raft microdomains. Although the amount of CNGA2 in soluble gradient fractions correlates well with the level of intracellular protein in transfected HEK-293 cells, it may also reflect the existence of channel protein in non-raft domains at the plasma membrane. Again, it is important to note that the biochemical isolation of lipid rafts is only a qualitative, and not a quantitative, assessment of protein affinity for cholesterol-rich, detergent-insoluble membranes²⁰⁵. For this reason, it is difficult to calculate the fraction of CNGA2 that resides in raft and non-raft membranes based on our biochemical data. However, the variability in the effect of methyl- β -cyclodextrin on the apparent affinity of CNGA2 channels supports the idea that channels exist in both raft and non-raft environments, and it is the PGE₁-stimulated channel that is compartmentized in rafts and sensitive to cholesterol depletion. It will be interesting to determine whether agonists for other G-protein coupled receptors activate CNGA2 channels that are insensitive to cholesterol depletion.

The localization of CNG channels to lipid rafts may play a role in organizing cyclic nucleotide-mediated signaling compartments in neurons of the olfactory epithelium. Schreiber and colleagues²⁴⁴ demonstrated that the G-protein and adenylyl cyclase isoforms involved in odorant signaling associate with lipid rafts. The affinity of

odorant signaling proteins and CNG channels for physically distinct lipid raft membranes may facilitate their coassembly into signaling microdomains. Additionally, lipid rafts may play a role in targeting the channel and signaling proteins to defined regions of the dendritic cilia. Schreiber and colleagues also reported that G_{olf} and ACIII bind caveolin and that disruption of caveolin binding inhibits odorant-induced cAMP production in OSNs. Although we found no direct interaction between CNGA2 and caveolin in rat olfactory membranes, we cannot exclude the possibility that the native olfactory CNG channel localizes to caveolae *in vivo*. Further work with CNG channels in OSNs is required to clarify the involvement of caveolin.

The large shift in the apparent affinity of CNGA2 channels for cAMP following cholesterol depletion may have physiological significance for olfactory signaling. Modulation of channel cAMP affinity is believed to provide the main adaptive feedback mechanism for desensitization of the olfactory signaling pathway^{158,275}. Our results suggest that alteration of membrane lipid, either by disease or by clinical use of lipid-lowering drugs, can affect olfaction by altering the function of raft-localized CNG channels.

Acknowledgements. We thank William Connor for the total cellular cholesterol measurements, Daniel J. Menasco, Andrea DeBarber, and the PKCore for cholesterol measurements of gradient fractions, Kaili Song for making the FLAG- and CFP-CNGA2 constructs, and U. Benjamin Kaupp for the anti-wtCNGA2 antibody.

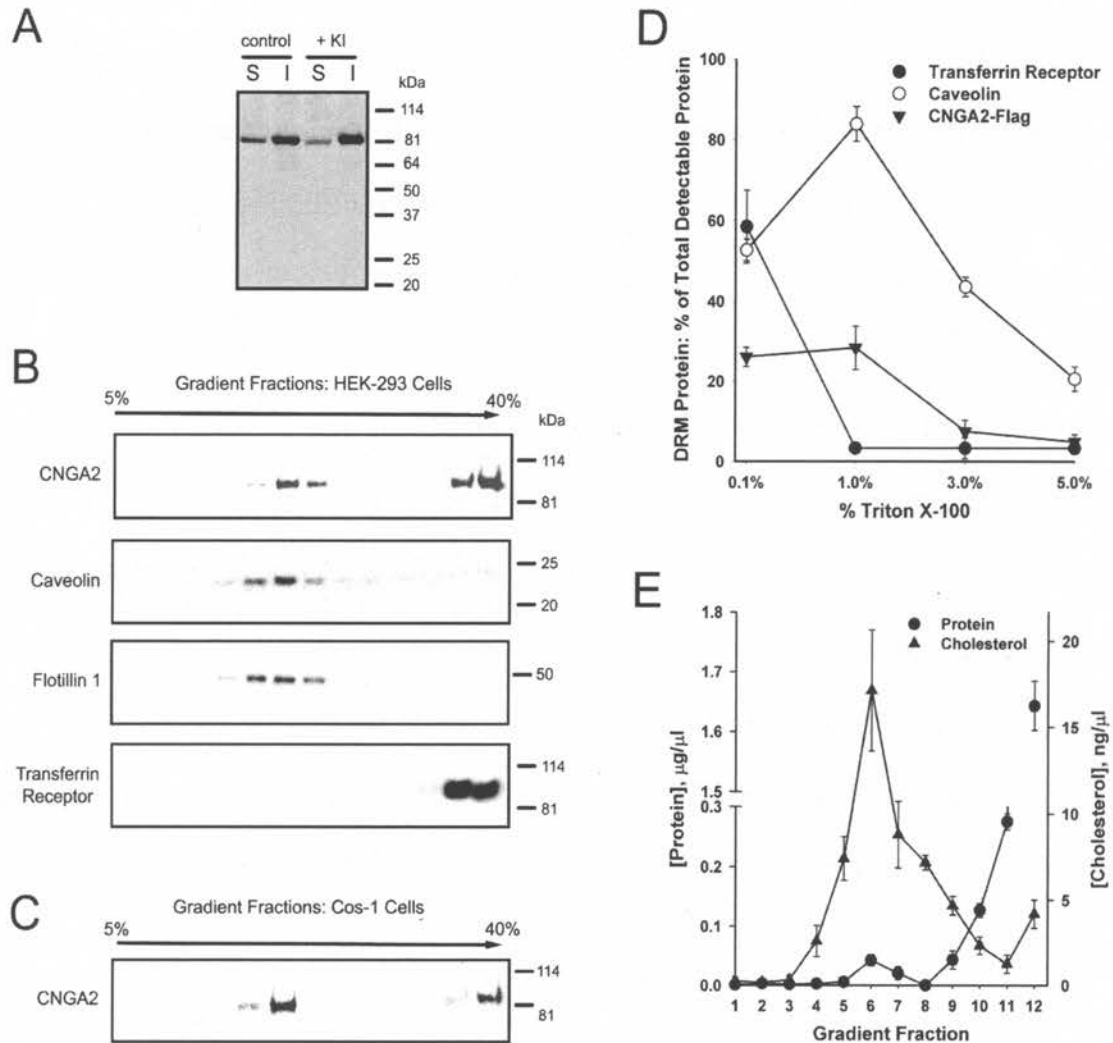


Figure 5. CNGA2 localizes to lipid rafts in heterologous expression systems. (A) Cell lysates from HEK-293 cells transiently transfected with FLAG-CNGA2 were homogenized in 1% Triton X-100 with or without 0.6 M KI to disrupt protein-protein interactions. Western blots of detergent soluble (S) and insoluble (I) proteins were probed with anti-FLAG antibody. FLAG-CNGA2 appears as a sharp band at approximately 85 kDa. The presence of 0.6 M KI during homogenization had no effect on the solubility of CNGA2 in Triton X-100. (B-C) Sucrose density gradient centrifugation of 1% Triton X-100 solubilized extracts from HEK-293 cells (B) or COS-1 cells (C) expressing FLAG-

CNGA2 were prepared as described in the “Materials and Methods”. Western blots probed with anti-FLAG demonstrate that CNGA2 is present in detergent-insoluble, low-density lipid raft fractions, which are also enriched in endogenous caveolin and flotillin 1, but lack endogenous transferrin receptor. Shown is a representative example from 4 experiments. 5% and 40% refer to the sucrose concentration at the top and bottom of the gradient, respectively. (D) Detergent-Resistant Membranes (DRM) were isolated by homogenizing HEK-293 cells in different concentrations of Triton X-100 and subjecting the lysates to sucrose density gradient centrifugation. Western blots of gradient fractions were probed with appropriate antibodies. The integrated optical density of detectable protein in the low-density fractions was measured using Labworks software (UVP, Inc.), then expressed as a percentage of the total detectable protein along the entire gradient (error bars represent SEM, n=3). (E) Following homogenization of HEK-293 cells in 1% Triton X-100 and sucrose density gradient centrifugation, the protein and cholesterol content of each gradient fraction was determined as described in “Materials and Methods” (error bars represent SEM, n=3).

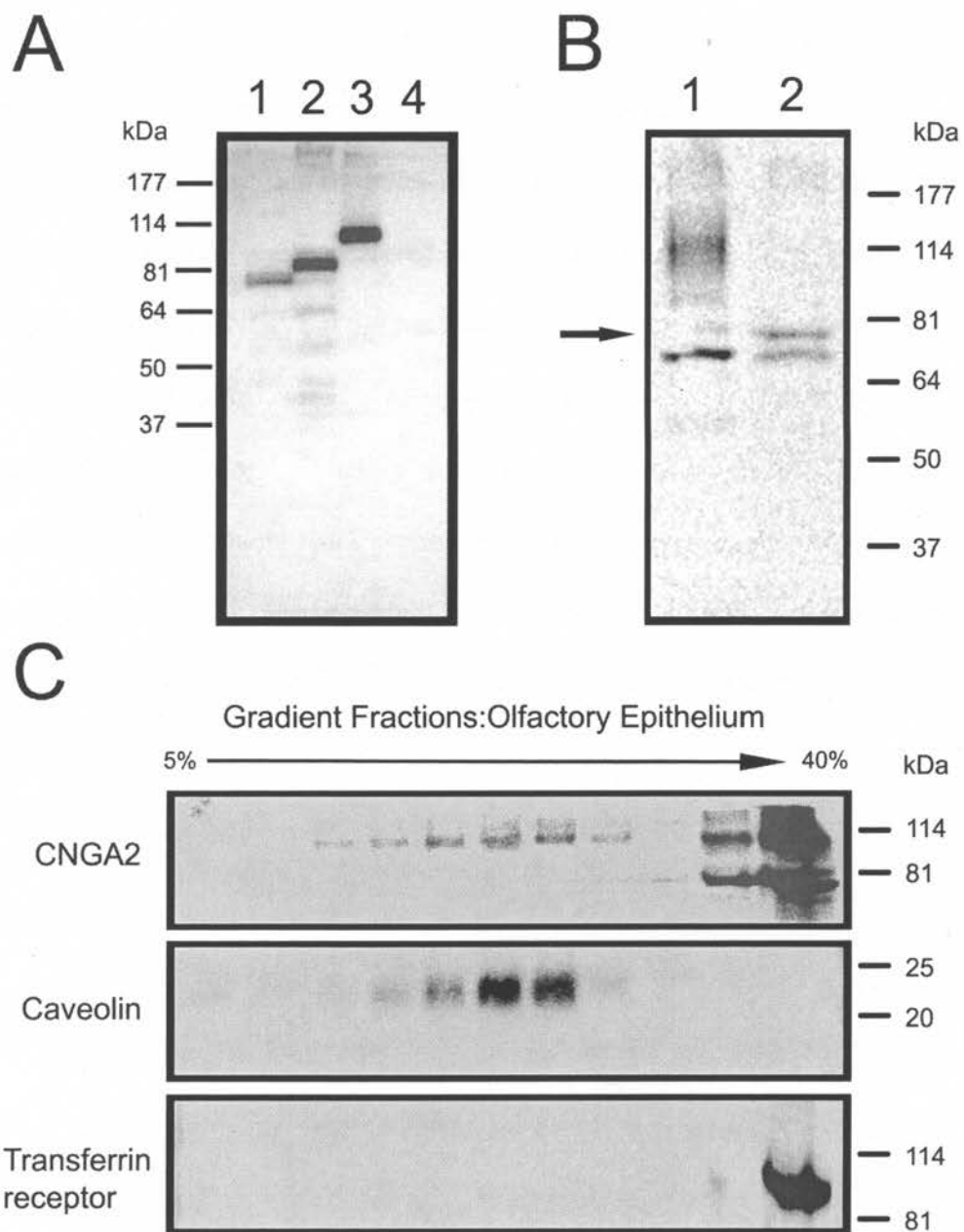


Figure 6. Glycosylated CNGA2 localizes to lipid rafts in membranes from rat olfactory tissue. (A) Cellular membranes prepared from HEK-293 cells transiently transfected with wtCNGA2 (Lane 1), FLAG-CNGA2 (Lane 2), or CFP-CNGA2 (Lane 3), and membranes from untransfected HEK-293 cells (Lane 4) were subjected to SDS-

PAGE, transferred to nitrocellulose, and probed with an antibody raised against native CNGA2. (B) Membranes prepared from rat nasal tissue were subjected to SDS-PAGE before (Lane 1) or after (Lane 2) incubation with N-glycosidase F for 1 h at 37°C. Western blot analysis demonstrates that the anti-CNGA2 antibody recognizes glycosylated CNGA2 (smear centered at 114 kDa in Lane 1) as well as the non-glycosylated form of CNGA2 at approximately 75 kDa, indicated by the arrow (Lane 2). The lowest band in both lanes is a non-specific band stained by the secondary antibody alone. (C) Western blot of sucrose density gradient fractions of 3% Triton X-100 extracted rat olfactory membranes probed for CNGA2, caveolin, and transferrin receptor. Glycosylated CNGA2 is clearly present in low-density lipid raft fractions (n=3). 5% and 40% refer to the sucrose concentration at the top and bottom of the gradient, respectively.

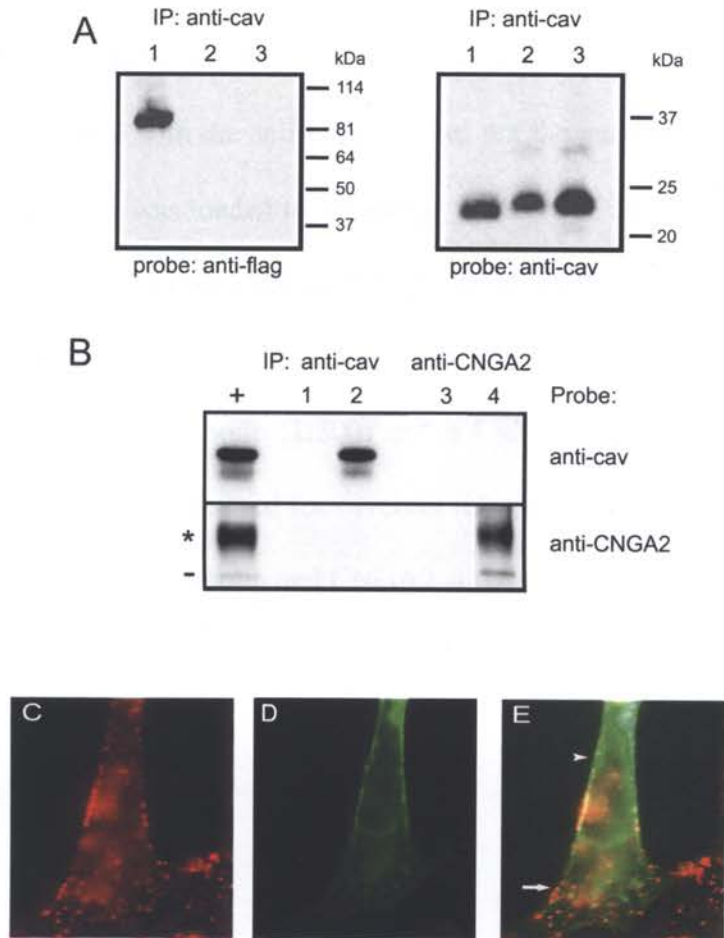


Figure 7. CNGA2 does not directly bind caveolin and is only partially colocalized with caveolin at the surface of HEK-293 cells. (A) Solubilized membranes from HEK-293 cells transfected with FLAG-CNGA2 (Lane 2) and from untransfected HEK-293 cells (Lane 3) were immunoprecipitated with anti-caveolin antibodies. Western blots of immunoprecipitates were probed with anti-FLAG and anti-caveolin antibodies. Lane 1 contains membranes from transfected cells as a positive protein control. The results demonstrate that caveolin (~23 kDa) does not immunoprecipitate CNGA2 (85 kDa). (B) Solubilized membranes from rat nasal tissue (200 μ g) were immunoprecipitated with anti-caveolin (Lane 2), anti-CNGA2 (Lane 4), or no primary antibodies (Lanes 1 & 3).

Western blots of the immunoprecipitates were probed with both anti-caveolin and anti-CNGA2 antibodies. Both the glycosylated (*) and unprocessed (-) forms of CNGA2 were precipitated with the anti-CNGA2, but not the anti-caveolin, antibody. 20 µg of rat nasal membranes was loaded to determine the level of caveolin and CNGA2 immunoreactivity before immunoprecipitation (+). The IP efficiency was approximately 20%. (C-E) HEK-293 cells transiently expressing CFP-CNGA2 were immunofluorescently labeled with anti-caveolin antibody (1:500) and a Cy3-conjugated fluorochrome. Individual images were pseudocolored red for caveolin (C) and green for CNGA2 (D). The overlap (yellow in E) between caveolin and CNGA2 at the cell surface is limited.

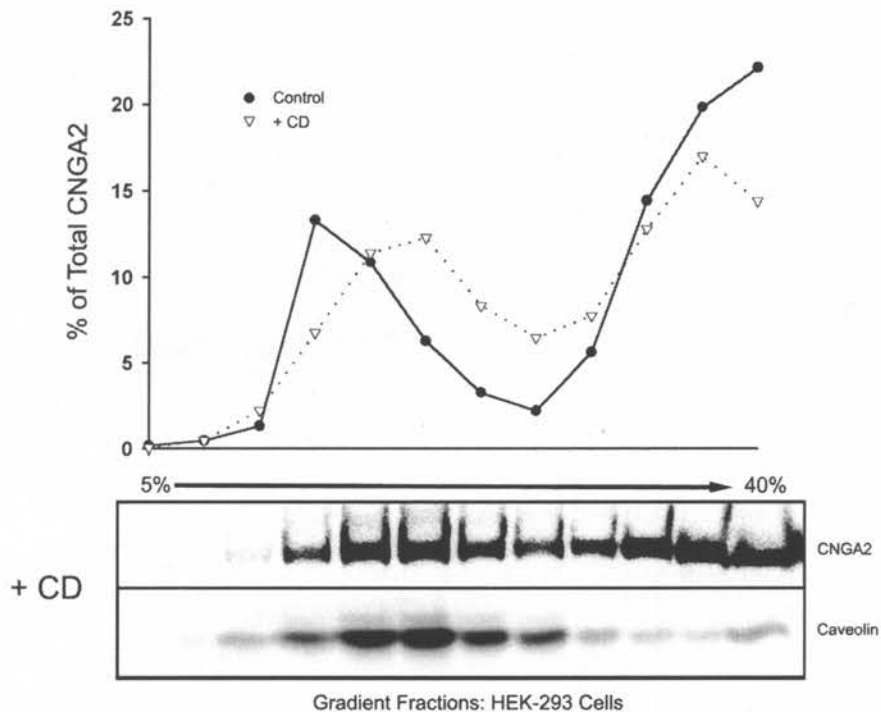


Figure 8. Cholesterol depletion increases the density of CNGA2-containing lipid raft membranes. HEK-293 cells expressing FLAG-CNGA2 were treated with 2% CD prior to solubilization in 1% Triton X-100 and sucrose density centrifugation. Western blots of sucrose gradient fractions were probed with anti-FLAG and anti-caveolin antibodies, and the optical density of CNGA2 immunoreactivity in each lane was measured and expressed as a percent of the total CNGA2 optical density. 5% and 40% refer to the sucrose concentration at the top and bottom of the gradient, respectively. Compared to results from untreated controls (filled circles, see Fig. 5), CD produced a smear of CNGA2 immunoreactivity (open triangles) through the gradient.

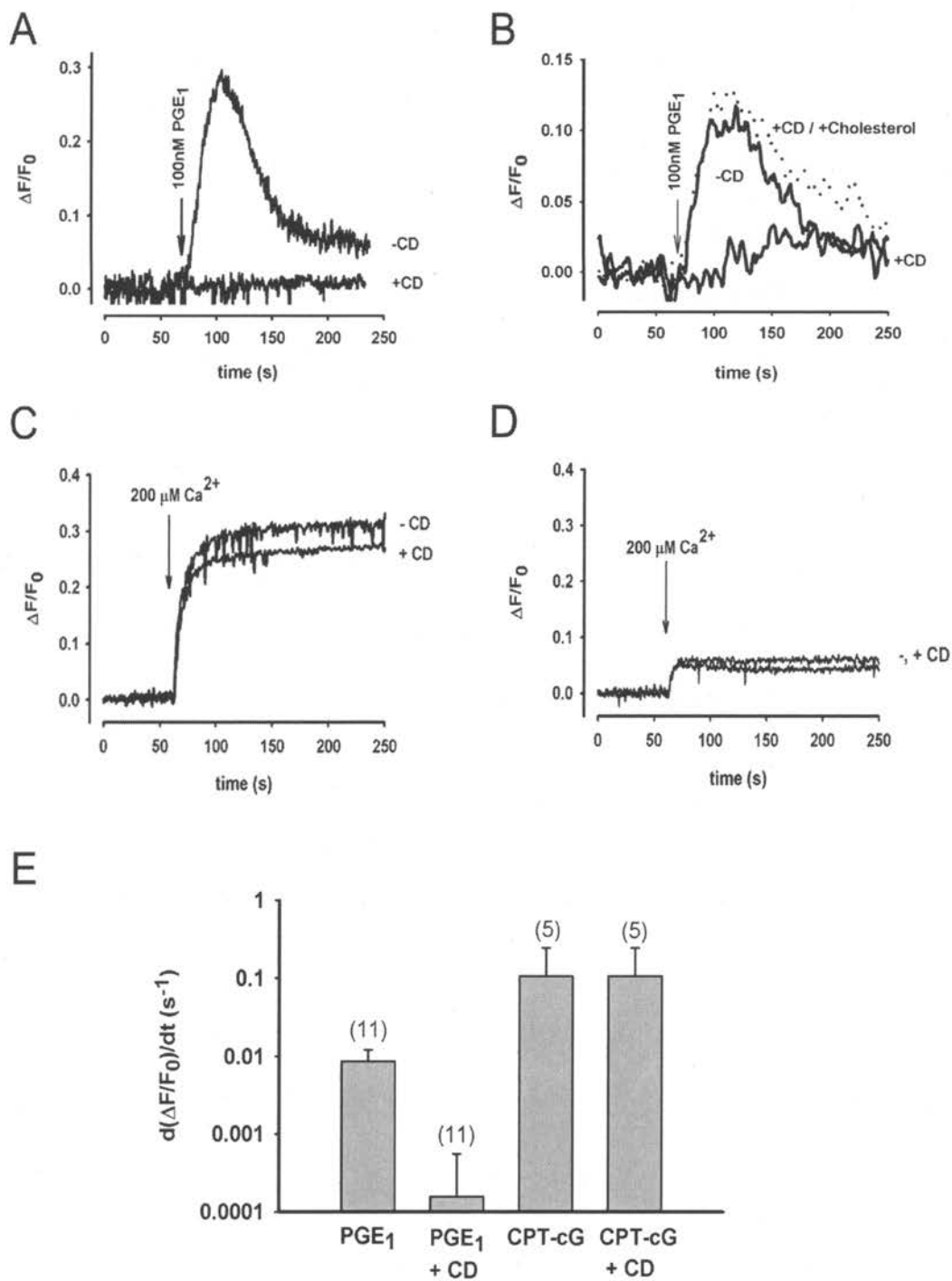


Figure 9. Cholesterol depletion abolishes PGE₁-stimulated CNGA2 channel activity in intact cells. (A-D) The fluorescent indicator fura-2 was used to monitor Ca²⁺ influx in HEK-293 cell populations expressing CNGA2. In this assay, an increase in local cAMP

concentration causes activation of homomeric CNGA2 channels and a subsequent increase in Ca^{2+} entry. Ca^{2+} influx causes a decrease in fluorescence (ΔF), which was expressed relative to the prestimulus fluorescence (F_0). $\Delta F/F_0$ was plotted with inverted polarity so that increases in Ca^{2+} influx are represented as positive deflections. (A) 100 nM PGE_1 stimulated an increase in calcium influx through CNGA2 channels (-CD, n = 11). Pretreatment of cells with 2% CD eliminated the response (+CD, n = 11). (B) Pretreatment of cells with 2% CD and 1 mM cholesterol (+CD/+Cholesterol) blocked the effect of 2% CD pretreatment alone (+CD). (C) Incubation in supersaturating (1 mM) CPT-cGMP for 1 h followed by the addition of 200 μM Ca^{2+} stimulated an increase in calcium influx (-CD, n = 5) that was only mildly reduced by pretreatment of cells with 2% CD (+CD, n = 5). (D) Only a small calcium influx was observed in uninfected cells following incubation in CPT-cGMP (1mM) and addition of 200 μM Ca^{2+} , both with and without 2% CD pretreatment. (E) Bar graph showing the maximal rate of calcium influx for the experiments shown in panels (A) and (C). Bars represent the averages from the number of experiments shown above the bar, and error bars represent the standard deviations. CD pretreatment significantly reduced the calcium influx following PGE_1 stimulation (t-test, $p < .00001$).

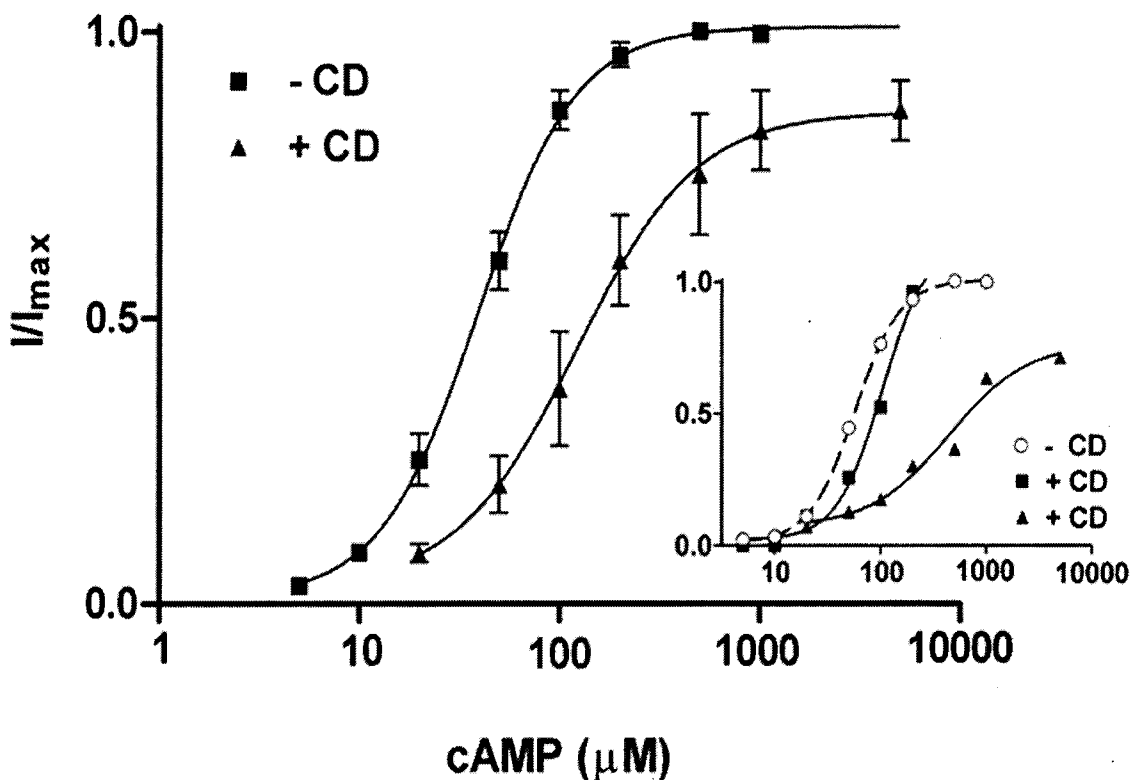


Figure 10. Cholesterol depletion reduces the apparent cAMP binding affinity of CNGA2 channels in isolated patches. CNGA2 channel activity was measured in inside-out patches pulled from HEK-293 cells expressing wtCNGA2 either before or after treatment with 2% CD for 15 – 30 minutes at 37 °C. Currents activated by bath application of increasing concentrations of cAMP (5 – 5000 μM) were measured at +50 mV, and the current at each cAMP concentration was expressed relative to the maximal current activated by 1 mM cGMP. The inset shows representative examples of single patch recordings from untreated (open circles) and 2%-CD-treated cells (closed symbols). All curves are fit to the Hill equation. The average $K_{1/2}$ increased from approximately 39 μM to 123 μM following CD incubation. Error bars represent SEM.

CHAPTER 2.2

**MBCD Does Not Inhibit Olfactory CNG Channels By
Disrupting Lipid Rafts.**

Our previous manuscript showed that heterologously expressed CNGA2 channels were associated with detergent resistant lipid raft membranes and inhibited by MBCD treatment, yet it was unclear whether the change in channel function following MBCD treatment was directly due to lipid raft disruption. To test this possibility, I first searched for related CNG channels that did not associate with lipid rafts, and therefore might not be expected to exhibit functional changes following MBCD treatment. I discovered that CNGA3 subunits expressed in HEK-293 cells were associated with Triton X-100 soluble membranes rich in transferrin receptors, rather than with caveolin-rich, detergent resistant membranes (Figure 11). This finding demonstrates that CNGA3 channels do not reside in lipid raft membranes.

Inconsistent with these biochemical results however, measurements of cGMP sensitivity in inside-out patches revealed that both CNGA2 and CNGA3 channels were similarly inhibited by 15 mM MBCD treatment at 37°C for 5-15 minutes (Figure 12). Together, these findings imply that MBCD inhibition of CNGA2 channels is not due to lipid raft disruption.

To further test the hypothesis that MBCD treatment inhibits CNGA2 channels by disrupting lipid rafts, I examined channel function following different MBCD treatment conditions. Evidence from studies employing a variety of methods to remove cellular cholesterol shows that at least two different kinetic pools of cholesterol exist within the plasma membrane: a temperature-insensitive, rapidly extractable pool, and a second pool that extracts more gradually and becomes harder to remove at lower extraction temperatures^{222,276-278}. These authors have hypothesized that the slowly-extractable pool represents tightly-bound plasma membrane cholesterol within microdomains resembling

lipid rafts. I therefore analyzed CNGA2 channel cyclic nucleotide sensitivity following 15 mM MBCD treatment at 22°C, for periods of up to 2 hours. Unlike the 3-fold average shift in cAMP sensitivity seen following MBCD treatment at 37°C, the $K_{1/2}$ for cAMP following MBCD treatment at 22°C remained largely unchanged (Figure 13A). This finding seemed to support the idea that MBCD treatment at 37°C inhibited CNGA2 channels by disrupting lipid rafts. However, when I lowered the concentration of MBCD to 5 mM, and treated cells at 37°C for up to 2 hours, I saw no change in the cyclic nucleotide sensitivity of CNGA2 channels (Figure 13B). In these experiments, the higher treatment temperature should still facilitate lipid raft disruption. This last finding and the CNGA3 data discussed above support the idea that MBCD inhibits CNGA2 channels through a mechanism that does not involve changes in lipid raft integrity.

However, it is also possible that at lower temperatures or lower MBCD concentrations, the amount of cholesterol removed is too small to promote lipid raft disruption. To test this idea, I measured the amount of cholesterol in HEK membranes following various MBCD treatment conditions, using either mass spectroscopy or a cholesterol oxidase-based fluorimetric assay. Both methods reported identical relative changes in cholesterol levels. As figure 14A demonstrates, 15 mM MBCD treatment at 37°C removes approximately 50% of total cellular cholesterol within the first 10 minutes, and eventually removes nearly all cellular cholesterol over the next 2 hours. 15 mM MBCD treatment at 22°C produces a similar cholesterol extraction profile, but after 2 hours of treatment approximately 30% of the total cholesterol still remains. Still, by 10-15 minutes at 37°C and after 1 hour at 22°C, the conditions used for electrophysiological analysis, nearly the same relative amount of cholesterol is removed. Figure 14B shows

that all of the various treatment conditions used for the functional experiments remove identical amounts of total cholesterol. Thus the lack of CNGA2 inhibition following 5 mM or 22°C MBCD treatment cannot be attributed to a higher concentration of remaining cholesterol. Following a 30 minute pretreatment with 15 mM MBCD at 37°C, up to 95% of the cellular cholesterol could be replaced by a subsequent 30 minute incubation with 15mM MBCD complexed with 1mM cholesterol. This treatment, however, resulted in a dramatic decrease in cell viability (assessed by cell counting and protein measurement), and isolating patches from the surviving cells proved extremely difficult.

An additional observation I made during these experiments was that after treating cells in suspension with 15 mM MBCD at 37°C beyond 15 minutes, or attached cells beyond 30 minutes, I was unable to achieve gigaohm seals or isolate stable patches. However, with 5 mM MBCD at 37°C, or 15 mM MBCD at 22°C, I could treat cells for up to 2 hours and still achieve strong seals and stable patches. These findings further demonstrate that 15 mM MBCD pretreatment at 37°C, independent of the quantity of cholesterol removed, leads to more dramatic changes in membrane integrity than the other treatment conditions.

In summary, I have found that the degree to which MBCD inhibits CNGA2 channels does not correlate with its ability to disrupt lipid rafts or with the amount of cholesterol removed. These findings suggest that CNGA2 channel function is not stabilized by specific interactions with cholesterol molecules, or by the integrity of cholesterol-rich plasma membrane microdomains. Rather, MBCD likely alters CNGA2 channel function through non-cholesterol mediated effects on membrane structure, or by

changing the concentration of another channel modulator.

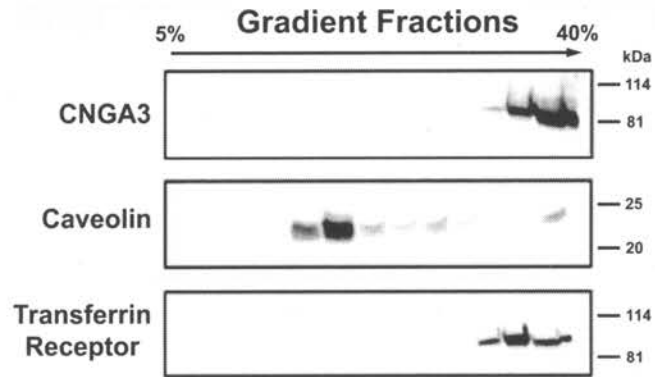


Figure 11: CNGA3 Raft Preparation Lipid raft membranes were isolated from HEK-293 cells expressing FLAG-CNGA3 subunits, as described in materials and methods. Proteins in the sucrose gradient fractions were separated by SDS-PAGE. Western blots probed with appropriate antibodies show that caveolin was present in low-density sucrose fractions, while transferrin receptor and CNGA3 were found in detergent-soluble fractions (40%).

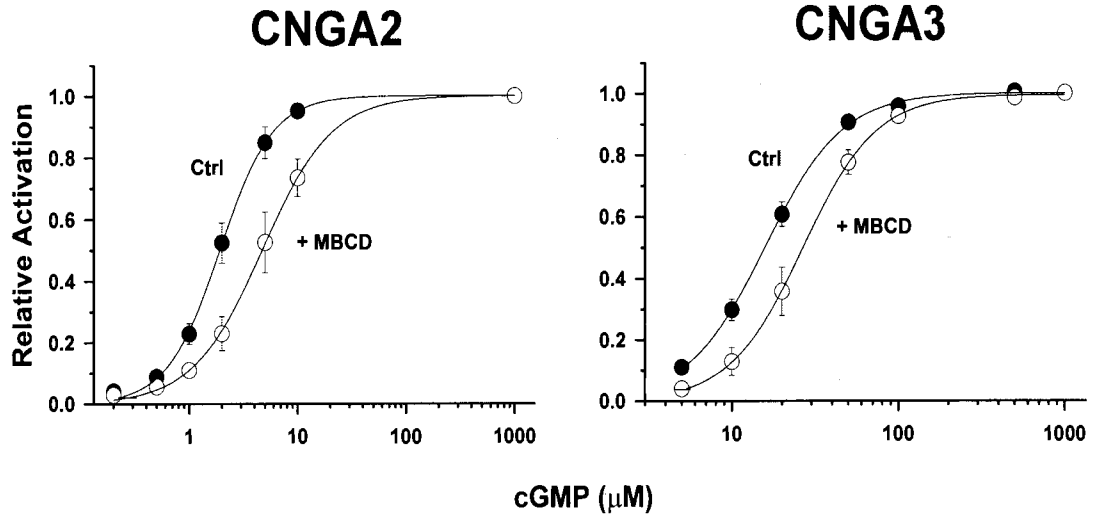


Figure 12: CNGA2 vs. CNGA3 Activation Curves Following MBCD Treatment

Inside-out patches were pulled from HEK-293 cells expressing either wtCNGA2 or wtCNGA3 subunits, either before (Ctrl) or after (+MBCD) incubation with 15 mM MBCD for 5-15 minutes at 37°C. Currents activated by the indicated concentrations of cGMP at +50 mV were normalized to the current activated by 1 mM cGMP.

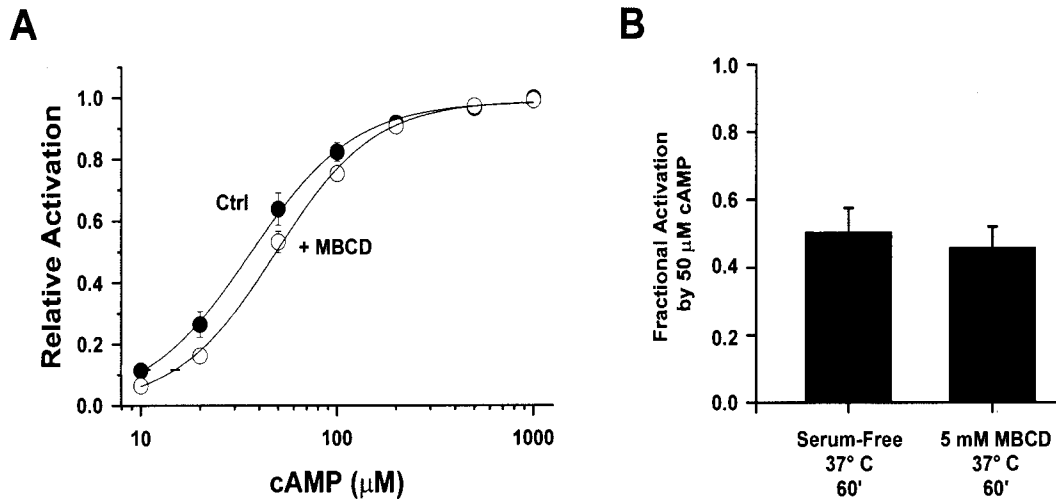


Figure 13: Effect of Different MBCD Treatment Conditions on CNGA2 Channels

(A) Inside-out patches from HEK-293 cells expressing CNGA2 subunits were exposed to the indicated concentrations of cAMP, either before (Ctrl) or after (+MBCD) pretreatment of cells with 15 mM MBCD at 22°C for 40-60 minutes. In (B), cells were pretreated with 5 mM MBCD at 37°C for 60 minutes. All currents were collected at +50 mV, and normalized to the current activated by 1 mM cGMP.

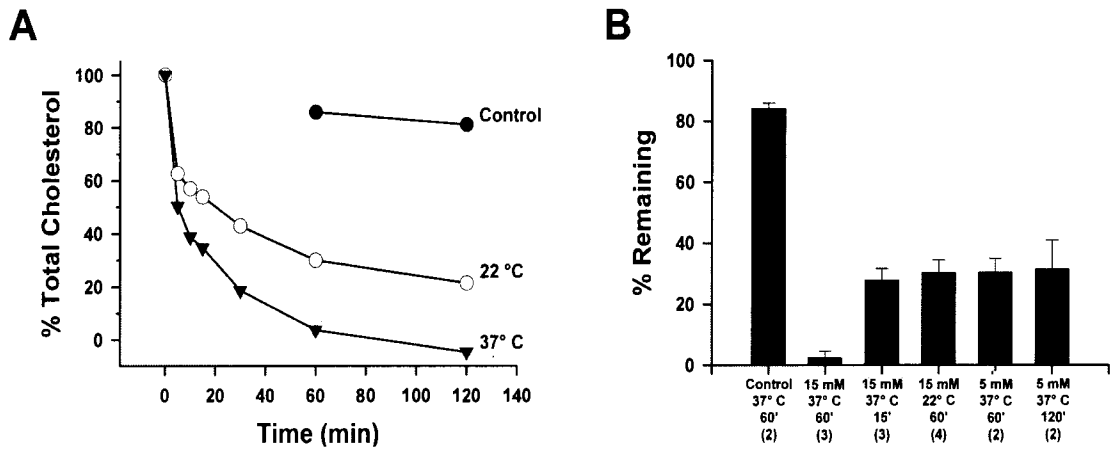


Figure 14: Cholesterol Extraction Data (A) The total cholesterol content of HEK-293 cells was measured following 15 mM MBCD treatment at the indicated temperatures using mass spectroscopy, as described in the materials and methods. Control cells were incubated in serum-free media at 37°C. Data points were normalized to the protein content and to the amount of cholesterol present before exposure to MBCD (time 0). The data are representative of 3 separate experiments, as well as 3 experiments using a biochemical assay, described in the methods. **(B)** HEK-293 cells were treated with MBCD as indicated on the X axis, and the total cholesterol content was measured with either mass spectroscopy or a biochemical assay. Data were normalized to the protein content and to the amount of cholesterol present before treatment. Numbers in parenthesis indicate the number of experiments performed.

CHAPTER 2.3

Interplay Between PIP₃ and Calmodulin Regulation of
Olfactory CNG Channels.

Interplay Between PIP₃ and Calmodulin

Regulation of Olfactory Cyclic Nucleotide-Gated Channels

James D. Brady¹, Elizabeth D. Rich³, Jeffrey R. Martens⁴,
Jeffrey W. Karpen², Michael D. Varnum³, & R. Lane Brown¹

¹Neurological Sciences Institute & ²Department of Physiology & Pharmacology, Oregon Health & Science University, Portland, OR.

³Department of Veterinary and Comparative Anatomy, Pharmacology and Physiology, and Program in Neuroscience, Washington State University, Pullman, WA.

⁴Department of Pharmacology, University of Michigan, Ann Arbor, MI

Phosphatidylinositol-3,4,5-trisphosphate (PIP₃) has been proposed to modulate the odorant sensitivity of olfactory sensory neurons (OSNs) by inhibiting activation of cyclic nucleotide-gated (CNG) channels in the cilia. When applied to the intracellular face of excised patches, PIP₃ has been shown to inhibit activation of heteromeric olfactory CNG channels, composed of CNGA2, CNGA4, and CNGB1b subunits, as well as homomeric CNGA2 channels. In contrast, we discovered that channels formed by CNGA3 subunits from cone photoreceptors were unaffected by PIP₃. Using chimeric channels and a deletion mutant, we determined that residues 61-90 within the N-terminus of CNGA2 are necessary for PIP₃ regulation, and a biochemical “pull-down” assay suggests that PIP₃ directly binds this region. The N-terminus of CNGA2 contains a previously identified calcium-calmodulin (Ca²⁺/CaM) binding domain (residues 68-81) that mediates Ca²⁺/CaM inhibition of homomeric CNGA2 channels, but is functionally silent in heteromeric channels. We discovered, however, that this region is required for PIP₃ regulation of both homomeric and heteromeric channels. Furthermore, PIP₃ occluded the action of Ca²⁺/CaM on both homomeric and heteromeric channels, in part by blocking Ca²⁺/CaM binding. Our results establish the importance of the CNGA2 N-terminus for PIP₃ inhibition of olfactory CNG channels, and suggest that PIP₃ inhibits channel activation by disrupting an autoexcitatory interaction between the N- and C-termini of adjacent subunits. By dramatically suppressing channel currents, PIP₃ may generate a shift in odorant sensitivity that does not require prior channel activity.

Odorant binding to specialized receptors in the cilia of olfactory sensory neurons (OSNs) triggers an increase in intracellular cAMP²⁷⁹⁻²⁸², which directly opens cyclic nucleotide-gated (CNG) channels⁴⁴. Calcium influx through CNG channels activates an atypical chloride current²⁸³⁻²⁸⁵, leading to depolarization of the cell membrane. The elevated calcium also causes rapid adaptation to odorants by triggering a Ca²⁺/CaM-dependent decrease in the sensitivity of CNG channels to cAMP²⁸⁶. Recent evidence suggests that PIP₃ also decreases the sensitivity of olfactory CNG channels and reduces the response of OSNs to complex odors, but the mechanism has yet to be elucidated^{180,181}.

Ca²⁺/CaM inhibits homomeric CNGA2 channel activation by binding to a Baa-like motif in the N-terminus^{161,287,288}, thereby disrupting an autostimulatory interaction with the C-terminus of an adjacent subunit²⁸⁹⁻²⁹¹. Deletion of the Ca²⁺/CaM-binding domain (amino acids 68-81) in CNGA2 produces channels that are resistant to inhibition by Ca²⁺/CaM, and also exhibit dramatically reduced sensitivity to cyclic nucleotides due to loss of the autostimulatory interaction. Native olfactory CNG channels are tetrameric assemblies of 3 different pore-forming subunits – CNGA2, CNGA4, and CNGB1b – in a 2:1:1 stoichiometry^{63,292,293}. Surprisingly, the N-terminal Ca²⁺/CaM-binding site on CNGA2 is functionally silent in heteromeric channels; instead, Ca²⁺/CaM exerts its inhibitory effect by binding to IQ-like motifs in the CNGA4 and CNGB1b subunits²⁹⁴.

More recently, several lipids have been shown to regulate the activity of CNG channels. Activation of rod channels is dramatically reduced by application of diacylglycerol derivatives^{295,296}, *all-trans*-retinal²⁹⁷, and PIP₂¹⁷⁹, and activation of olfactory CNG channels is inhibited by cholesterol depletion²⁹⁸. Zhainazarov and colleagues reported that PIP₃ inhibits heterologously-expressed CNGA2 homomeric

channels or CNGA2/CNGA4 heteromeric channels to nearly the same extent as native channels in OSN membranes¹⁸¹. Interestingly, inhibition by PIP₃ in many respects resembles that of Ca²⁺/CaM – in both cases the apparent affinity of the channel for cAMP is reduced by at least 10-fold with no change in the single channel conductance. While the mechanism of Ca²⁺/CaM inhibition has been well characterized, the molecular mechanisms underlying PIP₃ inhibition remain unknown. Furthermore, it is unclear how these two regulatory processes interact to modulate the odorant response.

Results

CNGA3 channels are insensitive to PIP₃. To investigate the effects of PIP₃ on CNG channel function, we expressed cloned channel subunits in HEK-293 cells, and exposed inside-out patches to varying concentrations of cyclic nucleotides. As shown in Fig. 15A & B, exposure of patches containing homomeric CNGA2 channels to 10 μM dipalmitoyl-PIP₃ produced, on average, a 17- and 13-fold shift in the apparent affinity for cGMP (N = 8) and cAMP (N = 12), respectively. In addition, dipalmitoyl-PIP₃ (referred to as PIP₃ in the rest of the manuscript) decreased the efficacy of saturating cAMP by approximately 70%, an effect typically ascribed to stabilization of closed channel states. The decrease in cyclic nucleotide sensitivity generally occurred within 20 seconds of exposure to 10 μM PIP₃; similar results were observed with concentrations of PIP₃ as low as 1 μM, but the time-course was generally slower (Fig. 15E). We were unable to reverse the effect of PIP₃, even with wash times of more than 60 minutes, which we attribute to the high affinity of PIP₃ for the hydrophobic membrane environment. Application of 50 μM dioctanoyl-PIP₃ (a more water soluble analog with shorter acyl substituents) caused only

a mild decrease in the apparent cAMP affinity (less than 2-fold), while 10 μ M dioctanoyl-PIP₃ and 10 μ M IP₄ had no effect (Figures 16A & B). In about half of the patches, PIP₃ reduced the saturating cGMP current by 20-30%. This effect developed gradually with prolonged exposure to PIP₃, suggesting that high concentrations of patch-resident PIP₃ were required (Figure 16C). We found no correlation between the size of the apparent affinity shift and the decrease in the maximum cGMP-activated current.

In contrast, application of 10 μ M PIP₃ had no effect on channels formed by CNGA3, the α subunit from cone photoreceptors (Fig. 15C & D). Neither the apparent affinity for cGMP nor the maximum current elicited by saturating cGMP concentrations was significantly altered by even prolonged exposure to 10 μ M PIP₃ (up to 4 min). Similarly, the apparent affinity and efficacy of cAMP, a weak partial agonist for CNGA3, were also unaffected.

Molecular determinants of PIP₃ regulation. To identify channel regions involved in PIP₃ regulation, we constructed chimeric channels by exchanging different regions of CNGA2 and CNGA3. These two subunits are approximately 60% identical and 75% homologous, with most of their differences lying in the cytoplasmic N- and C-termini. Exchanging the pore domain and C-terminus did not eliminate the PIP₃ sensitivity of the parent channel; CNGA2 containing the CNGA3 pore and cyclic nucleotide-binding (CNB) domain (chimera 2233) was still inhibited by PIP₃ (by approximately 5-fold), and CNGA3 channels containing the CNGA2 pore and CNB domain (chimera 3322) were unaffected by PIP₃ (Fig. 17A). We then assessed the PIP₃ sensitivity of chimeric channels containing only the cytoplasmic N-terminus of CNGA2, and found that transplantation of

this region onto CNGA3 was sufficient to confer PIP₃ inhibition. Exposure of patches containing these chimeric channels (A2nA3) to 10 μM PIP₃ caused a 5-fold decrease in their cGMP sensitivity, and a severe reduction in the current elicited by saturating cAMP. (Fig.17A & B).

Calmodulin inhibition of CNGA2 channels resembles PIP₃ inhibition, and also relies on residues within the N-terminus (residues 68-81). We therefore hypothesized that the two modulators share a common inhibitory mechanism or binding site. In support of this, we found that channels formed by CNGA2 subunits lacking residues 61-90 (Δ61-90-CNGA2) were virtually unaffected by application of 10 μM PIP₃ (Figure 18A). However, with prolonged PIP₃ exposure, these channels, like wild-type CNGA2 channels, often exhibited a reduction in the maximum cGMP-activated current, but no change in the maximum cAMP-activated current. Although difficult to explain based on current models of CNG channel activation, this effect was not investigated further.

Several mechanistic scenarios might explain the loss of PIP₃ sensitivity in the Δ61-90-CNGA2 channels. First, PIP₃ might interact directly with amino acids within this region. Alternatively, PIP₃ might bind to adjacent sites, and inhibit channels by disrupting the autostimulatory interaction between the N- and C-termini, which is already absent in the deletion mutant. To test for a direct interaction between PIP₃ and the N-terminus of CNGA2, we incubated a GST-tagged peptide containing the cytoplasmic N-terminus of CNGA2 (GST-A2N) with PIP₃-conjugated beads. The beads and bound protein were recovered by centrifugation and washed to reduce non-specific binding. As shown in Figure 18B, GST alone did not adhere to the PIP₃ beads, but the high affinity PIP₃-binding domain from Grp1 (GST-Grp1PH) was enriched by the PIP₃ beads. A fraction of

the GST-A2N peptide was also recovered with the PIP₃-conjugated beads. In contrast, a CNGA2 N-terminal peptide lacking residues 61-90 (GST-A2NΔ) did not adhere to the PIP₃-coated beads. This biochemical result suggests that PIP₃ directly binds to residues in the region between amino acids 61 and 90. Surprisingly, we found that the CNGA3 N-terminus also adhered to PIP₃-coated beads (Fig. 18B), even though PIP₃ does not alter CNGA3 channel activity. When the Ca²⁺-CaM binding site was removed from the CNGA3 N-terminal peptide (GST-A3NΔ), binding to PIP₃ beads was no longer observed. Interestingly, previous biochemical experiments have established that the N-terminus of CNGA3 binds Ca²⁺/CaM, but this binding is functionally silent²⁹⁹.

Native-type olfactory CNG channels, formed by CNGA2, CNGA4 and CNGB1b subunits, were also strongly inhibited by PIP₃. Heteromeric channels containing wild-type CNGA2 subunits exhibited a 5-fold average increase in their K_{1/2} for cGMP from 2.6 ± 0.6 μM to 15.7 ± 7.1 μM following brief exposures to 10 μM PIP₃ (5 patches, Fig. 18C). To test the functional relevance of the CNGA2 N-terminal PIP₃-binding site in the context of the heteromeric channel, we expressed the Δ61-90-CNGA2 subunits along with CNGA4 and CNGB1b. We found that exposure to 10 μM PIP₃ had no appreciable effect on the apparent cGMP affinity of these channels (K_{1/2} before PIP₃ = 14.7 ± 3.1 μM, K_{1/2} after = 19.9 ± 9.1 μM, 3 patches, Fig. 18D). Similar results were observed with cAMP for both wild type and mutant channels (Fig 18C & D). These observations demonstrate that residues 61-90 of CNGA2 are necessary for PIP₃ regulation of heteromeric olfactory CNG channels.

Interplay between PIP₃ and Ca²⁺/CaM regulation. Since our biochemical data imply that the PIP₃-binding site overlaps that of Ca²⁺/CaM on CNGA2, we predicted that PIP₃ might occlude the action of Ca²⁺/CaM on homomeric CNGA2 channels. As shown in Figure 19A, CNGA2 channels exhibited a reversible decrease in their apparent affinity for cGMP following exposure to 250 nM Ca²⁺/CaM ($K_{1/2}$ before Ca²⁺/CaM = 2.3 ± 1.2 μ M, after Ca²⁺/CaM = 19.2 ± 5.3 μ M, after EDTA wash = 1.6 ± 0.4 μ M, 4 patches). Subsequently, a brief exposure to 10 μ M PIP₃ inhibited channel activation to an equal, or greater, extent ($K_{1/2}$ = 29.9 ± 11.4 μ M, 4 patches). Thereafter, a second exposure to Ca²⁺/CaM produced no further decrease in apparent affinity ($K_{1/2}$ = 29.6 ± 14.7 μ M, 4 patches). This finding suggests that PIP₃ and Ca²⁺/CaM exert their effects through a common mechanism or that PIP₃ inhibits Ca²⁺/CaM binding. To test the latter hypothesis, we measured Ca²⁺/CaM binding to the CNGA2 N-terminus using a calmodulin overlay assay (Fig. 19D). We found that the presence of 100 μ M PIP₃ reduced the binding of FLAG-tagged Ca²⁺/CaM to a GST-tagged CNGA2 N-terminal peptide by almost 70 % under our assay conditions (67.3 ± 0.06 %; N = 6). Thus, PIP₃ appears to mimic and occlude Ca²⁺/CaM inhibition of homomeric CNGA2 channels, in part by interfering with Ca²⁺/CaM binding to the CNGA2 N-terminus.

In heteromeric olfactory channels, the CNGA2 N-terminal CaM-binding site is functionally silent; instead, Ca²⁺/CaM exerts its inhibitory effects by binding to IQ-like motifs in the CNGA4 and CNGB1b subunits. Therefore, we expected that PIP₃ and Ca²⁺/CaM inhibition would be additive. Surprisingly, we found that wild-type heteromeric channels were unaffected by application of Ca²⁺/CaM following exposure to 10 μ M PIP₃ (Fig. 19B). Exposure of heteromeric channels containing $\Delta 61-90$ -CNGA2 to

10 μM PIP_3 also occluded inhibition by $\text{Ca}^{2+}/\text{CaM}$ (Fig. 19C), even though PIP_3 had no direct effect on the apparent affinity of the channels. Using calmodulin overlay assays (Fig. 19D), we found that the presence of 100 μM PIP_3 inhibited the binding of FLAG-tagged calmodulin to peptides containing the IQ motifs from CNGA4 ($86.1 \pm 0.06 \%$; $N = 9$) and CNGB1b ($87.4 \pm .08 \%$; $N = 7$).

Discussion

We have shown that PIP_3 dramatically shifts the cyclic nucleotide sensitivity of olfactory CNG channels by direct interaction with residues in the N-terminus of CNGA2. This interaction mimics and occludes $\text{Ca}^{2+}/\text{CaM}$ regulation in homomeric CNGA2 channels. In heteromeric channels containing CNGA2, CNGA4, and CNGB1b, PIP_3 and $\text{Ca}^{2+}/\text{CaM}$ produce distinct functional changes by binding to different subunits, yet PIP_3 still blocks $\text{Ca}^{2+}/\text{CaM}$ regulation. To the best of our knowledge this is the first example of a PIP_3 -protein interaction that prevents $\text{Ca}^{2+}/\text{CaM}$ regulation. Our findings reaffirm the regulatory significance of the CNGA2 N-terminus in the heteromeric channel, and indicate that each subunit in native olfactory CNG channels has a distinct and important role in channel regulation and trafficking³⁰⁰⁻³⁰².

Based on our observations, a possible mechanism for PIP_3 inhibition of olfactory CNG channels can be inferred. In homomeric CNGA2 channels, removal of residues 61-90, exposure to $\text{Ca}^{2+}/\text{CaM}$, and exposure to PIP_3 produce nearly identical shifts in cyclic nucleotide sensitivity and in the maximum cAMP-activated current. The removal of residues 61-90 and regulation by $\text{Ca}^{2+}/\text{CaM}$ are both known to disrupt an autostimulatory interaction between the N- and C-termini of adjacent CNGA2 subunits^{289,291}. Since PIP_3

inhibition requires residues 61-90 and prevents $\text{Ca}^{2+}/\text{CaM}$ regulation, we postulate that PIP_3 binding may anchor the N-terminus of CNGA2 to the membrane surface, thereby disrupting the intersubunit autostimulatory interaction. This molecular mechanism resembles that recently proposed for prevention of K^+ channel N-type inactivation by phosphoinositides: sequestering of the N-terminal domain at the cytoplasmic face of the membrane¹⁹⁴. Although the N-terminus of CNGA3 can bind both PIP_3 and $\text{Ca}^{2+}/\text{CaM}$, these interactions appear to be functionally silent, most likely reflecting the absence of a pronounced autostimulatory interaction with the C-terminus²⁹⁹. Our data also suggest a possible mechanism for PIP_3 inhibition of heteromeric olfactory channels. As we and others have observed, PIP_3 inhibition of heteromeric channels causes a 10-fold shift in cyclic nucleotide sensitivity and a 2-fold reduction in the efficacy of cAMP¹⁸¹. In contrast, $\text{Ca}^{2+}/\text{CaM}$ produces a larger shift in cyclic nucleotide sensitivity without decreasing the efficacy of cAMP²⁸⁷. Taken together, the results suggest that autostimulatory interactions between CNGA2 subunits still occur in heteromeric channels, and that PIP_3 , but not $\text{Ca}^{2+}/\text{CaM}$, may act by disrupting these interactions. The mechanism of $\text{Ca}^{2+}/\text{CaM}$ inhibition of heteromeric channels remains unclear, although interactions with CNGA4 and CNGB1b are required (21).

Phosphatidylinositides are known to regulate the activity of an ever increasing number of ion channels. Binding of PIP_2 to both $\text{K}_{\text{ir}}1$ and $\text{K}_{\text{ir}}6$ channels promotes channel activation by stabilizing the open state^{182,186,303}, and PIP_3 has been proposed to activate both epithelial sodium channels and TRPC6 channels by direct binding^{195,304}. Like PIP_2 -binding regions identified in other ion channels^{187,188,190}, the stretch of amino acids between residues 61-90 of CNGA2 contains multiple basic residues that may be

important for the interaction with negatively charged phospholipids. Similar to PIP₂ inhibition of TRPV1 channels¹⁹², PIP₃ inhibited activation of olfactory CNG channels. PIP₂ and Ca²⁺/CaM have been shown to bind competitively and have antagonistic effects on the activity of many proteins, like RGS4 and MARCKS^{172,173}. In contrast, PIP₃ partially mimics and occludes Ca²⁺/CaM regulation of olfactory CNG channels. Our data suggest that for both homomeric and heteromeric olfactory CNG channels, PIP₃ interferes with Ca²⁺/CaM binding to several channel subunits. Additionally, in homomeric channels, binding of PIP₃ may induce a separation of the N- and C-termini, thereby preventing Ca²⁺/CaM from having any further effect on channel function.

Olfactory sensory adaptation is mediated by Ca²⁺/CaM-dependent channel inhibition, and depends upon activation of the odorant signaling pathway and the subsequent influx of Ca²⁺ through open CNG channels²⁸⁶. In contrast, inhibition of olfactory signaling by PIP₃ does not require prior channel activity, and channel regulation by PIP₃ may serve to reduce overall olfactory sensitivity in the presence of complex odorant mixtures. One possible route for PIP₃ synthesis is suggested by the recent discovery of purinergic receptors in OSN membranes³⁰⁵. These G-protein coupled receptors are activated by ATP and have been reported to stimulate PIP₃ synthesis in astrocytes and C6 glioma cells^{306,307}. In the olfactory epithelium, noxious stimuli or prolonged exposure to odorants may lead to release of cellular ATP, causing activation of purinergic receptors and consequent production of PIP₃. We speculate, therefore, that the stimulation of PIP₃ synthesis by purinergic receptor activation may serve a neuroprotective role by preventing possibly toxic levels of calcium influx through CNG channels following excessive or noxious stimulation.

Acknowledgements We would like to acknowledge Dr. Martin Biel for providing the DNA encoding CNGA3, CNGA4, and CNGB1b, and Dr. William Zagotta for the DNA encoding CNGA2 & the GST-fusion peptides. This work was supported by the following NIH grants: Ruth Kirchstein National Predoctoral Research Service Award NS052103 to J.D.B.; EY009275 to J.W.K.; EY12836 to M.D.V.; EY12837 to R.L.B.

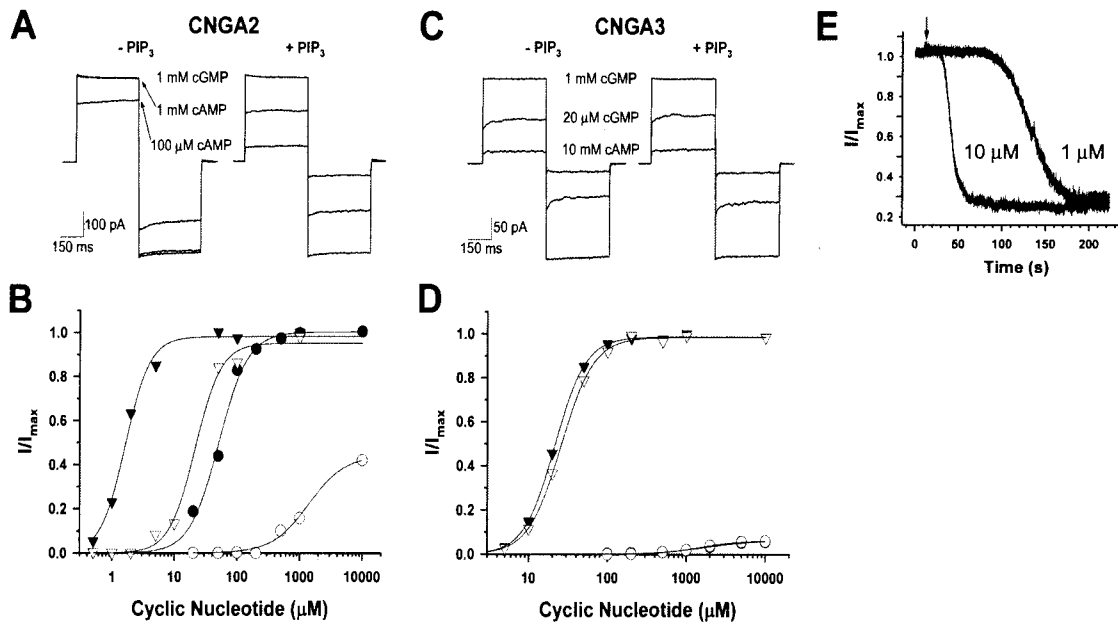


Figure 15: PIP₃ inhibits CNGA2 channels, but not CNGA3 channels. Representative traces from CNGA2 (A) and CNGA3 (C) before and after application of 10 μM PIP₃. Currents were elicited by voltage steps to +50 and -50 mV in the presence of the indicated concentration of cyclic nucleotides. Data are representative of 12 patches for CNGA2 and 6 patches for CNGA3. Representative CNGA2 (B) and CNGA3 (D) cyclic nucleotide dose-response relations, before (dark symbols) and after (open symbols) application of 10 μM PIP₃. Hill parameters ($K_{1/2}$, n) for CNGA2: (▼) cGMP = 1.6 μM, 2.2 before PIP₃, and (▽) 21.5 μM, 2.1 after PIP₃; (●) cAMP = 51.2 μM, 1.9 before PIP₃, and (○) 1.4 mM, 1.5 after PIP₃; for CNGA3 (▼) cGMP = 21.6 μM, 2.2 before PIP₃, and (▽) 25.8 μM, 2.1 after PIP₃; (●) cAMP = 1.8 mM, 1.3 before PIP₃, and (○) 1.5 mM, 1.7 after PIP₃. The open circles in panel D overlap and hide the filled circles. Data are representative of 3 separate experiments each for CNGA2 and CNGA3. (E) Two different patches containing CNGA2 channels activated by 1 mM cAMP and held at -50

mV were exposed to 10 μM or 1 μM PIP_3 at 15 s (denoted by arrow). Data were normalized to the current level before PIP_3 exposure.

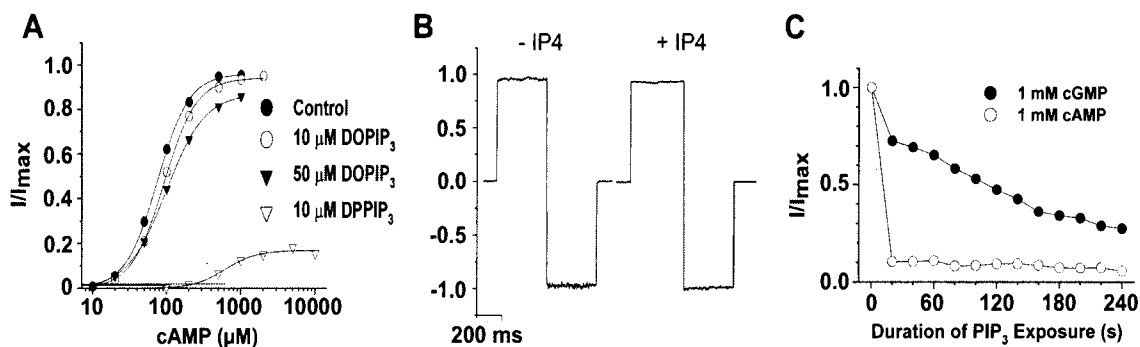


Figure 16: Effects of PIP3 Analogs on CNGA2 Channels (A) An inside-out patch from a CNGA2-expressing HEK293 cell was exposed to the indicated substances and concentrations for 1-5 minutes. Data are representative of 2 separate experiments. DOPIP = dioctanoyl-PIP, DPPPIP = dipalmitoyl-PIP. (B) An inside-out patch from a CNGA2-expressing HEK293 cell was exposed to 200 μ M cAMP in the presence or absence of 50 μ M inositol-1,3,4,5-phosphate (IP4). The currents were normalized to the current activated by 1 mM cGMP. Data are representative of 2 separate experiments. (C) An inside-out patch from a CNGA2-expressing HEK293 cell was continuously exposed to 10 μ M PIP3. Every 30 seconds, channels were activated by 1 mM cGMP or 1 mM cAMP and currents recorded at +50 mV. All currents were normalized to the current activated by 1 mM cGMP at time 0.

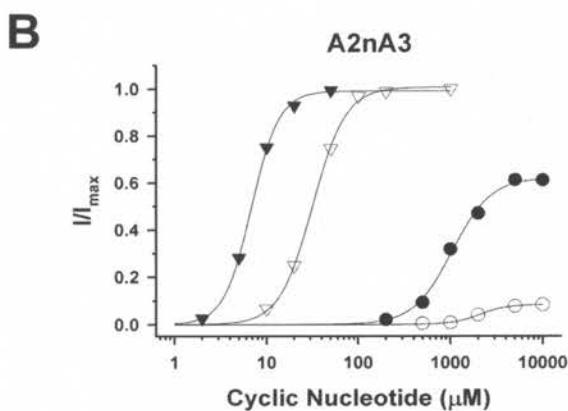
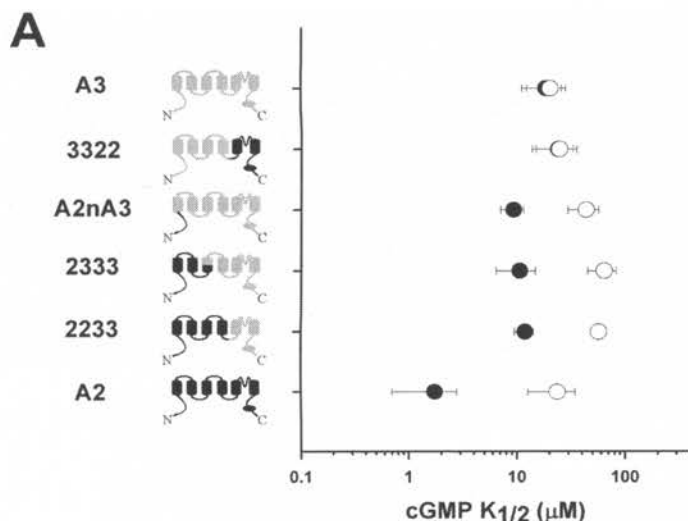


Figure 17: The N-terminus of CNGA2 confers PIP₃ sensitivity to CNGA3 channels.

(A) Diagrams depicting CNGA2/CNGA3 chimeric subunits are shown on the left (see methods for splice site locations). Portions of the channel sequence derived from CNGA2 are shown in black; portions derived from CNGA3 are shown in gray. Plotted adjacent is the mean $K_{1/2}$ for cGMP before (●) and after 10 μM PIP₃ (○). $K_{1/2}$ values \pm SD are: **A3**, $18.6 \pm 7 \mu\text{M}$ before PIP₃ and $20.5 \pm 8 \mu\text{M}$ after PIP₃, 3 patches; **3322**, $24.0 \pm 9 \mu\text{M}$ before PIP₃ and $24.6 \pm 11 \mu\text{M}$ after PIP₃, 3 patches; **A2nA3** $9.3 \pm 2.3 \mu\text{M}$ before and $43.5 \pm 13.8 \mu\text{M}$ after, 5 patches; **2333** $10.6 \pm 4 \mu\text{M}$ before and $64 \pm 19 \mu\text{M}$ after, 4 patches; **2233** $12.0 \pm 2.4 \mu\text{M}$ before and $57.3 \pm 7 \mu\text{M}$ after, 3 patches; **CNGA2** $1.8 \pm 1 \mu\text{M}$ before

and $23.9 \pm 11 \mu\text{M}$ after, 9 patches. (B) Representative cyclic nucleotide dose-response relations, before (dark symbols) and after (open symbols) application of $10 \mu\text{M PIP}_3$, for channels containing A2nA3 subunits. Hill equation parameters ($K_{1/2}$, n): (\blacktriangledown) cGMP = $11.6 \mu\text{M}$, 2.5 before PIP_3 and (∇) $51.1 \mu\text{M}$, 1.9 after PIP_3 ; (\bullet) cAMP = $1.1 \mu\text{M}$, 2.9 before PIP_3 and (\circ) $K_{1/2} = \text{ND}$, ND after PIP_3 . Data are representative of 4 different patches.

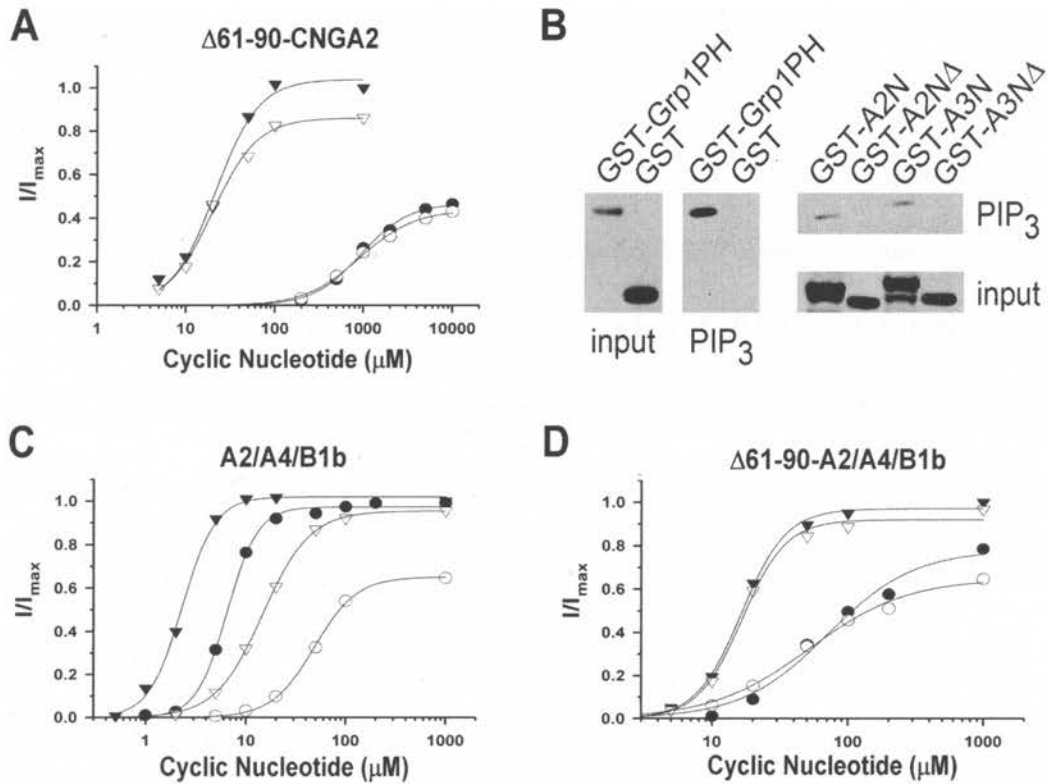


Figure 18: PIP₃ inhibits olfactory CNG channels through a direct interaction with the N-terminus of CNGA2. (A) Shown are representative cyclic nucleotide dose-response relations for $\Delta 61-90$ -CNGA2, measured before (dark symbols) and after (open symbols) treatment with 10 μM PIP₃. Hill equation parameters ($K_{1/2}$, n): (\blacktriangledown) cGMP 22.6 μM , 2.8 before PIP₃ and (\triangledown) 26.9 μM , 2.2 after PIP₃; (\bullet) cAMP = 1.2 mM, 1.4 before PIP₃ and (\circ) 917 μM , 1.6 after PIP₃. Data are representative of 3 different experiments. (B) Amino terminal regions of CNGA2 and CNGA3 were expressed as GST-fusion proteins, and tested for PIP₃ binding *in vitro* using PIP₃-agarose beads. Input proteins (far left and lower panels) and bound proteins (middle and upper panels) were identified by immunoblotting with anti-GST antibodies. GST-Grp1PH, positive control pleckstrin homology domain (Echelon); GST-A2N, amino terminal cytoplasmic domain (amino

acids 1-138) of rat CNGA2 (AF126808); GST-A2N□, amino acids 61-90 deleted; GST-A3N, amino terminal cytoplasmic domain (amino acids 1-164) of human CNGA3 (AF065314); GST-A3N□, amino acids 51-108 deleted. Data are representative of four different experiments. (C) Representative cyclic GMP dose-response relations before (dark symbols) and after (open symbols) application of 10 μM PIP₃ to a patch containing wtCNGA2/A4/B1b channels. Hill equation parameters ($K_{1/2}$, n): (▼) cGMP 2.3 μM , 2.6 before PIP₃ and (▽) 14.6 μM , 1.8 after PIP₃; (●) cAMP = 6.4 μM , 2.8 before PIP₃ and (○) 48.4 μM , after PIP₃. (D) Representative cyclic GMP dose-response relations before and after application of 10 μM PIP₃ to a patch containing Δ 61-90-CNGA2/A4/B1b channels. Hill equation parameters ($K_{1/2}$, n): (▼) cGMP = 16.3 μM , 2.6 before PIP₃ and (▽) 16.5 μM , 2.7 after PIP₃; (●) cAMP = 70.4 μM , 1.4 before PIP₃ and (○) 51.4 μM , 1.2 after PIP₃. Data are representative of 5 patches for wt channels, and 3 patches for deletion mutants.

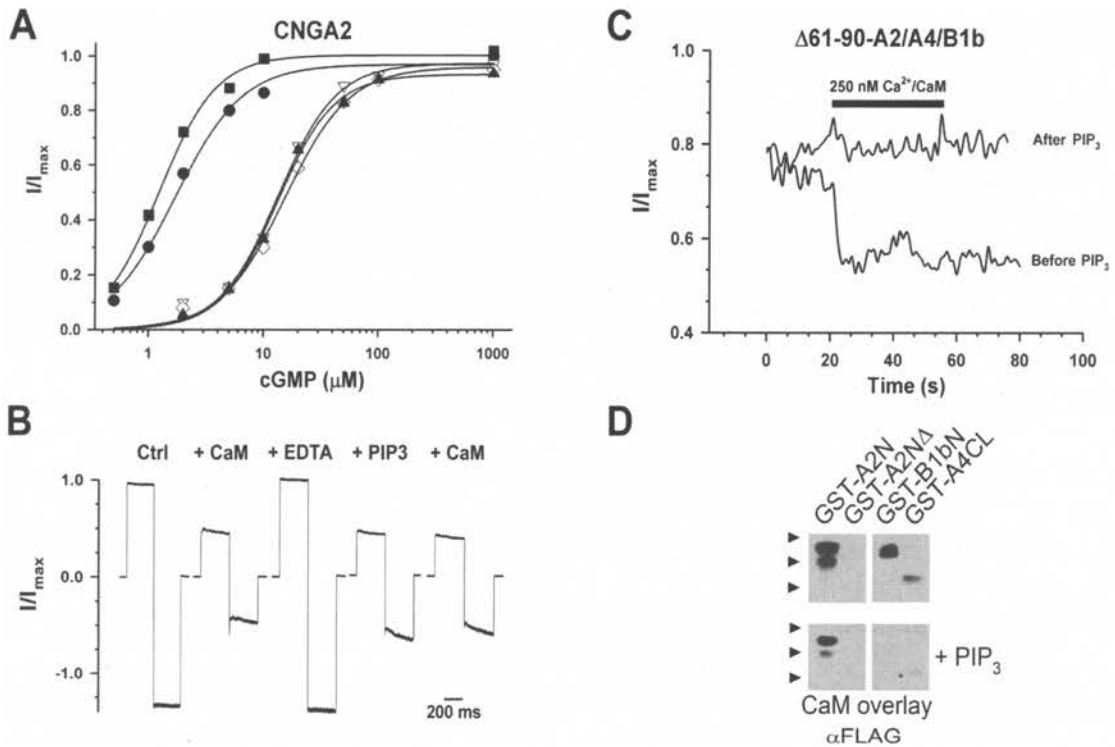


Figure 19: PIP3 prevents calmodulin regulation of olfactory CNG channels. (A) CNGA2 cGMP dose-response relations were measured before (●) and after (▽) application of 250 nM $\text{Ca}^{2+}/\text{CaM}$. The patch was then washed with 0.5 mM EDTA (■) to remove the CaM. 10 μM PIP₃ (◇) caused a right shift that occluded a response to subsequent application of CaM (▲). $K_{1/2}$ values: before CaM, 1.7 μM ; after CaM, 13.3 μM ; EDTA wash, 1.2 μM ; after PIP₃, 15.3 μM ; PIP₃ + CaM, 13.2 μM . Data are representative of 4 separate experiments. (B) Representative traces from an inside-out patch containing wtCNGA2/A4/B1b channels stepped to +50 mV and -50 mV, and exposed to solutions containing either 500 nM $\text{Ca}^{2+}/\text{CaM}$ or 10 μM PIP₃. Data are representative of 3 separate experiments. (C) Representative trace from an inside-out patch containing $\Delta 61-90$ -CNGA2/A4/B1b channels, before and after exposure to 10 μM PIP₃. The current activated by 50 μM cGMP was measured at +50 mV every second, and

normalized to the current activated by 1 mM cGMP. 250 nM Ca^{2+} /CaM was added at 20 s. Data are representative of 3 separate experiments. (D) After blotting, GST-fusion proteins were probed in an overlay assay using ~ 50 nM FLAG-tagged CaM in 10 μM buffered calcium, either in the presence (below) or absence (above) of 100 μM PIP_3 . GST-A2N and GST-A2N Δ as in Figure 18B; GST-B1bN, proximal amino-terminal region (amino acids 677-764) of bovine CNGB1; GST-A4CL, C-linker region (amino acids 271-339) of rat CNGA4. Bound CaM-FLAG was detected using M2 anti-FLAG antibody. Arrow heads indicate approximate location of molecular weight markers: 49, 38 and 28 kD. Corresponding blots above and below each other represent identical exposure times. Data are representative of six different experiments.

Chapter 3: Summary and Discussion

In my first manuscript, I provided evidence suggesting that homomeric CNGA2 and heteromeric olfactory CNG channels associate with biochemically-isolated cholesterol-rich lipid raft membrane microdomains. This association did not involve interactions with caveolin, a cholesterol-binding protein implicated in raft formation. Treatment of cells with the cholesterol-depleting agent, MBCD, decreased cAMP production following PGE1-stimulation and reduced the cyclic nucleotide sensitivity of CNGA2 channels.

The decreased sensitivity of CNGA2 channels following MBCD treatment, however, was not related to lipid raft disruption or cholesterol removal. CNGA3 channels, which did not associate with biochemically-isolated cholesterol-rich lipid rafts, exhibited a shift in cGMP sensitivity following MBCD treatment similar to that observed for CNGA2 channels. Also, different MBCD treatment conditions, all of which removed identical amounts of cholesterol, had varying effects on CNGA2 channel function.

In a separate line of investigation, I defined a region within the N-terminus of CNGA2 subunits that is required for PIP₃ inhibition of homomeric CNGA2 channels and heteromeric CNGA2/A4/B1b channels. I also found that PIP₃ occludes calmodulin inhibition of homomeric and heteromeric channels. Biochemical experiments revealed that this effect involves the ability of PIP₃ to block the binding of calmodulin to several channel subunits.

3.1 Relationship between CNG channels and lipid rafts.

In biochemical studies, a significant percentage of CNGA2 channels fractionate with detergent-insoluble membranes rich in cholesterol, or lipid rafts. Approximately half of the channels, however, are found in detergent-soluble, cholesterol-poor membrane fractions. This behavior is very different from that observed for the strongly raft-associated proteins caveolin and flotillin (Figure 5B). The reasons for the existence of two different channel populations remain unclear, and I cannot at this time firmly conclude that functional CNGA2 channels at the plasma membrane reside in lipid rafts.

One possible explanation for the existence of two distinct fractions of CNGA2 channels is that both raft-resident and non-resident channel populations exist in the plasma membrane. The basis for separate channel populations with different affinities for lipid rafts may involve interactions with other proteins, or covalent modifications such as phosphorylation. If any proteins directly interact with CNGA2 channels, they have not yet been discovered. Coimmunoprecipitation experiments and yeast two-hybrid screens may be helpful in this regard. In particular, interactions with cytoskeletal proteins may be important. With respect to covalent modification, CNGA2 subunits can be phosphorylated at a serine residue in their amino terminus. This increases the apparent affinity for cAMP by approximately 5-fold. Although I found no evidence for the existence of phosphorylated channels in my patch experiments, a small number of such channels might be unnoticeable in macroscopic current recordings. To more specifically investigate the role of CNGA2 channel phosphorylation on lipid raft affinity,

phosphorylation could be induced prior to detergent lysis by briefly pretreating cells with phorbol esters to activate PKC¹⁴⁵.

An alternative explanation for the existence of two channel populations with different detergent-resistance profiles is that one fraction represents channels within intracellular membranes, while the other fraction represents channels in the plasma membrane. My immunofluorescent imaging experiments, similar to those shown in Figure 6, reveal that in many CNGA2-expressing HEK-293 cells large amounts of the subunit remain within intracellular compartments and do not reach the plasma membrane. Since the plasmids used in our studies do not contain all of the genetic regulatory elements that normally limit protein expression, the amount of subunit produced may overwhelm the processing capability of HEK-293 cells. The intracellular fraction likely represents subunits trapped within the endoplasmic reticulum, the golgi complex, post-golgi transport vesicles, or endocytosed regions of the plasma membrane. Endoplasmic reticulum membranes contain very low levels of cholesterol and are therefore detergent-soluble^{213,258,308-310}. However, golgi and post-golgi vesicle membranes can exhibit detergent resistance^{258,308}. Therefore, it is difficult to determine from my data whether the detergent-resistant fraction of CNGA2 represents subunits within intracellular compartments or at the plasma membrane. In a preliminary experiment with heterologously expressed CNGA4 (not shown), a significant fraction of the subunit was detected in detergent-resistant membranes, although only a miniscule percentage of these subunits actually reaches the plasma membrane in the absence of CNGA2. This suggests that intracellularly trapped CNG channel subunits can be both detergent-soluble and insoluble. Also, in my experience, CNGA3-expressing cells produce larger patch

currents, and unpublished observations of CNGA3-expressing cells shows that these subunits exhibit very little accumulation in the cytosol relative to CNGA2. Thus, while CNGA3 channels more effectively reach the plasma membrane, these channels are not found in detergent-resistant membranes.

Further experiments are necessary to determine whether CNGA2 channels at the plasma membrane are entirely contained within lipid rafts, partially contained, or not associated at all. Imaging experiments provide little information, since to date no reliable visual assay of lipid rafts in living cells has been developed, largely owing to the small predicted size of these domains in living cells²¹⁷. It may be possible to determine whether the detergent-resistant fraction is associated with the plasma membrane using cell surface biotinylation experiments. This could be achieved by introducing a FLAG epitope tag, which contains multiple lysines, into one of the extracellularly-exposed loops of the subunit. With such a construct, covalent biotinylation of extracellularly exposed lysine residues before cell lysis would allow subsequent identification of the plasma membrane channel population on western blots of sucrose gradient fractions.

The fact that CNGA3 subunits reside almost entirely within detergent-soluble membranes may also provide a useful tool for analyzing the lipid raft affinity of CNGA2 subunits (Figure 11). The chimeric subunits used for defining the PIP₃-binding domain of CNGA2 could also be used in lipid raft assays to define channel regions important for detergent-resistance. This approach could also be combined with a method for analyzing surface expression to create a very powerful assay for the molecular determinants of raft association. To date, beyond post-translational modifications, such as GPI-attachment

and palmitoylation, little is known about the sequence elements responsible for targeting proteins to lipid rafts^{241,242}.

Our data shows that only a small percentage of native CNGA2 associates with detergent-resistant membranes (Figure 6C). While this assay is generally not considered to provide quantitative information, the results do make it difficult to conclude that native olfactory CNG channels in the cilia preferentially reside in lipid raft microdomains. One possible problem with the experiment involves the use of membranes from whole olfactory epithelium, which contain the cilia and cell bodies of OSNs and supporting cells. Methods have been developed for isolating a relatively pure preparation of OSN cilia, and use of this technique may provide a better source of membranes for the detergent-resistance assay. Still, CNGA2 in the olfactory epithelium is overwhelmingly expressed in the OSN cilia, thus even our preparation should be suitable for lipid raft analysis. A more likely explanation is that the presence of CNGA4 or CNGB1b subunits, or other proteins that interact with the channels, reduces lipid raft association. This possibility could be initially addressed by heterologous expression of heteromeric channels in mammalian cells, as long as methods are developed to identify the plasma membrane population.

Another approach for assessing the lipid raft affinity of olfactory CNG channels involves the use of artificial lipid bilayers, where large raft domains can be created through the precise control of lipid composition, and the domains can be visualized with fluorescent dyes that either fluoresce or quench when in a liquid-ordered environment²¹⁷. Artificial membranes can also be solubilized with Triton X-100, and raft membranes with their associated proteins can be isolated on sucrose gradients. These techniques have been

used previously to study the affinity of reconstituted proteins for lipid rafts^{206-208,258,311}. To date, only native heteromeric rod channels have been successfully purified and reconstituted into liposomes, but similar techniques may be useful for purifying CNGA2 from cultured mammalian cells or native channels from olfactory cilia preparations^{49,64,312}. The use of epitope-tagged subunits may facilitate purification from cultured cells. Although the appropriate purification and reconstitution conditions may be difficult to develop, this technique will allow a more controlled environment for determining whether olfactory CNG channels have a preference for cholesterol-rich membranes.

3.2 MBCD inhibition of CNGA2 channels

Pretreatment of cells expressing CNGA2 channels with 15 mM MBCD at 37°C for 5-15 minutes decreased the apparent affinity of the channels for cAMP by approximately 3-fold, and decreased the average cAMP efficacy by about 20% (Figure 10). The decrease in cAMP efficacy is highly indicative of an effect on channel gating, that is, the transition from an open state to a closed state. Previous modeling of similar effects caused by point mutations and sulfhydryl-reactive agents have found that a change in the free energy of the gating transition can entirely account for shifts in apparent affinity when accompanied by a decrease in cAMP efficacy^{113,123}. However, a change in cyclic nucleotide binding affinity can never be completely ruled out unless direct assays are employed. No such work has been performed for CNG channels, and such experiments would be difficult since multiple regions of the channel subunits may influence ligand binding. One possibility for indirectly determining whether MBCD

affects ligand binding or gating, is to record from patches containing single channels in the presence of super-saturating amounts of ligand. Under these conditions, all binding sites should be occupied at nearly all times, and any change in open probability without a change in the single channel conductance would reflect alterations of the gating mechanism. If MBCD affected only ligand binding, a decrease in the single channel conductance would be required to explain the reduced cAMP efficacy.

Why MBCD changes the apparent affinity of CNGA2 channels remains an unanswered question, but multiple scenarios can be envisioned. First, while MBCD is too large to fit into or pass through the channel pore, it might directly interact with extracellular channel regions. However, MBCD does not adhere to cell membranes; therefore the compound appears to have little or no affinity for membrane lipids and proteins²²¹. Also, following incubation of the cells with MBCD, they were diluted approximately 100- to 1000-fold into MBCD-free bath solution. Any MBCD attached to the channels would be expected to almost completely dissociate over time. Yet patches pulled from cells immediately after placement in the recording chamber showed similar shifts in affinity to those pulled up to two hours after dilution. Only an extremely strong association between MBCD and the channels could explain such findings, which is highly unlikely based on the literature.

A second possibility for the effect of MBCD treatment on CNGA2 channel function may be that MBCD removes a membrane lipid that directly interacts with the channels. The most likely candidate for this lipid is cholesterol, since MBCD shows a strong selectivity for cholesterol over other membrane lipids^{220,221}. But the effect of MBCD on channel affinity did not reflect a simple correlation with the amount of

cholesterol removed (Figures 13 & 14). This could be explained if the channel affinity for cholesterol was high, such that lower MBCD concentrations and lower extraction temperatures did not provide enough energy to break the interaction. Alternatively, MBCD at high concentrations and high temperatures may be removing another lipid that directly interacts with CNGA2 channels.

It may be possible to test whether cholesterol is specifically required for CNGA2 channel function by using other agents that remove cellular cholesterol, though these other compounds have severe disadvantages. The enzyme cholesterol oxidase is probably the best choice because it is membrane impermeant and highly specific, but its action is much slower than MBCD, and it does not actually remove cholesterol from the membrane but simply cleaves off a functional group. Filipin is a pore forming antibiotic that interacts with membrane cholesterol, but can also promote the removal of cholesterol from intracellular membranes, and it is not highly specific. Instead of removing cholesterol, alpha-cyclodextrins remove phospholipids to a similar extent as that seen with higher concentrations of MBCD, thus this compound could be used to control for non-cholesterol mediated effects of MBCD²²⁰.

I attempted to address the issue of cholesterol specificity by first treating cells with MBCD, then replacing only cellular cholesterol by incubating with MBCD/cholesterol complexes. While I was successful at replacing up to 95% of the cellular cholesterol using this method, I was unable to isolate stable patches for channel recordings. The extraction/replacement technique appeared to dramatically reduce cell viability, but with further refinement the technique may prove useful.

Instead of disrupting a direct interaction between CNGA2 channels and membrane lipids, MBCD might induce a change in membrane structure, such as disrupting lipid raft organization. However, several lines of evidence suggest that lipid raft microdomains are not involved in the effect of MBCD treatment on CNGA2 channels. First, CNGA3 and CNGA2 were both similarly affected by MBCD treatment, even though CNGA3 does not associate with detergent resistant membranes. Second, different MBCD treatment conditions produced varying degrees of channel inhibition, or no inhibition at all, despite the fact that all of the conditions removed identical amounts of cholesterol. Initially, I suspected that the lack of an effect of room temperature MBCD treatment on channel function was the result of lipid rafts remaining intact under these conditions. Many other laboratories, using numerous cholesterol extraction tools, have observed that two distinct kinetic pools of cholesterol exist within membranes^{221,222,276-278}. One pool is readily extractable with relatively linear temperature dependence. Extraction of the second pool, though, occurs more gradually, and exhibits non-linear temperature dependence, becoming nearly unextractable at lower temperatures. These two pools have been observed in both native and artificial membranes. With artificial membranes, where the concentrations of other lipids can be more precisely controlled, data show that the existence of a second cholesterol pool often depends on the presence of lipids that support liquid-ordered domain formation, such as sphingolipids. In these systems, cholesterol extraction at lower temperatures leaves the liquid-ordered domains largely intact. Therefore, if the effects I observed were due to differences in lipid raft integrity, treatment with a lower concentration of MBCD at 37°C would still be expected to dramatically alter CNG channel function. This was not what I observed, however.

While 15 mM MBCD treatment at 37°C produced, on average, a 3- to 4-fold decrease in the current activated by a subsaturating concentration of cAMP (Figure 10), 5 mM MBCD treatment at 37°C produced no change (Figure 13), despite the fact that both conditions removed the same amount of cholesterol (Figure 14). Since the temperature of extraction in both cases should allow cholesterol removal from lipid rafts, these findings seem to support the conclusion that MBCD treatment does not alter CNGA2 channel activity by disrupting lipid rafts.

It may be possible to further investigate the contribution of lipid rafts to CNGA2 function through the use of cholesterol analogues which differ in their ability to form liquid-ordered membrane environments. This would require an initial treatment with MBCD followed by incubation with MBCD/cholesterol analogue complexes, a strategy which has been successful in the past^{248,249}. Though my replacement strategy did not allow for stable patch recordings, further refinement guided by the literature should be possible, or the use of different cell lines may be necessary. It may also be instructive to employ the membrane soluble dye, Laurdan. This dye reportedly changes emission properties in response to changes of membrane fluidity, which may be useful for understanding the effects of different MBCD treatment conditions on HEK-293 membrane organization³¹³.

Instead of specifically altering lipid raft integrity, high concentrations of MBCD at high temperatures may induce changes in general membrane structure that would be predicted to affect the function of a variety of membrane proteins. The finding that both CNGA2 and CNGA3 are similarly affected by 15 mM MBCD treatment at 37°C supports this idea. Changes in general membrane structure are also thought to underlie the effect

of DAG on CNGA2 channel function¹⁷⁷. Furthermore, studies shows that some lipid soluble odorants are capable of mildly inhibiting olfactory channels at relatively high concentrations, and the authors of these reports provide some evidence that their results are due to alterations of membrane structure^{314,315}.

Finally, MBCD may alter CNGA2 channel function by inducing changes in second messenger molecules that can act on the channels. To date, the only channel modulators identified that produce effects similar to those observed following MBCD treatment are $\text{Ca}^{2+}/\text{CaM}$ and PIP_3 . Changes in $\text{Ca}^{2+}/\text{CaM}$ levels are likely not involved, since my calcium-free recording conditions should remove such effects. MBCD has been shown, however, to cause ligand-independent activation of growth factor receptors and increased PIP_3 synthesis, which would inhibit CNGA2 channels^{225,316}. My work with PIP_3 regulation was initiated, in part, to investigate this possibility, though my work does not clearly answer the question. If MBCD treatment led to inhibition of CNG channels through increased PIP_3 production, in theory, treatment of isolated patches with anti- PIP_3 antibodies should reverse the MBCD effect. My attempts to reverse PIP_3 inhibition in patches with antibodies were unsuccessful, thus this line of experiments is not currently possible. An alternative approach would be to block PI3K, which is largely responsible for stimulus-induced PIP_3 synthesis. However, a negative result with this experiment would not confirm that PIP_3 is not involved, since changes in phosphatase activity could also underlie a MBCD-induced increase in PIP_3 levels. Currently, there are no good tools for altering phosphatase activity in living cells during MBCD treatment. Perhaps further defining the molecular determinants of PIP_3 inhibition will allow the use of PIP_3 -insensitive channels that may then show no response to MBCD treatment.

3.3 Lipid rafts as organizers of cAMP signaling compartments

Prior studies have found that when CNGA2 channels are used as sensors of membrane-localized, stimulus-induced changes in cAMP levels, the channels are present within diffusion restricted signaling compartments. The nature of these compartments is unknown, but our data showing that MBCD dramatically reduces the influx of calcium through CNGA2 channels following PGE1 stimulation suggest that membrane lipid organization may play a role in establishing or maintaining the signaling compartments. Still, while our data imply that lipid rafts may be involved, they also raise many questions and indicate that much work needs to be done.

An overwhelmingly large number of studies propose that lipid rafts organize signaling events at the plasma membrane, and at least one study reports that caveolin and lipid rafts facilitate odorant-induced cAMP synthesis in olfactory cilia^{215,244}. But the true role of lipid rafts in membrane signaling remains a highly controversial topic for many reasons. As mentioned previously, lipid rafts cannot be directly observed, except in a few notable instances, for example in polarized lymphocytes²³⁰. Yet even in these cases, it cannot be established that a liquid-crystalline microenvironment is responsible for proper signaling. Currently, no reliable method for selectively disrupting lipid raft integrity without perturbing other membrane regions is available. The problems associated with the most common tool, cholesterol removal, have already been discussed. When cholesterol removal causes a functional change, the proteins underlying the activity under

investigation are often associated with biochemically-defined lipid rafts, yet this is only a correlation. My work with CNGA3 channels demonstrates that cholesterol removal can change the function of a protein that is not associated with lipid rafts. These concerns over the effects of cholesterol removal make it difficult to firmly conclude that MBCD treatment alters PGE1 signaling by disrupting lipid rafts.

My data shows that pretreating cells with MBCD reduced forskolin-stimulated cAMP production. The nature of this effect is unclear, and may involve effects on membrane structure or more direct effects on the structure and function of AC. Other investigators have found that multiple AC isoforms associate with lipid rafts and exhibit functional changes following MBCD treatment^{232,234-237,317,318}. Unfortunately, the mechanism underlying the MBCD effect in these studies has not been seriously examined, therefore any claim that MBCD alters AC activity by disrupting lipid rafts is still largely unproven. Replacement of membrane cholesterol with structural analogues and the introduction of cyclase isoforms into artificial membranes may help address this issue. A recent report has identified cytoplasmic regions of certain AC isoforms that are important for targeting the proteins to detergent-resistant membranes²³³. Mutant AC proteins lacking the raft targeting sequences were not tested for MBCD sensitivity, but further work in this direction should provide valuable information pertaining to the relationship between MBCD effects and lipid raft association. By introducing mutant AC proteins lacking the raft targeting domain into our system, we may be able to better understand the role of lipid rafts in cAMP compartmentation.

While we find that MBCD reduces PGE1-stimulated cAMP production, the limited literature available implies that prostanoid receptors do not associate with

biochemically-isolated lipid raft microdomains³¹⁸. It is important, therefore, that we identify which receptor is involved in PGE1 signaling in HEK-293 cells, and determine whether these receptors associate with lipid rafts. I attempted to identify the type of receptor using commercially available antibodies, but produced inconclusive results since the level of receptor expression appears to be extremely low. A better approach would be to clone prostanoid receptor subtypes from a HEK-293 cell cDNA library. Once identified, each receptor could be tested for MBCD sensitivity following heterologous expression. To control for problems with overexpression, stable cells lines could be generated with different expression levels.

One final consideration is the influence of the cytoskeleton on the organization of signaling compartments. Multiple studies report that MBCD alters cytoskeletal integrity, thus the change we observe could result from loss of interactions between the cytoskeleton and the membrane or the signaling proteins²²⁷⁻²²⁹. If so, effects similar to those produced by MBCD should also be observed following treatment with agents that disrupt the cytoskeleton.

3.4 Mechanism of PIP₃ inhibition of olfactory CNG channels

PIP₃ applied to the intracellular side of inside-out membrane patches decreases the cAMP sensitivity of CNGA2 channels by more than one order of magnitude, and lowers the efficacy of cAMP by about 50%. For reasons similar to those discussed above concerning the MBCD effect on CNGA2 channels, the most likely mechanism

underlying PIP₃ inhibition of homomeric and heteromeric olfactory CNG channels is a change in the free energy of gating. The large decrease in cAMP efficacy following PIP₃ exposure is difficult to explain otherwise. Furthermore, the initial report on PIP₃ inhibition of olfactory CNG channels observed no change in the single channel conductance following PIP₃ exposure, suggesting that the decreased cAMP efficacy is due to increased stability of the closed state relative to the open state when ligand is bound. Still, while the entire effect of PIP₃ cannot be explained by a change in binding affinity, such a change could partially contribute.

The localization of the PIP₃ interaction site to the N-terminus of CNGA2 subunits suggests that the mechanism of inhibition involves a disruption of the intersubunit interaction between the N- and C- termini, similar to the mechanism underlying Ca²⁺/CaM inhibition¹⁰¹. Residues between amino acids 61 and 90 interact with regions in the C-linker and CNBD to facilitate channel opening at lower cyclic nucleotide concentrations¹⁰⁰. Removal of amino acids 61-90 dramatically decreases the apparent affinity for both cGMP and cAMP, and reduces the efficacy of cAMP (see Figure 20 for functional comparisons)^{100,101}. PIP₃ mimicked these effects, and removal of amino acids 61-90 blocked PIP₃ inhibition (Figures 15 & 17). By attaching YFP to one terminus of CNGA2 and CFP to the other terminus, Zheng and colleagues¹⁰¹ observed emission from YFP following excitation of CFP (FRET), demonstrating that the two fluorophores, and thus the two termini, were in close proximity. Addition of Ca²⁺/CaM reduced this FRET effect, implying that inhibition involved a separation of the two ends of the channel. Similar experiments could be used to test whether PIP₃ also regulates CNGA2 channels in this fashion. Biochemical overlay assays could also be employed with western blots

containing one terminal peptide exposed to tagged fragments of the alternate terminal, in the absence and presence of PIP₃, similar to the CaM overlay experiments in Paper 2 (Figure 18)¹⁰⁰. It might also be possible to covalently link the N- and C- terminals with disulfide bonds. The C-linker of CNGA2 contains an endogenous cysteine residue, and the equivalent residue in CNGA1 is capable of crosslinking with an endogenous cysteine in the N-terminus⁹⁹. While the N-terminus of CNGA2 does not contain the appropriate cysteine, by introducing single cysteines upstream and downstream of residue 90, it may be possible to identify one that crosslinks with the C-terminus. This should lock the terminals together, thereby preventing PIP₃ from inhibiting the channels.

The exact residues required for PIP₃ inhibition remain to be identified. Numerous basic residues reside between amino acids 61 and 90, and work in other ion channels shows that clusters of basic residues are often vital for PIP₂ and PIP₃ binding¹⁸²⁻¹⁹⁵. The fact that the N-terminals of both CNGA2 and CNGA3 interact with PIP₃ in pulldown assays suggests that conserved residues between the two channels may be important. Converting conserved basic residues, either singly or in combination, to neutral amino acids, followed by electrophysiological analysis should lead to a better understanding of the molecular determinants of PIP₃ inhibition. Ideally, it would be beneficial to identify one or a few changes that remove PIP₃ inhibition without dramatically altering normal channel function.

The results from preliminary work to establish which portions of the PIP₃ molecule are involved in binding to CNGA2 are inconclusive. I discovered that DOPIP₃ and IP₄ have little or no impact on channel function, which may suggest that the lipid portion of PIP₃ makes specific contacts with the channels or that it is important for strong

membrane anchoring of the CNGA2 amino terminus. While 10 μM DOPIP₃ had no effect on channel function, 50 μM DOPIP₃ could produce a mild shift in cyclic nucleotide sensitivity. Since DOPIP₃ is far more soluble in the aqueous environment than DPPIP₃, DOPIP₃ may not build to significant levels within the membrane to produce maximal channel inhibition. Zhainazarov *et al*¹⁸¹ report that CNGA2 channels are insensitive to PIP₂, thus CNGA2 channels may also show headgroup selectivity. However, when I applied PIP₂ to a few CNGA2-containing patches, I observed a dramatic shift in cyclic nucleotide sensitivity (Supplemental Figure 3). This discrepancy with the results of Zhainazarov *et al* begs further investigation.

While molecular mechanisms underlying gating in heteromeric channels are poorly understood, our data hint at possible molecular interactions involved in gating. As in homomeric channels, removing residues 61-90 from CNGA2 dramatically reduced the cyclic nucleotide sensitivity of heteromeric channels (see Figure 18), and eliminated the ability of PIP₃ to reduce channel activity. These observations suggest that in both homomeric and heteromeric channels, a similar mechanism may underlie PIP₃ inhibition, namely the disruption of interactions between the CNGA2 N-terminus and other channel regions. In heteromeric channels, though, the CNGA2 N-terminus may be interacting with regions in CNGA4 or CNGB1b to produce an autoexcitatory effect. FRET experiments could be used to test this possibility by attaching one fluorophore, such as CFP, to the N-terminus of CNGA2, and another fluorophore, YFP, to the N- or C-termini of CNGA4 or CNGB1b.

Comparing the quantitatively different effects of Ca²⁺/CaM and PIP₃ on heteromeric channel cAMP sensitivity suggests that distinct modulatory mechanisms

underlie the two forms of inhibition (see Figure 20B functional comparison). $\text{Ca}^{2+}/\text{CaM}$ produces a 20-fold shift in the cAMP sensitivity of heteromeric channels without altering efficacy. In contrast, PIP_3 shifted the cAMP sensitivity by only 8-fold, yet decreased the efficacy by 30% or more. Neither $\text{Ca}^{2+}/\text{CaM}$ nor PIP_3 reportedly reduce the maximum single channel conductance of heteromeric channels in the presence of saturating cAMP concentrations^{163,181}. The effects of $\text{Ca}^{2+}/\text{CaM}$ could be fit with current models of CNG channel activation by assuming that cAMP and cGMP are almost equally effective channel activators. In this case, however, the behavior of channels in the presence of PIP_3 cannot be accurately fit with the same models. This suggests that more complex kinetic models are required to fully explain the activation process of heteromeric channels. Perhaps PIP_3 binding can force channels into an additional open state with reduced or blocked conductance. Alternatively, the observation that PIP_3 generally reduces the Hill coefficient for cAMP activation of heteromeric channels suggests that cooperative intersubunit interactions are affected (Figure 20B). This may reflect a situation where each subunit in the heteromer contributes different gating properties to whole channels. PIP_3 may then change these contributions, allowing subunits with lower apparent affinities for cAMP to dominate the gating process. Testing these possibilities is a difficult task. I attempted to determine whether PIP_3 binds better to the closed or open state by exposing patches to PIP_3 in the presence or absence of cAMP, and measuring the timecourse of inhibition. I observed a large variability in the inhibition time courses with or without cAMP present, and no difference between the two conditions was evident. Perhaps lower concentrations of PIP_3 , which inhibit channels more gradually, would reveal a difference. But if my preliminary data are accurate, then PIP_3 appears to bind

both open and closed channel states. Still, more single channel data are required, as well as the construction of more complex models to fit the data.

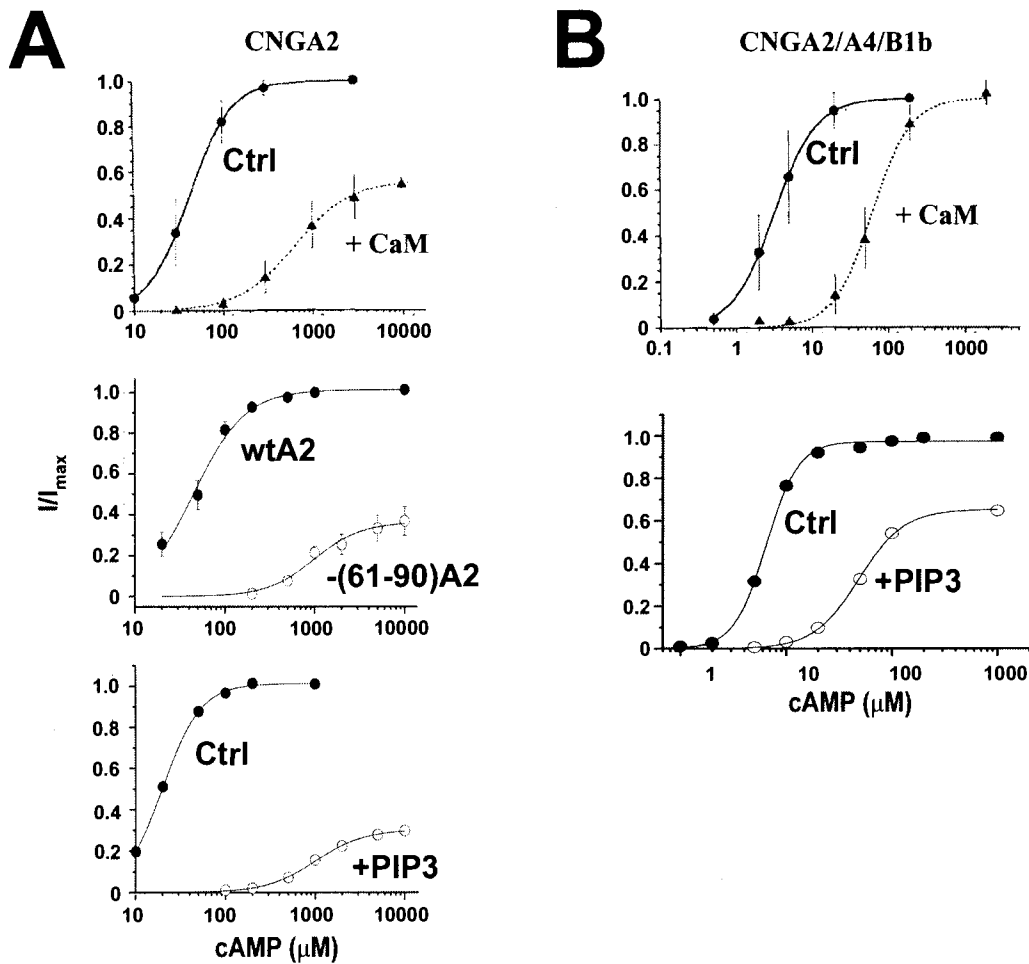


Figure 20: Calmodulin vs. PIP3 Inhibition of Olfactory CNG Channels (A) Calmodulin inhibition, PIP₃ inhibition, and removal of amino acids 61-90 in the N-terminus all have similar effects on the cAMP sensitivity of CNGA2 channels. Shown are activation curves for CNGA2 channels before (Ctrl) and after (+CaM) calmodulin exposure (top), with (wtA2) or without (-(61-90)A2) residues 61-90 in the amino terminus (middle), and before (Ctrl) or after PIP₃ (+PIP3) exposure (bottom). Solid lines are fits to the Hill equation with the following parameters ($K_{1/2}$ in μM , n): top panel, Ctrl = 43.4, 1.8, +CaM = 645, 1.4; middle panel, wtA2 = 45, 1.5, -(61-90)A2 = 981, 1.7; bottom panel, Ctrl = 20, 2.0, +PIP3 = 996, 1.6. Top panel modified from reference 161,

middle and bottom panels are my data. **(B)** Calmodulin and PIP₃ produce distinct effects on CNGA2/A4/B1b channels. Shown are activation curves before (Ctrl) and after (+CaM) exposure to Ca²⁺/CaM (top panel) and before (Ctrl) and after (+PIP₃) exposure to PIP₃ (bottom panel). Solid lines are fits to the Hill equation using the following parameters ($K_{1/2}$, n): top panel, Ctrl = 3.2, 1.6, +CaM = 63, 1.7; bottom panel, Ctrl = 6.4, 2.8, +PIP₃ = 48.4, 1.8. Top panel modified from reference 161. Bottom panel is my data.

3.5 Interplay between PIP₃ and calmodulin inhibition.

As discussed above, the mechanism underlying PIP₃ and Ca²⁺/CaM inhibition of CNGA2 channels appears to be identical. Our data also suggest that PIP₃ can partially prevent Ca²⁺/CaM from binding to the N-terminus of CNGA2 subunits (Figure 19). I was unable to determine whether previous exposure of CNGA2 channels to Ca²⁺/CaM could prevent PIP₃ inhibition or binding, because PIP₃ was ineffective at the free calcium concentrations required to maintain Ca²⁺/CaM binding (10-20 μM). Little is known about this effect, but it may involve the ability of divalent cations to stabilize the formation of large liposome clusters or sheets by neutralizing the normally repulsive interactions between highly negatively charged headgroups.

For heteromeric channels, PIP₃ and Ca²⁺/CaM interact with different subunits and produce distinct changes in channel function. While PIP₃ inhibition requires the calmodulin binding motif in CNGA2, Ca²⁺/CaM inhibition requires the presence of IQ-like calmodulin binding motifs in both CNGA4 and CNGB1b. Still, PIP₃ prevents Ca²⁺/CaM inhibition, even in Δ60-90A2/A4/B1b mutant channels that are not affected by PIP₃. We also found that PIP₃ can almost completely block Ca²⁺/CaM binding to the N-terminus of CNGB1b, and partially block Ca²⁺/CaM binding to the C-linker region of CNGA4. The fact that PIP₃ can block Ca²⁺/CaM binding without altering channel function suggests a possible mechanism for Ca²⁺/CaM inhibition of heteromeric

channels, which until now has remained a mystery. I propose that $\text{Ca}^{2+}/\text{CaM}$ normally facilitates an interaction between the N-terminus of CNGB1b and the C-linker of CNGA4, which leads to decreased channel sensitivity. PIP_3 binding to the IQ-like motifs blocks $\text{Ca}^{2+}/\text{CaM}$ inhibition by preventing this interaction from forming. This idea can be tested by fluorescently modifying cysteines introduced within the C-linker of CNGA4, and measuring changes in FRET with a fluorophore appended to the N-terminus of CNGB1b. A possible biochemical approach would involve, for example, incubating western blots carrying the CNGA4 C-terminus with solutions containing epitope-tagged CNGB1b N-terminals in the presence or absence of $\text{Ca}^{2+}/\text{CaM}$. If my model is correct, The CNGB1b fragment will only be detected on the gel in the presence of $\text{Ca}^{2+}/\text{CaM}$. The presence of PIP_3 would be expected to inhibit this interaction.

3.6 Physiological implications of PIP_3 Inhibition

The idea that PIP_3 regulation of olfactory CNG channels plays a role in the odorant response is relatively new, and little work has been done to confirm or deny the possibility. The identification of a region in CNGA2 that is necessary for PIP_3 inhibition of heteromeric channels is a significant step toward a more refined understanding of the physiological role of PIP_3 modulation. Further refining the molecular determinants of PIP_3 inhibition may eventually allow studies with transgenic animals expressing PIP_3 -insensitive CNGA2 subunits. This will reveal the behavioral consequences of loss of PIP_3 inhibition. A more immediate avenue for understanding the physiological role of PIP_3 involves work with isolated slices of olfactory epithelium³⁰⁵. Staining of such slices for the various isoforms of PI3K would reveal where in the cell PIP_3 synthesis can occur.

The introduction of fluorescent PIP₃ binding proteins into neurons in slice preparations would also help identify the cellular locations and dynamics of odorant-stimulated PIP₃ synthesis. Recordings from slices may allow investigators to test the involvement of both odorant and non-odorant receptors in PIP₃ synthesis and CNG channel inhibition.

PIP₃ and Ca²⁺/CaM produce quantitatively different effects on heteromeric olfactory CNG channel activity, which suggests that they serve very distinct roles in OSNs. In isolated patches, PIP₃ not only decreased the cAMP sensitivity of heteromeric olfactory CNG channels by about 8-fold, it also reduced the efficacy of cAMP by about 30-50% (Figure 18). Therefore, in OSNs PIP₃ inhibition would be expected to not only shift the odorant sensitivity but also reduce the maximum amount of calcium that enters the cilia with saturating odorant doses. This effect differs from that seen with Ca²⁺/CaM inhibition, which leads to a 20-fold decrease in the cAMP sensitivity but no change in the efficacy of cAMP¹⁶⁰. Physiologically, the large shift in cAMP sensitivity following Ca²⁺/CaM inhibition is vital for rapid adaptation to high levels of background odorants^{65,164}. By only shifting channel sensitivity, Ca²⁺/CaM decreases the response to the present concentration of background odorant, while still allowing increases in the level of odorants to trigger a maximal OSN response. While the role of PIP₃ may overlap that of Ca²⁺/CaM, the dramatic decrease in cAMP efficacy caused by PIP₃ is an additional level of control that is not necessarily useful for rapid adaptation.

Instead of regulating sensory adaptation, PIP₃ inhibition may play a protective role in OSNs. Spehr *et al*¹⁸⁰ reported that PI3K inhibition in OSNs resulted in enhanced calcium influx only when OSNs were exposed to complex odorant mixtures containing over one hundred distinct compounds. Therefore PIP₃ does not appear to be important for

regulating the response to simple odorants, but may be important for limiting calcium influx in the presence of large concentrations of mixed odorants. The results of Kawai & Miyachi suggest that high concentrations of odorant molecules destabilize the plasma membrane by decreasing its resistance³¹⁴. Perhaps PIP₃ inhibition of olfactory CNG channels serves as a mechanism for preventing potentially toxic levels of calcium influx under conditions where many ions are already passing through the membrane.

In any case, why would PIP₃ prevent further channel inhibition by Ca²⁺/CaM? It is possible that this phenomenon is a result of exogenous PIP₃ accumulating in patches to levels never found in OSN membranes. However, since very brief exposures to PIP₃ (10 seconds or less) were often sufficient to cause inhibition and block Ca²⁺/CaM modulation, this explanation seems unlikely. Perhaps the ability of the IQ-like motifs to bind PIP₃ is a side effect of such domains that leads to no real benefit or harm in OSNs, thus there exists no evolutionary pressure to eliminate the phenomenon even though it serves no purpose. Alternatively, since the combined effect of PIP₃ and Ca²⁺/CaM inhibition might leave channels completely unresponsive to odorants, the occlusion of Ca²⁺/CaM inhibition by PIP₃ may serve to maintain some level of responsiveness to simple salient odors within a background of mixed chemicals. Finally, if PIP₃ regulation of olfactory CNG channels does not occur in the cilia, the interplay with Ca²⁺/CaM regulation may not be relevant. Much more investigation is required to make any strong conclusions.

One important question is how PIP₃ is produced in the OSNs. Spehr *et al* provide evidence that PIP₃ is synthesized following an odorant-stimulated increase in PI3K activity¹⁸⁰. Our current understanding of odorant receptor function, which states that

odorant binding triggers activation of a G alpha protein which stimulates AC activity, provides no explanation for this effect. Perhaps the beta or gamma subunits of the olfactory G protein can stimulate PI3K activity. Alternatively, other receptor proteins may become activated with high levels of complex odorants. Mary Lucero's work shows that activation of purine receptors in OSN membranes can lead to decreased cyclic nucleotide channel activation, and that supporting cells in the olfactory epithelium may release ATP to modulate olfactory signaling through purine receptors³⁰⁵. Yet the results of Spehr *et al* were obtained from isolated neurons, therefore their results could not be explained by the release of ATP from supporting cells. Still, it is possible that the complex odorants used in their study non-specifically activate purinergic receptors on OSNs and stimulate PI3K activity, perhaps by destabilizing general membrane structure³¹⁵.

Chapter 4: Conclusions

- CNGA2 channels in HEK-293 cells and native olfactory CNG channels may reside in cholesterol-rich, lipid raft membrane microdomains.
- CNGA3 channels in HEK-293 cells do not reside in cholesterol-rich lipid raft microdomains.
- The oligosaccharide, lipid-extracting compound, MBCD, decreases the cyclic nucleotide sensitivity of CNGA2 channels at high concentrations and physiological temperature. This effect does not appear related to the disruption of cholesterol-rich lipid rafts or specific cholesterol-channel interactions.
- MBCD treatment reduces cAMP synthesis following PGE1 stimulation of HEK-293 cells, which may involve disruption of lipid rafts and membrane-localized signaling compartments.
- PIP₃ inhibits olfactory CNG channels through interactions with amino acids 61-90 of the CNGA2 amino terminus.
- PIP₃ inhibition of both homomeric and heteromeric olfactory CNG channels may result from a disruption of CNGA2 intersubunit autoexcitatory interactions.
- PIP₃ occludes Ca²⁺/CaM inhibition of olfactory CNG channels, in part by directly interacting with Ca²⁺/CaM-binding domains in several channel subunits.

Chapter 5: Materials and Methods

Materials. A mouse monoclonal antibody (CRO2H7) raised against the C-terminal region of rat CNGA2 (amino acids Y482–E664) fused to a maltose binding protein was provided by Dr. U. Benjamin Kaupp. Anti-FLAG M2 monoclonal antibody and anti-flotillin antibodies were obtained from Sigma. Polyclonal antibodies raised against caveolin that recognize all 3 caveolin isoforms were from BD Transduction Laboratories (Lexington, KY); monoclonal antibodies against the human transferrin receptor were from Zymed (South San Francisco, CA); and polyclonal antibodies against GFP were from BD Biosciences Clontech (Palo Alto, CA). Prostaglandin E1 (PGE1) was obtained from Calbiochem (San Diego, CA); forskolin, methyl- β -cyclodextrin (MBCD), and 8-(p-chlorophenylthio)-cGMP (CPT-cGMP) were from Sigma-Aldrich (St. Louis, MO).

Statistical Analysis. To determine whether the data obtained following experimental manipulations significantly differed from control conditions, two-tailed t-tests were performed using either SigmaStat (SPSS Inc., IL) or Excel (Microsoft Inc., WA) software. To compare dose-response relationships, $\log[K_{1/2}]$ values were used for t-tests, since actual $K_{1/2}$ values extrapolated from the Hill equation do not provide a normal distribution.

DNA and Mutagenesis. The wild-type CNGA2 in a pCIS vector was a gift from R. Reed (Johns Hopkins University, Baltimore, MD). The 3XFLAG-CNGA2 was made by inserting the wtCNGA2 into the p3xFLAG-CMV-7.1 vector (Sigma). CFP-CNGA2 was made by inserting the wtCNGA2 gene into the p-ECFPC1 vector (BD Biosciences Clontech). For electrophysiological studies with PIP_3 wild type bovine CNGA3, rat

CNGA2, rat CNGA4, and rat CNGB1b, including the 5' and 3' untranslated regions, and all chimeras, were cloned into pcDNA3.0 (Invitrogen, Carlsbad, CA). A YFP tagged CNGA2 was occasionally used (pEYFP-C1, Clontech, Mountain View, CA) and was functionally indistinguishable from the native subunit. Construction of chimeric subunits has been described previously, with splice sites after S229, I277, and R401 in CNGA2, and after V276, I322, and R446 in CNGA3³¹⁹. The A2nA3 chimera was constructed using overlapping PCR, with residues 1-140 of CNGA2 spliced to residues 186-706 of CNGA3. DNAs encoding the N-terminal regions of rat CNGA2 (residues 1-138) and human CNGA3 (residues 1-164) were genetically fused with DNA encoding glutathione-S-transferase (GE Healthcare Biosciences, Piscataway, NJ) as previously described^{289,320}. DNAs encoding the proximal amino-terminal region of bovine CNGB1b (amino acids 677-764) and the C-linker region of rat CNGA4 (amino acids 271-339) were fused to GST to form CNGB1bN and GST-A4CL.

Cell Culture, Transfection, and Infection. Human embryonic kidney 293 and COS-1 cells were maintained in 100 mm culture dishes in Dulbecco's modified Eagle's medium supplemented with 10% fetal bovine serum and 1-2% penicillin/streptomycin (Invitrogen, Carlsbad, CA) (plus 0.1% Gentamicin (Invitrogen) for cells used in biochemical experiments) at 37°C in a humidified atmosphere of 95% air/5% CO₂. For detergent resistance and imaging experiments, cells were transfected at 60 to 80% confluence with 3 µg of DNA combined with 25 µl of LipofectAMINE reagent (Invitrogen) in serum-free Dulbecco's modified Eagle's medium for 6 to 7 h, and used for experiments 18 to 48 h after return to serum-supplemented media. For electrophysiology, Cells were transfected with either Fugene 6 (Roche) in a 2.5 µg DNA: 15 µl Fugene reagent ration, or with

Effectene (Qiagen) by combining 650 µg of total DNA with 5.2 µl of enhancer and 16.25 µl of effectene reagent. For both the Fugene and Effectene protocols, transfection mixes remained on the cells for 18-72 hrs, until the time of recording. Equal amounts of the 3 different subunits were transfected for heteromeric channel expression. For adenoviral infection, HEK-293 cells were maintained in MEM (Life Technologies Inc.) supplemented with 26.2 mM NaHCO₃, 10% (vol/vol) FBS (Gemini), penicillin (50 µg/ml), and streptomycin (50 µg/ml), pH 7.0, at 37° C in a humidified atmosphere of 95% air and 5% CO₂. Cells were plated at 60% confluence in 100-mm culture dishes 24 h before infection with the CNG channel–encoding adenovirus constructs (multiplicity of infection = 10 plaque forming units per cell). 2 h after infection, hydroxyurea was added to the cell media at 2 mM final concentration to partially inhibit viral replication. 24 h after infection cells were detached with PBS containing 0.03% EDTA, resuspended in serum-containing medium, and assayed within 12 h.

Detergent Extraction and Cholesterol Depletion. To assess detergent insolubility, cells from a single confluent 100 mm culture dish were homogenized in MES-buffered saline (25mM MES, pH 6.5, 150 mM NaCl) containing 1% Triton X-100. The homogenate was then centrifuged at 13,400 rpm in a microcentrifuge at 4°C for 30 min. After removal of the supernatant, the pellet was resuspended in phosphate-buffered saline (PBS), and both the pellet and supernatant were mixed with SDS-PAGE sample buffer. For isolation of low-density, Triton X-100–insoluble complexes confluent cells from a single 100-mm dish were homogenized in MES-buffered saline containing 1% Triton X-100 (unless otherwise indicated), and sucrose was added to a final concentration of 40%. A 5-to-30% discontinuous sucrose gradient was layered on top of this detergent extract followed by

ultracentrifugation [54,000 rpm in a rotor (Beckman Coulter, Fullerton, CA)] for 18 to 24 h at 4°C in a TL-100 ultracentrifuge (Beckman Coulter). Successive gradient fractions were collected from the top and subjected to SDS-PAGE and Western blot analysis. Cholesterol depletion for detergent resistance assays was achieved by incubating cells for 1 h in 2% methyl- β -cyclodextrin in serum-free media at 37°C, with shaking every 5 min. Preparation of crude olfactory membranes was performed by scraping the epithelial lining from the nasal turbinates into a sucrose phosphate solution containing protease inhibitors and centrifuged at 1000 rpm to remove bone or cartilage. The pellet was removed and the supernatant was centrifuged at 13,000 rpm in a Beckman Coulter JA25.5 rotor. The resulting pellet was resuspended in PBS. Raft preparations of rat nasal membranes were performed with 3% Triton X-100. For deglycosylation, samples of rat nasal membranes containing 20 μ g of protein were incubated with 500 units of N-glycosidase F (New England Biolabs, Beverly, MA) for 1 h at 37°C.

Protein and Cholesterol Measurements. The protein concentration of cell lysates and sucrose gradient fractions was determined with a Bradford protein assay kit (Bio-Rad, Hercules, CA). The total cholesterol in sonicated cell lysates and density-gradient fractions was determined using a liquid chromatography-mass spectroscopy (MS) protocol developed by the Pharmacokinetics Core Laboratory in the Department of Physiology and Pharmacology at Oregon Health and Science University. The protocol is a modified version of the method employed by Trinder *et al*³²¹. 120 μ l of isopropyl alcohol was added to each 100 μ l sample. After addition of 1000 ng of d6-cholesterol as an internal standard, samples were hydrolyzed in 1 ml of ethanolic potassium hydroxide (25:1) at 100°C for 5 min, and cholesterol was then extracted in 2 ml of hexane. The

Pharmacokinetics Core Laboratory performed positive atmospheric pressure chemical ionization-MS with an ion trap mass spectrometer (LCQ Advantage; Thermo Finnigan, San Jose, CA), which gave a predominant ion for cholesterol at 369 [MH⁺-H₂O]. A tandem MS transition from 369 to 243 was monitored in a selected-reaction monitoring scan event (for d₆-cholesterol, the transition from 375 to 249 was monitored). The atmospheric pressure-chemical ionization interface was operated using the following settings: sheath and aux gas flow rates, 70 and 29, respectively; vaporizer temperature, 450°C; and capillary temperature, 225°C. Cholesterol concentrations were calculated by comparing the area ratio of unknowns to standard curves generated with cholesterol oleate (0–2000 ng) and 1000 ng of d₆-cholesterol. For some experiments, cholesterol was measured using the Amplex Red assay kit from Molecular Probes. The absolute cholesterol amounts reported by the two different methods at each timepoint varied, but when the absolute values at each time point were expressed relative to the total amount at time 0, the two methods produced nearly identical results.

Immunoprecipitation. HEK-293 cell membranes or rat nasal membranes were solubilized in 10 mM Tris, pH 8.0, 150 mM NaCl, 1% Triton X-100, and 60 mM octylglucoside, supplemented with protease inhibitors (complete tablets; Roche). After incubation for 45 min at 4°C, the solubilized membranes were centrifuged in a microcentrifuge at 13,400 rpm for 15 min at 4°C. Solubilized membranes were then incubated with polyclonal anti-caveolin (1:500) or monoclonal anti-CNGA2 (1:250) antibody overnight at 4°C with gentle mixing. The next day, 250 µl of a 1:5 dilution of Sepharose-conjugated protein A (anti-caveolin) or protein G (anti-CNGA2) beads (Sigma) was added, and the samples were incubated for 3 h at 4°C with gentle mixing.

The beads with bound antibody-antigen complex were pelleted and washed three times with 0.5% Triton X-100, 150 mM NaCl, 50 mM Tris-Cl, 1 mM EDTA pH 7.5, followed by a wash in 1% Triton X-100. The final pellet was resuspended in 40 μ l of PBS and SDS-PAGE sample buffer, briefly centrifuged to remove the beads, then subjected to SDS-PAGE and Western Blot analysis.

Immunostaining. For immunofluorescent labeling of caveolin cells were fixed and permeabilized before incubation with anti-caveolin antibodies (1:500). After incubation in biotinylated secondary antibody (1:200), the staining was visualized with a Cy3-conjugated streptavidin (1:500). The secondary antibody and streptavidin were obtained from Jackson ImmunoResearch Laboratories Inc. (West Grove, PA). Imaging was performed on a Zeiss Axiovert 200 M microscope equipped with standard epifluorescence and a Photometrics Cool Snap HQ charge-coupled device camera (Roper Scientific, Trenton, NJ).

Detection of CNG Channel Activity in Cell Populations. The fluorescent indicator fura-2 was used to monitor Ca^{2+} influx through CNGA2 channels in cell suspensions. HEK 293 cells were infected with an adenovirus construct encoding a CNGA2 channel containing two mutations, C460W and E583M, that increase cAMP sensitivity and decrease cGMP sensitivity, respectively^{116,200}. Cells were loaded with 4 μ M fura-2/AM (the membrane-permeant form) and 0.02% pluronic F-127 at room temperature for 30–40 min in a buffer containing Ham's F-10 medium supplemented with 1 mg/ml BSA fraction V (BSA, Fisher) and 20 mM HEPES, pH 7.4. Cells were washed twice, then resuspended in a solution containing the following (in mM): 145 NaCl, 11 d-Glucose, 10 HEPES, 4 KCl, 1 CaCl_2 , 1 MgCl_2 , and 1 mg/ml BSA, pH 7.4 ($3\text{--}4 \times 10^6$ cells /3 ml

buffer solution), and assayed using an LS-50B spectrofluorimeter (Perkin Elmer). Additions were made by pipetting stock solutions into a stirred cuvette. The mixing time was estimated to be on the order of 5 s. Fluorescence was measured at an excitation wavelength of 380nm and an emission wavelength of 510 nm. Under these conditions, Ca^{2+} influx causes a decrease in fluorescence (ΔF), which was expressed relative to the pre-stimulus fluorescence (F_0) to correct for variations in dye concentration, and to allow for comparison of results on different batches of cells. Data were sampled at 0.5 Hz and filtered at 0.1 Hz. After fura-2 loading, some cells were exposed to 2% MBCD for 1 h or 2% MBCD along with 1 mM cholesterol, whereas control cells were otherwise treated identically.

Patch Clamp Recordings. HEK-293 cells were lifted into room temperature normal media 18-72 hours following transfection, and used for recording within 6 hours. Cell aliquots were added to a bath solution containing, in mM: 130 NaCl, 5 KCl, 20 HEPES, 0.5 EDTA, 5 MgCl_2 , 2 CaCl_2 , pH 7.4. Pipettes were filled with a solution matching that in the bath, without MgCl_2 and CaCl_2 , and had resistances ranging from 1.5-4.0 M Ω . Following the formation of a G Ω seal, inside-out patches were excised and placed in front of a perfusion head controlled by a Biologic RSC-100 rapid solution changer (Molecular Kinetics, Pullman, WA). Patches were first washed in a solution containing, in mM, 130 KCl, 5 NaCl, 20 HEPES, 0.5 EDTA pH 7.4, then exposed to varying concentrations of cAMP and cGMP (Sigma, St. Louis, MO) dissolved in the perfusion solution. Dose-response curves were generated by subtracting the current recorded at +50 mV in cyclic nucleotide-free solution from the current recorded in the presence of cyclic nucleotide at the same voltage. The leak-subtracted currents were normalized to the

current elicited by 1 mM cGMP. Curves are fits to the Hill equation, $I/I_{\max} = C^n/[C^n + (K_{1/2})^n]$, where C is the cyclic nucleotide concentration and n is the Hill coefficient. For Ca^{2+} /CaM experiments, perfusion solutions typically contained 250 nM bovine brain calmodulin (Sigma), 2 mM NTA instead of EDTA, and 704 μM total CaCl_2 (50 μM free Ca^{2+}). All phosphoinositides were obtained from Matreya LLC (Pleasant Gap, PA) as sodium salts, and reconstituted with water to stock concentrations of 100 μM . The stock solutions were sonicated at low power for 30 min on ice, and stored at -20°C . Perfusion solutions containing phosphoinositides were sonicated for an additional 30 min before use. Recordings were made with a CV201 headstage attached to an Axopatch 200A amplifier and a Digidata 1200 interface (Molecular Devices, Corp., Sunnyvale, CA). Currents were sampled at 10 kHz and digitally filtered at 1 kHz.

PLEASE NOTE: The following methods were performed by members of Michael Varnum's lab.

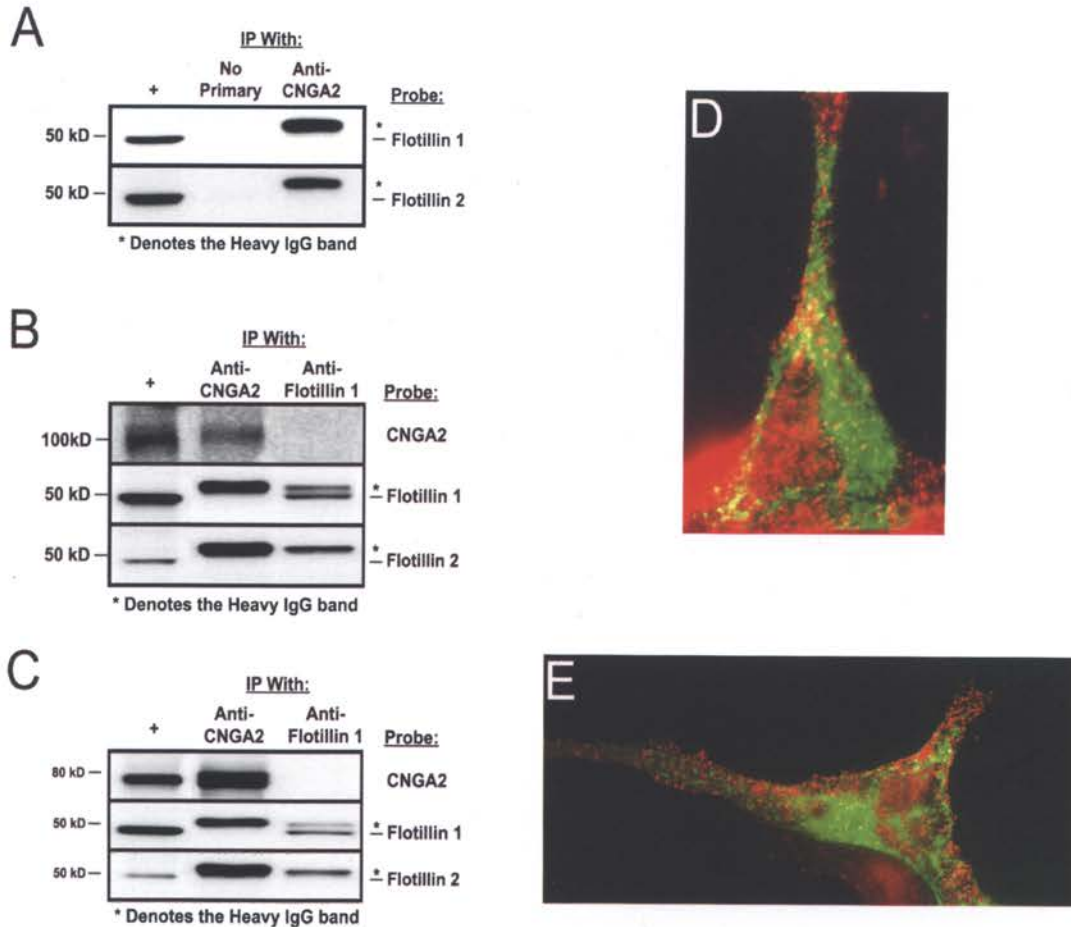
PIP₃ Binding and CaM Overlay Assays. Expression of recombinant protein in bacteria and purification were carried out as previously described^{289,320}. Briefly, cells were harvested and resuspended in buffer S [50 mM Tris-HCl (pH 7.8), 150 mM NaCl, 25 mM imidazole, 1% NDSB (Calbiochem, San Diego, CA), 0.5% CHAPS, and 0.25% Tween 20] containing protease inhibitors (Roche Applied Science), then lysed using a French pressure cell (SLM Instruments, Rochester, NY) or sonication. Soluble proteins were isolated by centrifugation at 20,000 X g and 4 °C for 30 min. GST fusion proteins were purified using glutathione-Sepharose beads (Amersham Biosciences). Purified GST-fusion proteins were used for *in vitro* PIP₃-binding assays in buffer containing 10 mM

HEPES (pH 7.4), 150 mM NaCl, 5 mM EDTA and 0.25% NP40. PIP₃-agarose beads and the GST-Grp1PH positive-control protein were from Echelon Biosciences. 50 µl of a 50% slurry of PIP₃ beads and purified protein (2 µg/ml) were incubated in 0.5 ml of binding buffer for 2 hours at 4 °C with rocking. Beads were gently pelleted and washed five times with excess binding buffer; PIP₃-interacting proteins were eluted with 1x NuPAGE sample buffer (Invitrogen). Protein samples were then separated under reducing conditions in 4-12% Bis-Tris gels and blotted onto nitrocellulose using the NuPAGE transfer buffer system (Invitrogen). Blotted proteins were detected using B-14 anti-GST monoclonal antibody (Santa Cruz Biotechnology, Santa Cruz, CA) at a dilution of 1:2000 in 1% milk/TTBS, HRP-conjugated anti-mouse IgG secondary antibody and the SuperSignal West Dura Extended Duration chemiluminescence substrate (Pierce Biotechnology, Rockford, IL).

Calmodulin-overlay assays were carried out essentially as described previously¹⁵². After blotting, GST-fusion proteins were probed for 1 hr. at room temperature with recombinant FLAG-tagged calmodulin (at ~ 50 nM) in 10 mM HEPES (pH 7.4), 150 mM NaCl, 0.5% NP-40, 0.5% BSA, 2 mM NTA and 170 µM CaCl₂ (10 µM free Ca²⁺), either with or without prior and concomitant incubation with 100 µM PIP₃. Bound calmodulin was visualized using M2 anti-FLAG antibody (Sigma) and the calmodulin signal was quantified using Kodak 1D Image Analysis Software (Eastman Kodak, New Haven, CT). Blots were subsequently stripped and reprobed with an antibody against GST to ensure that equivalent amounts of fusion protein were blotted in all lanes. Control western blots for CaM demonstrated that incubation with PIP₃ did not interfere with antibody binding

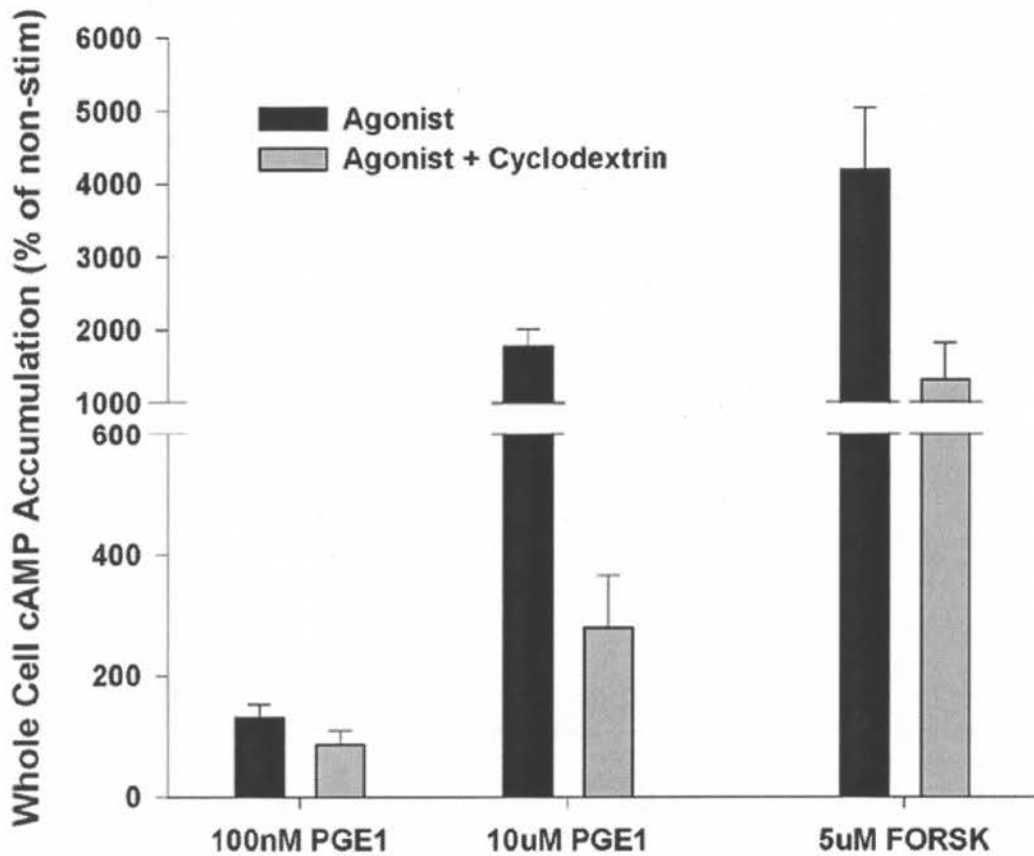
or blot processing (data not shown). Inhibition of CaM binding is expressed as a percentage reduction compared to control \pm SEM.

Appendix: Supplemental Figures

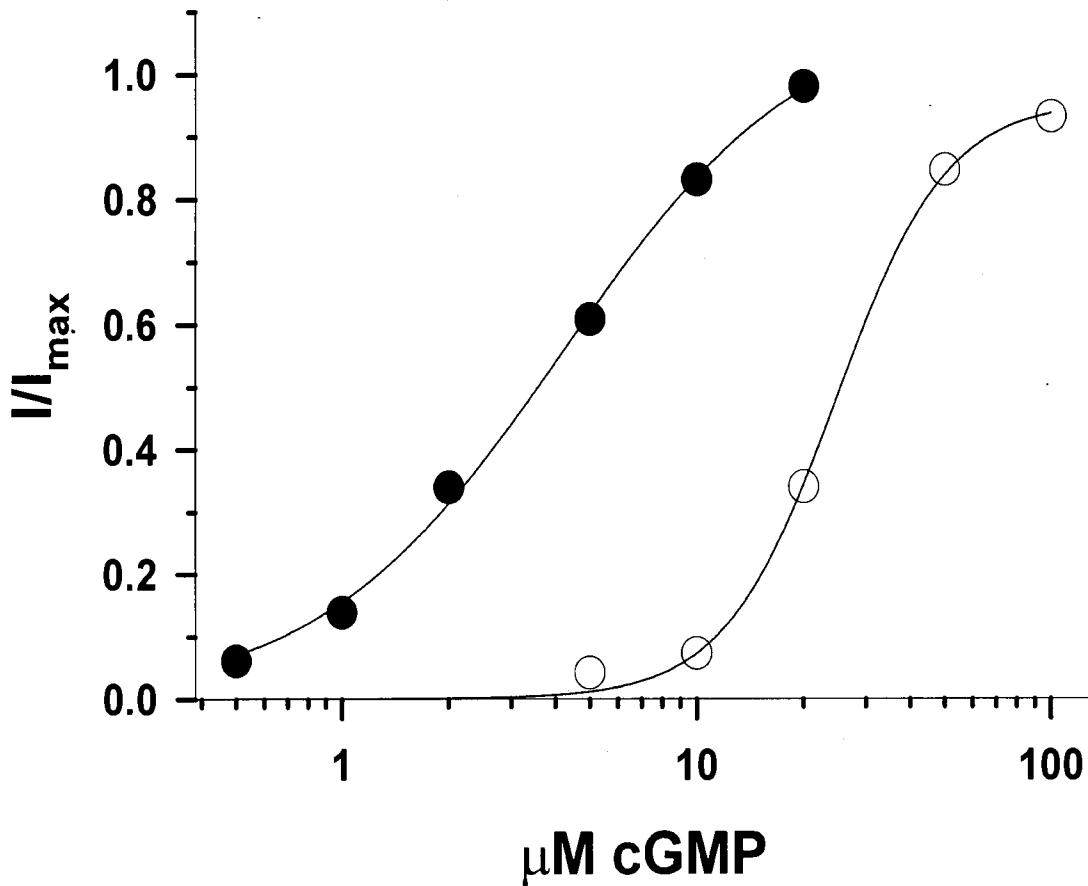


Supplemental Figure 1: CNGA2 does not directly bind or colocalize with flotillin 1 or 2. (A) Same samples as in Figure 7B probed with monoclonal antibodies against flotillin 1 and flotillin 2. (B) Solubilized membranes from rat nasal tissue (200 mg) were immunoprecipitated with anti-flotillin 1 (1:125) or anti-CNGA2 (1:125) antibodies. Western blots of the immunoprecipitates were probed with the antibodies listed on the right side of the blots. (C) Solubilized membranes from HEK-293 cells transfected with FLAG-CNGA2 were immunoprecipitated with anti-flotillin 1 (1:125) or anti-CNGA2

(1:125) antibodies. Western blots of the immunoprecipitates were probed with the antibodies indicated on the right side of the blots. (D-E) HEK-293 cells transiently expressing YFP-CNGA2 were immunofluorescently labeled with anti-flotillin 1 (D, 1:250) or anti-flotillin 2 (E, 1:250) antibodies and a Cy3-conjugated secondary antibody. YFP-CNGA2 alone is green, antibody labeled flotillin is red, and any overlap is yellow.



Supplemental Figure 2: Cyclodextrin reduces PGE1- and forskolin-stimulated whole-cell cAMP production. Untreated HEK293 cells and cells treated with 2% methyl- β -cyclodextrin were stimulated for 5 min with 100 nM prostaglandin E1 (PGE1), 10 μ M prostaglandin E1, or 5 mM forskolin (FORSK) and whole-cell cAMP levels were measured with an enzyme-coupled immunoassay (Amersham Biosciences). cAMP levels are expressed relative to the amount of protein in cell lysates and as a percentage of the per protein levels in unstimulated controls. 100 nM prostaglandin E1 did not stimulate an increase in whole-cell cAMP over the levels measured in unstimulated controls.



Supplemental Figure 3: PIP₂ inhibits CNGA2 channels. Shown is the dose-response relationship of a single patch containing CNGA2 channels before (●) and after (○) exposure to 10 μM PIP₂ (Sigma). Solid lines are fits to the Hill equation with the following parameters: before PIP₂, $K_{1/2} = 4.2 \mu\text{M}$, $n = 1.3$; after PIP₂, $K_{1/2} = 24.6 \mu\text{M}$, $n = 2.8$. Data are representative of 4 individual patches.

References

1. Pugh, E.N., Jr. The nature and identity of the internal excitational transmitter of vertebrate phototransduction. *Annu Rev Physiol* **49**, 715-41 (1987).
2. Yau, K.W. & Baylor, D.A. Cyclic GMP-activated conductance of retinal photoreceptor cells. *Annu Rev Neurosci* **12**, 289-327 (1989).
3. Owen, W.G. Ionic conductances in rod photoreceptors. *Annu Rev Physiol* **49**, 743-64 (1987).
4. Stryer, L. Cyclic GMP cascade of vision. *Annu Rev Neurosci* **9**, 87-119 (1986).
5. Lancet, D. Vertebrate olfactory reception. *Annu Rev Neurosci* **9**, 329-55 (1986).
6. Getchell, T.V. Functional properties of vertebrate olfactory receptor neurons. *Physiol Rev* **66**, 772-818 (1986).
7. Hagins, W.A., Penn, R.D. & Yoshikami, S. Dark current and photocurrent in retinal rods. *Biophys J* **10**, 380-412 (1970).
8. Baylor, D.A. & Fuortes, M.G. Electrical responses of single cones in the retina of the turtle. *J Physiol* **207**, 77-92 (1970).
9. Bitensky, M.W., Gorman, R.E. & Miller, W.H. Adenyl cyclase as a link between photon capture and changes in membrane permeability of frog photoreceptors. *Proc Natl Acad Sci U S A* **68**, 561-2 (1971).
10. Miller, W.H., Gorman, R.E. & Bitensky, M.W. Cyclic adenosine monophosphate: function in photoreceptors. *Science* **174**, 295-7 (1971).
11. Miki, N., Keirns, J.J., Marcus, F.R., Freeman, J. & Bitensky, M.W. Regulation of cyclic nucleotide concentrations in photoreceptors: an ATP-dependent stimulation of cyclic nucleotide phosphodiesterase by light. *Proc Natl Acad Sci U S A* **70**, 3820-4 (1973).
12. Lipton, S.A., Rasmussen, H. & Dowling, J.E. Electrical and adaptive properties of rod photoreceptors in *Bufo marinus*. II. Effects of cyclic nucleotides and prostaglandins. *J Gen Physiol* **70**, 771-91 (1977).
13. Nicol, G.D. & Miller, W.H. Cyclic GMP injected into retinal rod outer segments increases latency and amplitude of response to illumination. *Proc Natl Acad Sci U S A* **75**, 5217-20 (1978).
14. Miller, W.H. Physiological evidence that light-mediated decrease in cyclic GMP is an intermediary process in retinal rod transduction. *J Gen Physiol* **80**, 103-23 (1982).
15. Cobbs, W.H. & Pugh, E.N., Jr. Cyclic GMP can increase rod outer-segment light-sensitive current 10-fold without delay of excitation. *Nature* **313**, 585-7 (1985).
16. Matthews, H.R., Torre, V. & Lamb, T.D. Effects on the photoresponse of calcium buffers and cyclic GMP incorporated into the cytoplasm of retinal rods. *Nature* **313**, 582-5 (1985).
17. Fung, B.K., Hurley, J.B. & Stryer, L. Flow of information in the light-triggered cyclic nucleotide cascade of vision. *Proc Natl Acad Sci U S A* **78**, 152-6 (1981).
18. Kwok-Keung Fung, B. & Stryer, L. Photolyzed rhodopsin catalyzes the exchange of GTP for bound GDP in retinal rod outer segments. *Proc Natl Acad Sci U S A* **77**, 2500-4 (1980).

19. Fesenko, E.E., Kolesnikov, S.S. & Lyubarsky, A.L. Induction by cyclic GMP of cationic conductance in plasma membrane of retinal rod outer segment. *Nature* **313**, 310-3 (1985).
20. Yau, K.W. & Nakatani, K. Light-suppressible, cyclic GMP-sensitive conductance in the plasma membrane of a truncated rod outer segment. *Nature* **317**, 252-5 (1985).
21. Matthews, G. Comparison of the light-sensitive and cyclic GMP-sensitive conductances of the rod photoreceptor: noise characteristics. *J Neurosci* **6**, 2521-6 (1986).
22. Matthews, G. Single-channel recordings demonstrate that cGMP opens the light-sensitive ion channel of the rod photoreceptor. *Proc Natl Acad Sci U S A* **84**, 299-302 (1987).
23. Dryja, T.P., Finn, J.T., Peng, Y.W., McGee, T.L., Berson, E.L. & Yau, K.W. Mutations in the gene encoding the alpha subunit of the rod cGMP-gated channel in autosomal recessive retinitis pigmentosa. *Proc Natl Acad Sci U S A* **92**, 10177-81 (1995).
24. Bareil, C., Hamel, C.P., Delague, V., Arnaud, B., Demaille, J. & Claustres, M. Segregation of a mutation in CNGB1 encoding the beta-subunit of the rod cGMP-gated channel in a family with autosomal recessive retinitis pigmentosa. *Hum Genet* **108**, 328-34 (2001).
25. Kohl, S., Baumann, B., Broghammer, M., Jagle, H., Sieving, P., Kellner, U., Spegal, R., Anastasi, M., Zrenner, E., Sharpe, L.T. & Wissinger, B. Mutations in the CNGB3 gene encoding the beta-subunit of the cone photoreceptor cGMP-gated channel are responsible for achromatopsia (ACHM3) linked to chromosome 8q21. *Hum Mol Genet* **9**, 2107-16 (2000).
26. Kohl, S., Marx, T., Giddings, I., Jagle, H., Jacobson, S.G., Apfelstedt-Sylla, E., Zrenner, E., Sharpe, L.T. & Wissinger, B. Total colourblindness is caused by mutations in the gene encoding the alpha-subunit of the cone photoreceptor cGMP-gated cation channel. *Nat Genet* **19**, 257-9 (1998).
27. Burns, M.E. & Baylor, D.A. Activation, deactivation, and adaptation in vertebrate photoreceptor cells. *Annu Rev Neurosci* **24**, 779-805 (2001).
28. Pace, U., Hanski, E., Salomon, Y. & Lancet, D. Odorant-sensitive adenylate cyclase may mediate olfactory reception. *Nature* **316**, 255-8 (1985).
29. Sklar, P.B., Anholt, R.R. & Snyder, S.H. The odorant-sensitive adenylate cyclase of olfactory receptor cells. Differential stimulation by distinct classes of odorants. *J Biol Chem* **261**, 15538-43 (1986).
30. Lowe, G., Nakamura, T. & Gold, G.H. Adenylate cyclase mediates olfactory transduction for a wide variety of odorants. *Proc Natl Acad Sci U S A* **86**, 5641-5 (1989).
31. Getchell, T.V. Analysis of intracellular recordings from salamander olfactory epithelium. *Brain Res* **123**, 275-86 (1977).
32. Trotier, D. & MacLeod, P. Intracellular recordings from salamander olfactory receptor cells. *Brain Res* **268**, 225-37 (1983).
33. Nakamura, T. & Gold, G.H. A cyclic nucleotide-gated conductance in olfactory receptor cilia. *Nature* **325**, 442-4 (1987).

34. Kurahashi, T. Activation by odorants of cation-selective conductance in the olfactory receptor cell isolated from the newt. *J Physiol* **419**, 177-92 (1989).
35. Firestein, S. & Werblin, F. Odor-induced membrane currents in vertebrate-olfactory receptor neurons. *Science* **244**, 79-82 (1989).
36. Firestein, S., Zufall, F. & Shepherd, G.M. Single odor-sensitive channels in olfactory receptor neurons are also gated by cyclic nucleotides. *J Neurosci* **11**, 3565-72 (1991).
37. Zufall, F., Firestein, S. & Shepherd, G.M. Analysis of single cyclic nucleotide-gated channels in olfactory receptor cells. *J Neurosci* **11**, 3573-80 (1991).
38. Kolesnikov, S.S., Zhainazarov, A.B. & Kosolapov, A.V. Cyclic nucleotide-activated channels in the frog olfactory receptor plasma membrane. *FEBS Lett* **266**, 96-8 (1990).
39. Frings, S. & Lindemann, B. Current recording from sensory cilia of olfactory receptor cells in situ. I. The neuronal response to cyclic nucleotides. *J Gen Physiol* **97**, 1-16 (1991).
40. Reisert, J., Bauer, P.J., Yau, K.W. & Frings, S. The Ca-activated Cl channel and its control in rat olfactory receptor neurons. *J Gen Physiol* **122**, 349-63 (2003).
41. Matthews, H.R. & Reisert, J. Calcium, the two-faced messenger of olfactory transduction and adaptation. *Curr Opin Neurobiol* **13**, 469-75 (2003).
42. Brunet, L.J., Gold, G.H. & Ngai, J. General anosmia caused by a targeted disruption of the mouse olfactory cyclic nucleotide-gated cation channel. *Neuron* **17**, 681-93 (1996).
43. Zhao, H. & Reed, R.R. X inactivation of the OCNC1 channel gene reveals a role for activity-dependent competition in the olfactory system. *Cell* **104**, 651-60 (2001).
44. Kaupp, U.B. & Seifert, R. Cyclic nucleotide-gated ion channels. *Physiol Rev* **82**, 769-824 (2002).
45. Brown, R.L., Strassmaier, T., Brady, J.D. & Karpen, J.W. The Pharmacology of Cyclic Nucleotide-Gated Channels: Emerging from the Darkness. *Current Pharmaceutical Design* **In Press**(2006).
46. Parent, A., Schrader, K., Munger, S.D., Reed, R.R., Linden, D.J. & Ronnett, G.V. Synaptic transmission and hippocampal long-term potentiation in olfactory cyclic nucleotide-gated channel type 1 null mouse. *J Neurophysiol* **79**, 3295-301 (1998).
47. Kuzmiski, J.B. & MacVicar, B.A. Cyclic nucleotide-gated channels contribute to the cholinergic plateau potential in hippocampal CA1 pyramidal neurons. *J Neurosci* **21**, 8707-14 (2001).
48. Savchenko, A., Barnes, S. & Kramer, R.H. Cyclic-nucleotide-gated channels mediate synaptic feedback by nitric oxide. *Nature* **390**, 694-8 (1997).
49. Cook, N.J., Hanke, W. & Kaupp, U.B. Identification, purification, and functional reconstitution of the cyclic GMP-dependent channel from rod photoreceptors. *Proc Natl Acad Sci U S A* **84**, 585-9 (1987).
50. Kaupp, U.B., Niidome, T., Tanabe, T., Terada, S., Bonigk, W., Stuhmer, W., Cook, N.J., Kangawa, K., Matsuo, H., Hirose, T. & et al. Primary structure and functional expression from complementary DNA of the rod photoreceptor cyclic GMP-gated channel. *Nature* **342**, 762-6 (1989).

51. Biel, M., Zong, X., Ludwig, A., Sautter, A. & Hofmann, F. Molecular cloning and expression of the Modulatory subunit of the cyclic nucleotide-gated cation channel. *J Biol Chem* **271**, 6349-55 (1996).
52. Bonigk, W., Altenhofen, W., Muller, F., Dose, A., Illing, M., Molday, R.S. & Kaupp, U.B. Rod and cone photoreceptor cells express distinct genes for cGMP-gated channels. *Neuron* **10**, 865-77 (1993).
53. Bradley, J., Li, J., Davidson, N., Lester, H.A. & Zinn, K. Heteromeric olfactory cyclic nucleotide-gated channels: a subunit that confers increased sensitivity to cAMP. *Proc Natl Acad Sci U S A* **91**, 8890-4 (1994).
54. Chen, T.Y., Peng, Y.W., Dhallan, R.S., Ahamed, B., Reed, R.R. & Yau, K.W. A new subunit of the cyclic nucleotide-gated cation channel in retinal rods. *Nature* **362**, 764-7 (1993).
55. Gerstner, A., Zong, X., Hofmann, F. & Biel, M. Molecular cloning and functional characterization of a new modulatory cyclic nucleotide-gated channel subunit from mouse retina. *J Neurosci* **20**, 1324-32 (2000).
56. Goulding, E.H., Ngai, J., Kramer, R.H., Colicos, S., Axel, R., Siegelbaum, S.A. & Chess, A. Molecular cloning and single-channel properties of the cyclic nucleotide-gated channel from catfish olfactory neurons. *Neuron* **8**, 45-58 (1992).
57. Liman, E.R. & Buck, L.B. A second subunit of the olfactory cyclic nucleotide-gated channel confers high sensitivity to cAMP. *Neuron* **13**, 611-21 (1994).
58. Sautter, A., Zong, X., Hofmann, F. & Biel, M. An isoform of the rod photoreceptor cyclic nucleotide-gated channel beta subunit expressed in olfactory neurons. *Proc Natl Acad Sci U S A* **95**, 4696-701 (1998).
59. Zheng, J., Trudeau, M.C. & Zagotta, W.N. Rod cyclic nucleotide-gated channels have a stoichiometry of three CNGA1 subunits and one CNGB1 subunit. *Neuron* **36**, 891-6 (2002).
60. Weitz, D., Ficek, N., Kremmer, E., Bauer, P.J. & Kaupp, U.B. Subunit stoichiometry of the CNG channel of rod photoreceptors. *Neuron* **36**, 881-9 (2002).
61. Zhong, H., Molday, L.L., Molday, R.S. & Yau, K.W. The heteromeric cyclic nucleotide-gated channel adopts a 3A:1B stoichiometry. *Nature* **420**, 193-8 (2002).
62. Peng, C., Rich, E.D. & Varnum, M.D. Subunit configuration of heteromeric cone cyclic nucleotide-gated channels. *Neuron* **42**, 401-10 (2004).
63. Zheng, J. & Zagotta, W.N. Stoichiometry and assembly of olfactory cyclic nucleotide-gated channels. *Neuron* **42**, 411-21 (2004).
64. Bonigk, W., Bradley, J., Muller, F., Sesti, F., Boehhoff, I., Ronnett, G.V., Kaupp, U.B. & Frings, S. The native rat olfactory cyclic nucleotide-gated channel is composed of three distinct subunits. *J Neurosci* **19**, 5332-47 (1999).
65. Munger, S.D., Lane, A.P., Zhong, H., Leinders-Zufall, T., Yau, K.W., Zufall, F. & Reed, R.R. Central role of the CNGA4 channel subunit in Ca²⁺-calmodulin-dependent odor adaptation. *Science* **294**, 2172-5 (2001).
66. Colville, C.A. & Molday, R.S. Primary structure and expression of the human beta-subunit and related proteins of the rod photoreceptor cGMP-gated channel. *J Biol Chem* **271**, 32968-74 (1996).

67. Pittler, S.J., Lee, A.K., Altherr, M.R., Howard, T.A., Seldin, M.F., Hurwitz, R.L., Wasmuth, J.J. & Baehr, W. Primary structure and chromosomal localization of human and mouse rod photoreceptor cGMP-gated cation channel. *J Biol Chem* **267**, 6257-62 (1992).
68. Yu, W.P., Grunwald, M.E. & Yau, K.W. Molecular cloning, functional expression and chromosomal localization of a human homolog of the cyclic nucleotide-gated ion channel of retinal cone photoreceptors. *FEBS Lett* **393**, 211-5 (1996).
69. Jan, L.Y. & Jan, Y.N. A superfamily of ion channels. *Nature* **345**, 672 (1990).
70. Molday, R.S., Molday, L.L., Dose, A., Clark-Lewis, I., Illing, M., Cook, N.J., Eismann, E. & Kaupp, U.B. The cGMP-gated channel of the rod photoreceptor cell characterization and orientation of the amino terminus. *J Biol Chem* **266**, 21917-22 (1991).
71. Wohlfart, P., Haase, W., Molday, R.S. & Cook, N.J. Antibodies against synthetic peptides used to determine the topology and site of glycosylation of the cGMP-gated channel from bovine rod photoreceptors. *J Biol Chem* **267**, 644-8 (1992).
72. Henn, D.K., Baumann, A. & Kaupp, U.B. Probing the transmembrane topology of cyclic nucleotide-gated ion channels with a gene fusion approach. *Proc Natl Acad Sci U S A* **92**, 7425-9 (1995).
73. Bezanilla, F. Voltage sensor movements. *J Gen Physiol* **120**, 465-73 (2002).
74. Tang, C.Y. & Papazian, D.M. Transfer of voltage independence from a rat olfactory channel to the *Drosophila* ether-a-go-go K⁺ channel. *J Gen Physiol* **109**, 301-11 (1997).
75. Doyle, D.A., Morais Cabral, J., Pfuetzner, R.A., Kuo, A., Gulbis, J.M., Cohen, S.L., Chait, B.T. & MacKinnon, R. The structure of the potassium channel: molecular basis of K⁺ conduction and selectivity. *Science* **280**, 69-77 (1998).
76. Flynn, G.E., Johnson, J.P., Jr. & Zagotta, W.N. Cyclic nucleotide-gated channels: shedding light on the opening of a channel pore. *Nat Rev Neurosci* **2**, 643-51 (2001).
77. Heginbotham, L., Lu, Z., Abramson, T. & MacKinnon, R. Mutations in the K⁺ channel signature sequence. *Biophys J* **66**, 1061-7 (1994).
78. Seifert, R., Eismann, E., Ludwig, J., Baumann, A. & Kaupp, U.B. Molecular determinants of a Ca²⁺-binding site in the pore of cyclic nucleotide-gated channels: S5/S6 segments control affinity of intrapore glutamates. *Embo J* **18**, 119-30 (1999).
79. Root, M.J. & MacKinnon, R. Identification of an external divalent cation-binding site in the pore of a cGMP-activated channel. *Neuron* **11**, 459-66 (1993).
80. Eismann, E., Muller, F., Heinemann, S.H. & Kaupp, U.B. A single negative charge within the pore region of a cGMP-gated channel controls rectification, Ca²⁺ blockage, and ionic selectivity. *Proc Natl Acad Sci U S A* **91**, 1109-13 (1994).
81. Goulding, E.H., Tibbs, G.R., Liu, D. & Siegelbaum, S.A. Role of H5 domain in determining pore diameter and ion permeation through cyclic nucleotide-gated channels. *Nature* **364**, 61-4 (1993).

82. Heginbotham, L., Abramson, T. & MacKinnon, R. A functional connection between the pores of distantly related ion channels as revealed by mutant K⁺ channels. *Science* **258**, 1152-5 (1992).
83. Qu, W., Moorhouse, A.J., Chandra, M., Pierce, K.D., Lewis, T.M. & Barry, P.H. A single P-loop glutamate point mutation to either lysine or arginine switches the cation-anion selectivity of the CNGA2 channel. *J Gen Physiol* **127**, 375-89 (2006).
84. Becchetti, A., Gamel, K. & Torre, V. Cyclic nucleotide-gated channels. Pore topology studied through the accessibility of reporter cysteines. *J Gen Physiol* **114**, 377-92 (1999).
85. Karpen, J.W., Brown, R.L., Stryer, L. & Baylor, D.A. Interactions between divalent cations and the gating machinery of cyclic GMP-activated channels in salamander retinal rods. *J Gen Physiol* **101**, 1-25 (1993).
86. Brown, R.L., Bert, R.J., Evans, F.E. & Karpen, J.W. Activation of retinal rod cGMP-gated channels: what makes for an effective 8-substituted derivative of cGMP? *Biochemistry* **32**, 10089-95 (1993).
87. McKay, D.B. & Steitz, T.A. Structure of catabolite gene activator protein at 2.9 Å resolution suggests binding to left-handed B-DNA. *Nature* **290**, 744-9 (1981).
88. Su, Y., Dostmann, W.R., Herberg, F.W., Durick, K., Xuong, N.H., Ten Eyck, L., Taylor, S.S. & Varughese, K.I. Regulatory subunit of protein kinase A: structure of deletion mutant with cAMP binding domains. *Science* **269**, 807-13 (1995).
89. Zagotta, W.N., Olivier, N.B., Black, K.D., Young, E.C., Olson, R. & Gouaux, E. Structural basis for modulation and agonist specificity of HCN pacemaker channels. *Nature* **425**, 200-5 (2003).
90. Craven, K.B. & Zagotta, W.N. CNG and HCN channels: two peas, one pod. *Annu Rev Physiol* **68**, 375-401 (2006).
91. Craven, K.B. & Zagotta, W.N. Salt bridges and gating in the COOH-terminal region of HCN2 and CNGA1 channels. *J Gen Physiol* **124**, 663-77 (2004).
92. Higgins, M.K., Weitz, D., Warne, T., Schertler, G.F. & Kaupp, U.B. Molecular architecture of a retinal cGMP-gated channel: the arrangement of the cytoplasmic domains. *Embo J* **21**, 2087-94 (2002).
93. Johnson, J.P., Jr. & Zagotta, W.N. The carboxyl-terminal region of cyclic nucleotide-modulated channels is a gating ring, not a permeation path. *Proc Natl Acad Sci U S A* **102**, 2742-7 (2005).
94. MacKinnon, R. Determination of the subunit stoichiometry of a voltage-activated potassium channel. *Nature* **350**, 232-5 (1991).
95. Liu, D.T., Tibbs, G.R. & Siegelbaum, S.A. Subunit stoichiometry of cyclic nucleotide-gated channels and effects of subunit order on channel function. *Neuron* **16**, 983-90 (1996).
96. Matulef, K. & Zagotta, W. Multimerization of the ligand binding domains of cyclic nucleotide-gated channels. *Neuron* **36**, 93-103 (2002).
97. Johnson, J.P., Jr. & Zagotta, W.N. Rotational movement during cyclic nucleotide-gated channel opening. *Nature* **412**, 917-21 (2001).
98. Gordon, S.E., Downing-Park, J. & Zimmerman, A.L. Modulation of the cGMP-gated ion channel in frog rods by calmodulin and an endogenous inhibitory factor. *J Physiol* **486** (Pt 3), 533-46 (1995).

99. Gordon, S.E., Varnum, M.D. & Zagotta, W.N. Direct interaction between amino- and carboxyl-terminal domains of cyclic nucleotide-gated channels. *Neuron* **19**, 431-41 (1997).
100. Varnum, M.D. & Zagotta, W.N. Interdomain interactions underlying activation of cyclic nucleotide-gated channels. *Science* **278**, 110-3 (1997).
101. Zheng, J., Varnum, M.D. & Zagotta, W.N. Disruption of an intersubunit interaction underlies Ca²⁺-calmodulin modulation of cyclic nucleotide-gated channels. *J Neurosci* **23**, 8167-75 (2003).
102. Liu, M., Chen, T.Y., Ahamed, B., Li, J. & Yau, K.W. Calcium-calmodulin modulation of the olfactory cyclic nucleotide-gated cation channel. *Science* **266**, 1348-54 (1994).
103. Li, M., Jan, Y.N. & Jan, L.Y. Specification of subunit assembly by the hydrophilic amino-terminal domain of the Shaker potassium channel. *Science* **257**, 1225-30 (1992).
104. Haynes, L.W., Kay, A.R. & Yau, K.W. Single cyclic GMP-activated channel activity in excised patches of rod outer segment membrane. *Nature* **321**, 66-70 (1986).
105. Zimmerman, A.L. & Baylor, D.A. Cyclic GMP-sensitive conductance of retinal rods consists of aqueous pores. *Nature* **321**, 70-2 (1986).
106. Zufall, F. & Firestein, S. Divalent cations block the cyclic nucleotide-gated channel of olfactory receptor neurons. *J Neurophysiol* **69**, 1758-68 (1993).
107. Colamartino, G., Menini, A. & Torre, V. Blockage and permeation of divalent cations through the cyclic GMP-activated channel from tiger salamander retinal rods. *J Physiol* **440**, 189-206 (1991).
108. Zimmerman, A.L. & Baylor, D.A. Cation interactions within the cyclic GMP-activated channel of retinal rods from the tiger salamander. *J Physiol* **449**, 759-83 (1992).
109. Frings, S., Seifert, R., Godde, M. & Kaupp, U.B. Profoundly different calcium permeation and blockage determine the specific function of distinct cyclic nucleotide-gated channels. *Neuron* **15**, 169-79 (1995).
110. Gavazzo, P., Picco, C., Eismann, E., Kaupp, U.B. & Menini, A. A point mutation in the pore region alters gating, Ca(2+) blockage, and permeation of olfactory cyclic nucleotide-gated channels. *J Gen Physiol* **116**, 311-26 (2000).
111. Dzeja, C., Hagen, V., Kaupp, U.B. & Frings, S. Ca²⁺ permeation in cyclic nucleotide-gated channels. *Embo J* **18**, 131-44 (1999).
112. Richards, M.J. & Gordon, S.E. Cooperativity and cooperation in cyclic nucleotide-gated ion channels. *Biochemistry* **39**, 14003-11 (2000).
113. Gordon, S.E. & Zagotta, W.N. Localization of regions affecting an allosteric transition in cyclic nucleotide-activated channels. *Neuron* **14**, 857-64 (1995).
114. Altenhofen, W., Ludwig, J., Eismann, E., Kraus, W., Bonigk, W. & Kaupp, U.B. Control of ligand specificity in cyclic nucleotide-gated channels from rod photoreceptors and olfactory epithelium. *Proc Natl Acad Sci U S A* **88**, 9868-72 (1991).
115. Varnum, M.D., Black, K.D. & Zagotta, W.N. Molecular mechanism for ligand discrimination of cyclic nucleotide-gated channels. *Neuron* **15**, 619-25 (1995).

116. Rich, T.C., Tse, T.E., Rohan, J.G., Schaack, J. & Karpen, J.W. In vivo assessment of local phosphodiesterase activity using tailored cyclic nucleotide-gated channels as cAMP sensors. *J Gen Physiol* **118**, 63-78 (2001).
117. Matulef, K., Flynn, G.E. & Zagotta, W.N. Molecular rearrangements in the ligand-binding domain of cyclic nucleotide-gated channels. *Neuron* **24**, 443-52 (1999).
118. Goulding, E.H., Tibbs, G.R. & Siegelbaum, S.A. Molecular mechanism of cyclic-nucleotide-gated channel activation. *Nature* **372**, 369-74 (1994).
119. Bucossi, G., Nizzari, M. & Torre, V. Single-channel properties of ionic channels gated by cyclic nucleotides. *Biophys J* **72**, 1165-81 (1997).
120. Gordon, S.E. & Zagotta, W.N. A histidine residue associated with the gate of the cyclic nucleotide-activated channels in rod photoreceptors. *Neuron* **14**, 177-83 (1995).
121. Zong, X., Zucker, H., Hofmann, F. & Biel, M. Three amino acids in the C-linker are major determinants of gating in cyclic nucleotide-gated channels. *Embo J* **17**, 353-62 (1998).
122. Paoletti, P., Young, E.C. & Siegelbaum, S.A. C-Linker of cyclic nucleotide-gated channels controls coupling of ligand binding to channel gating. *J Gen Physiol* **113**, 17-34 (1999).
123. Brown, R.L., Snow, S.D. & Haley, T.L. Movement of gating machinery during the activation of rod cyclic nucleotide-gated channels. *Biophys J* **75**, 825-33 (1998).
124. Grunwald, M.E., Zhong, H., Lai, J. & Yau, K.W. Molecular determinants of the modulation of cyclic nucleotide-activated channels by calmodulin. *Proc Natl Acad Sci U S A* **96**, 13444-9 (1999).
125. Tibbs, G.R., Goulding, E.H. & Siegelbaum, S.A. Allosteric activation and tuning of ligand efficacy in cyclic-nucleotide-gated channels. *Nature* **386**, 612-5 (1997).
126. Trudeau, M.C. & Zagotta, W.N. An intersubunit interaction regulates trafficking of rod cyclic nucleotide-gated channels and is disrupted in an inherited form of blindness. *Neuron* **34**, 197-207 (2002).
127. Ruiz, M., Brown, R.L., He, Y., Haley, T.L. & Karpen, J.W. The single-channel dose-response relation is consistently steep for rod cyclic nucleotide-gated channels: implications for the interpretation of macroscopic dose-response relations. *Biochemistry* **38**, 10642-8 (1999).
128. Karpen, J.W., Zimmerman, A.L., Stryer, L. & Baylor, D.A. Gating kinetics of the cyclic-GMP-activated channel of retinal rods: flash photolysis and voltage-jump studies. *Proc Natl Acad Sci U S A* **85**, 1287-91 (1988).
129. Li, J. & Lester, H.A. Single-channel kinetics of the rat olfactory cyclic nucleotide-gated channel expressed in *Xenopus* oocytes. *Mol Pharmacol* **55**, 883-93 (1999).
130. Ruiz, M.L. & Karpen, J.W. Single cyclic nucleotide-gated channels locked in different ligand-bound states. *Nature* **389**, 389-92 (1997).
131. Ruiz, M. & Karpen, J.W. Opening mechanism of a cyclic nucleotide-gated channel based on analysis of single channels locked in each liganded state. *J Gen Physiol* **113**, 873-95 (1999).

132. Picones, A. & Korenbrot, J.I. Spontaneous, ligand-independent activity of the cGMP-gated ion channels in cone photoreceptors of fish. *J Physiol* **485** (Pt 3), 699-714 (1995).
133. Benndorf, K., Koopmann, R., Eismann, E. & Kaupp, U.B. Gating by cyclic GMP and voltage in the alpha subunit of the cyclic GMP-gated channel from rod photoreceptors. *J Gen Physiol* **114**, 477-90 (1999).
134. Hanke, W., Cook, N.J. & Kaupp, U.B. cGMP-dependent channel protein from photoreceptor membranes: single-channel activity of the purified and reconstituted protein. *Proc Natl Acad Sci U S A* **85**, 94-8 (1988).
135. Monod, J., Wyman, J. & Changeux, J.P. On the Nature of Allosteric Transitions: a Plausible Model. *J Mol Biol* **12**, 88-118 (1965).
136. Varnum, M.D. & Zagotta, W.N. Subunit interactions in the activation of cyclic nucleotide-gated ion channels. *Biophys J* **70**, 2667-79 (1996).
137. Liu, D.T., Tibbs, G.R., Paoletti, P. & Siegelbaum, S.A. Constraining ligand-binding site stoichiometry suggests that a cyclic nucleotide-gated channel is composed of two functional dimers. *Neuron* **21**, 235-48 (1998).
138. Nache, V., Schulz, E., Zimmer, T., Kusch, J., Biskup, C., Koopmann, R., Hagen, V. & Benndorf, K. Activation of olfactory-type cyclic nucleotide-gated channels is highly cooperative. *J Physiol* **569**, 91-102 (2005).
139. Gordon, S.E., Brautigan, D.L. & Zimmerman, A.L. Protein phosphatases modulate the apparent agonist affinity of the light-regulated ion channel in retinal rods. *Neuron* **9**, 739-48 (1992).
140. Molokanova, E., Trivedi, B., Savchenko, A. & Kramer, R.H. Modulation of rod photoreceptor cyclic nucleotide-gated channels by tyrosine phosphorylation. *J Neurosci* **17**, 9068-76 (1997).
141. Molokanova, E., Maddox, F., Luetje, C.W. & Kramer, R.H. Activity-dependent modulation of rod photoreceptor cyclic nucleotide-gated channels mediated by phosphorylation of a specific tyrosine residue. *J Neurosci* **19**, 4786-95 (1999).
142. Molokanova, E., Savchenko, A. & Kramer, R.H. Noncatalytic inhibition of cyclic nucleotide-gated channels by tyrosine kinase induced by genistein. *J Gen Physiol* **113**, 45-56 (1999).
143. Molokanova, E., Savchenko, A. & Kramer, R.H. Interactions of cyclic nucleotide-gated channel subunits and protein tyrosine kinase probed with genistein. *J Gen Physiol* **115**, 685-96 (2000).
144. Molokanova, E. & Kramer, R.H. Mechanism of inhibition of cyclic nucleotide-gated channel by protein tyrosine kinase probed with genistein. *J Gen Physiol* **117**, 219-34 (2001).
145. Muller, F., Bonigk, W., Sesti, F. & Frings, S. Phosphorylation of mammalian olfactory cyclic nucleotide-gated channels increases ligand sensitivity. *J Neurosci* **18**, 164-73 (1998).
146. Trudeau, M.C. & Zagotta, W.N. Calcium/calmodulin modulation of olfactory and rod cyclic nucleotide-gated ion channels. *J Biol Chem* **278**, 18705-8 (2003).
147. Chen, T.Y., Illing, M., Molday, L.L., Hsu, Y.T., Yau, K.W. & Molday, R.S. Subunit 2 (or beta) of retinal rod cGMP-gated cation channel is a component of the 240-kDa channel-associated protein and mediates Ca(2+)-calmodulin modulation. *Proc Natl Acad Sci U S A* **91**, 11757-61 (1994).

148. Grunwald, M.E., Yu, W.P., Yu, H.H. & Yau, K.W. Identification of a domain on the beta-subunit of the rod cGMP-gated cation channel that mediates inhibition by calcium-calmodulin. *J Biol Chem* **273**, 9148-57 (1998).
149. Weitz, D., Zoche, M., Muller, F., Beyermann, M., Korschen, H.G., Kaupp, U.B. & Koch, K.W. Calmodulin controls the rod photoreceptor CNG channel through an unconventional binding site in the N-terminus of the beta-subunit. *Embo J* **17**, 2273-84 (1998).
150. Trudeau, M.C. & Zagotta, W.N. Mechanism of calcium/calmodulin inhibition of rod cyclic nucleotide-gated channels. *Proc Natl Acad Sci U S A* **99**, 8424-9 (2002).
151. Trudeau, M.C. & Zagotta, W.N. Dynamics of Ca²⁺-calmodulin-dependent inhibition of rod cyclic nucleotide-gated channels measured by patch-clamp fluorometry. *J Gen Physiol* **124**, 211-23 (2004).
152. Peng, C., Rich, E.D., Thor, C.A. & Varnum, M.D. Functionally important calmodulin-binding sites in both NH₂- and COOH-terminal regions of the cone photoreceptor cyclic nucleotide-gated channel CNGB3 subunit. *J Biol Chem* **278**, 24617-23 (2003).
153. Hsu, Y.T. & Molday, R.S. Modulation of the cGMP-gated channel of rod photoreceptor cells by calmodulin. *Nature* **361**, 76-9 (1993).
154. Nakatani, K., Koutalos, Y. & Yau, K.W. Ca²⁺ modulation of the cGMP-gated channel of bullfrog retinal rod photoreceptors. *J Physiol* **484** (Pt 1), 69-76 (1995).
155. Hackos, D.H. & Korenbrot, J.I. Calcium modulation of ligand affinity in the cyclic GMP-gated ion channels of cone photoreceptors. *J Gen Physiol* **110**, 515-28 (1997).
156. Rebrik, T.I. & Korenbrot, J.I. In intact cone photoreceptors, a Ca²⁺-dependent, diffusible factor modulates the cGMP-gated ion channels differently than in rods. *J Gen Physiol* **112**, 537-48 (1998).
157. Kramer, R.H. & Siegelbaum, S.A. Intracellular Ca²⁺ regulates the sensitivity of cyclic nucleotide-gated channels in olfactory receptor neurons. *Neuron* **9**, 897-906 (1992).
158. Kurahashi, T. & Menini, A. Mechanism of odorant adaptation in the olfactory receptor cell. *Nature* **385**, 725-9 (1997).
159. Zufall, F. & Leinders-Zufall, T. The cellular and molecular basis of odor adaptation. *Chem Senses* **25**, 473-81 (2000).
160. Chen, T.Y. & Yau, K.W. Direct modulation by Ca²⁺-calmodulin of cyclic nucleotide-activated channel of rat olfactory receptor neurons. *Nature* **368**, 545-8 (1994).
161. O'Neil, K.T. & DeGrado, W.F. How calmodulin binds its targets: sequence independent recognition of amphiphilic alpha-helices. *Trends Biochem Sci* **15**, 59-64 (1990).
162. Bradley, J., Bonigk, W., Yau, K.W. & Frings, S. Calmodulin permanently associates with rat olfactory CNG channels under native conditions. *Nat Neurosci* **7**, 705-10 (2004).
163. Bradley, J., Reuter, D. & Frings, S. Facilitation of calmodulin-mediated odor adaptation by cAMP-gated channel subunits. *Science* **294**, 2176-8 (2001).

164. Kelliher, K.R., Ziesmann, J., Munger, S.D., Reed, R.R. & Zufall, F. Importance of the CNGA4 channel gene for odor discrimination and adaptation in behaving mice. *Proc Natl Acad Sci U S A* **100**, 4299-304 (2003).
165. Dean, D.M., Nguitragool, W., Miri, A., McCabe, S.L. & Zimmerman, A.L. All-trans-retinal shuts down rod cyclic nucleotide-gated ion channels: a novel role for photoreceptor retinoids in the response to bright light? *Proc Natl Acad Sci U S A* **99**, 8372-7 (2002).
166. McCabe, S.L., Pelosi, D.M., Tetreault, M., Miri, A., Nguitragool, W., Kovithathanaphong, P., Mahajan, R. & Zimmerman, A.L. All-trans-retinal is a closed-state inhibitor of rod cyclic nucleotide-gated ion channels. *J Gen Physiol* **123**, 521-31 (2004).
167. Horrigan, D.M., Tetreault, M.L., Tsomaia, N., Vasileiou, C., Borhan, B., Mierke, D.F., Crouch, R.K. & Zimmerman, A.L. Defining the retinoid binding site in the rod cyclic nucleotide-gated channel. *J Gen Physiol* **126**, 453-60 (2005).
168. Czech, M.P. PIP2 and PIP3: complex roles at the cell surface. *Cell* **100**, 603-6 (2000).
169. Cantley, L.C. The phosphoinositide 3-kinase pathway. *Science* **296**, 1655-7 (2002).
170. Lemmon, M.A. Phosphoinositide recognition domains. *Traffic* **4**, 201-13 (2003).
171. Insall, R.H. & Weiner, O.D. PIP3, PIP2, and cell movement--similar messages, different meanings? *Dev Cell* **1**, 743-7 (2001).
172. McLaughlin, S. & Murray, D. Plasma membrane phosphoinositide organization by protein electrostatics. *Nature* **438**, 605-11 (2005).
173. Ishii, M., Inanobe, A. & Kurachi, Y. PIP3 inhibition of RGS protein and its reversal by Ca²⁺/calmodulin mediate voltage-dependent control of the G protein cycle in a cardiac K⁺ channel. *Proc Natl Acad Sci U S A* **99**, 4325-30 (2002).
174. Hokanson, D.E. & Ostap, E.M. Myo1c binds tightly and specifically to phosphatidylinositol 4,5-bisphosphate and inositol 1,4,5-trisphosphate. *Proc Natl Acad Sci U S A* **103**, 3118-23 (2006).
175. Ananthanarayanan, B., Ni, Q. & Zhang, J. Signal propagation from membrane messengers to nuclear effectors revealed by reporters of phosphoinositide dynamics and Akt activity. *Proc Natl Acad Sci U S A* **102**, 15081-6 (2005).
176. Gordon, S.E., Downing-Park, J., Tam, B. & Zimmerman, A.L. Diacylglycerol analogs inhibit the rod cGMP-gated channel by a phosphorylation-independent mechanism. *Biophys J* **69**, 409-17 (1995).
177. Crary, J.I., Dean, D.M., Nguitragool, W., Kurshan, P.T. & Zimmerman, A.L. Mechanism of inhibition of cyclic nucleotide-gated ion channels by diacylglycerol. *J Gen Physiol* **116**, 755-68 (2000).
178. Crary, J.I., Dean, D.M., Maroof, F. & Zimmerman, A.L. Mutation of a single residue in the S2-S3 loop of CNG channels alters the gating properties and sensitivity to inhibitors. *J Gen Physiol* **116**, 769-80 (2000).
179. Womack, K.B., Gordon, S.E., He, F., Wensel, T.G., Lu, C.C. & Hilgemann, D.W. Do phosphatidylinositides modulate vertebrate phototransduction? *J Neurosci* **20**, 2792-9 (2000).

180. Spehr, M., Wetzel, C.H., Hatt, H. & Ache, B.W. 3-phosphoinositides modulate cyclic nucleotide signaling in olfactory receptor neurons. *Neuron* **33**, 731-9 (2002).
181. Zhainazarov, A.B., Spehr, M., Wetzel, C.H., Hatt, H. & Ache, B.W. Modulation of the olfactory CNG channel by PtdIns(3,4,5)P₃. *J Membr Biol* **201**, 51-7 (2004).
182. Huang, C.L., Feng, S. & Hilgemann, D.W. Direct activation of inward rectifier potassium channels by PIP₂ and its stabilization by Gbetagamma. *Nature* **391**, 803-6 (1998).
183. Rohacs, T., Lopes, C.M., Jin, T., Ramdya, P.P., Molnar, Z. & Logothetis, D.E. Specificity of activation by phosphoinositides determines lipid regulation of Kir channels. *Proc Natl Acad Sci U S A* **100**, 745-50 (2003).
184. MacGregor, G.G., Dong, K., Vanoye, C.G., Tang, L., Giebisch, G. & Hebert, S.C. Nucleotides and phospholipids compete for binding to the C terminus of KATP channels. *Proc Natl Acad Sci U S A* **99**, 2726-31 (2002).
185. Enkvetchakul, D., Jeliaskova, I. & Nichols, C.G. Direct modulation of Kir channel gating by membrane phosphatidylinositol 4,5-bisphosphate. *J Biol Chem* **280**, 35785-8 (2005).
186. Cukras, C.A., Jeliaskova, I. & Nichols, C.G. Structural and functional determinants of conserved lipid interaction domains of inward rectifying Kir6.2 channels. *J Gen Physiol* **119**, 581-91 (2002).
187. Dong, K., Tang, L., MacGregor, G.G. & Hebert, S.C. Localization of the ATP/phosphatidylinositol 4,5 diphosphate-binding site to a 39-amino acid region of the carboxyl terminus of the ATP-regulated K⁺ channel Kir1.1. *J Biol Chem* **277**, 49366-73 (2002).
188. Zhang, H., He, C., Yan, X., Mirshahi, T. & Logothetis, D.E. Activation of inwardly rectifying K⁺ channels by distinct PtdIns(4,5)P₂ interactions. *Nat Cell Biol* **1**, 183-8 (1999).
189. Shyng, S.L. & Nichols, C.G. Membrane phospholipid control of nucleotide sensitivity of KATP channels. *Science* **282**, 1138-41 (1998).
190. Shyng, S.L., Cukras, C.A., Harwood, J. & Nichols, C.G. Structural determinants of PIP(2) regulation of inward rectifier K(ATP) channels. *J Gen Physiol* **116**, 599-608 (2000).
191. Zhang, H., Craciun, L.C., Mirshahi, T., Rohacs, T., Lopes, C.M., Jin, T. & Logothetis, D.E. PIP(2) activates KCNQ channels, and its hydrolysis underlies receptor-mediated inhibition of M currents. *Neuron* **37**, 963-75 (2003).
192. Prescott, E.D. & Julius, D. A modular PIP₂ binding site as a determinant of capsaicin receptor sensitivity. *Science* **300**, 1284-8 (2003).
193. Chemin, J., Patel, A.J., Duprat, F., Lauritzen, I., Lazdunski, M. & Honore, E. A phospholipid sensor controls mechanogating of the K⁺ channel TREK-1. *Embo J* **24**, 44-53 (2005).
194. Oliver, D., Lien, C.C., Soom, M., Baukrowitz, T., Jonas, P. & Fakler, B. Functional conversion between A-type and delayed rectifier K⁺ channels by membrane lipids. *Science* **304**, 265-70 (2004).
195. Pochynyuk, O., Staruschenko, A., Tong, Q., Medina, J. & Stockand, J.D. Identification of a functional phosphatidylinositol 3,4,5-trisphosphate binding site in the epithelial Na⁺ channel. *J Biol Chem* **280**, 37565-71 (2005).

196. Hilgemann, D.W., Feng, S. & Nasuhoglu, C. The complex and intriguing lives of PIP2 with ion channels and transporters. *Sci STKE* **2001**, RE19 (2001).
197. Rich, T.C., Fagan, K.A., Nakata, H., Schaack, J., Cooper, D.M. & Karpen, J.W. Cyclic nucleotide-gated channels colocalize with adenylyl cyclase in regions of restricted cAMP diffusion. *J Gen Physiol* **116**, 147-61 (2000).
198. Fagan, K.A., Schaack, J., Zweifach, A. & Cooper, D.M. Adenovirus encoded cyclic nucleotide-gated channels: a new methodology for monitoring cAMP in living cells. *FEBS Lett* **500**, 85-90 (2001).
199. Rich, T.C., Xin, W., Mehats, C., Hassell, K.A., Piggott, L., Le, X., Karpen, J.W. & Conti, M. Cellular mechanisms underlying prostaglandin-induced transient cAMP signals near the plasma membrane of HEK-293 cells. *Am J Physiol Cell Physiol* (2006).
200. Rich, T.C., Fagan, K.A., Tse, T.E., Schaack, J., Cooper, D.M. & Karpen, J.W. A uniform extracellular stimulus triggers distinct cAMP signals in different compartments of a simple cell. *Proc Natl Acad Sci U S A* **98**, 13049-54 (2001).
201. Huttl, S., Michalakis, S., Seeliger, M., Luo, D.G., Acar, N., Geiger, H., Hudl, K., Mader, R., Haverkamp, S., Moser, M., Pfeifer, A., Gerstner, A., Yau, K.W. & Biel, M. Impaired channel targeting and retinal degeneration in mice lacking the cyclic nucleotide-gated channel subunit CNGB1. *J Neurosci* **25**, 130-8 (2005).
202. Jenkins, P.M., Hurd, T.W., Zhang, L., McEwen, D.P., Brown, R.L., Margolis, B., Verhey, K.J. & Martens, J.R. Ciliary targeting of olfactory CNG channels requires the CNGB1b subunit and the kinesin-2 motor protein, KIF17. *Curr Biol* **16**, 1211-6 (2006).
203. Martens, J.R., Navarro-Polanco, R., Coppock, E.A., Nishiyama, A., Parshley, L., Grobaski, T.D. & Tamkun, M.M. Differential targeting of Shaker-like potassium channels to lipid rafts. *J Biol Chem* **275**, 7443-6 (2000).
204. London, E. & Brown, D.A. Insolubility of lipids in triton X-100: physical origin and relationship to sphingolipid/cholesterol membrane domains (rafts). *Biochim Biophys Acta* **1508**, 182-95 (2000).
205. Shogomori, H. & Brown, D.A. Use of detergents to study membrane rafts: the good, the bad, and the ugly. *Biol Chem* **384**, 1259-63 (2003).
206. Silvius, J.R., del Giudice, D. & Lafleur, M. Cholesterol at different bilayer concentrations can promote or antagonize lateral segregation of phospholipids of differing acyl chain length. *Biochemistry* **35**, 15198-208 (1996).
207. Ahmed, S.N., Brown, D.A. & London, E. On the origin of sphingolipid/cholesterol-rich detergent-insoluble cell membranes: physiological concentrations of cholesterol and sphingolipid induce formation of a detergent-insoluble, liquid-ordered lipid phase in model membranes. *Biochemistry* **36**, 10944-53 (1997).
208. Schroeder, R.J., Ahmed, S.N., Zhu, Y., London, E. & Brown, D.A. Cholesterol and sphingolipid enhance the Triton X-100 insolubility of glycosylphosphatidylinositol-anchored proteins by promoting the formation of detergent-insoluble ordered membrane domains. *J Biol Chem* **273**, 1150-7 (1998).
209. Xu, X. & London, E. The effect of sterol structure on membrane lipid domains reveals how cholesterol can induce lipid domain formation. *Biochemistry* **39**, 843-9 (2000).

210. Hanada, K., Nishijima, M., Akamatsu, Y. & Pagano, R.E. Both sphingolipids and cholesterol participate in the detergent insolubility of alkaline phosphatase, a glycosylphosphatidylinositol-anchored protein, in mammalian membranes. *J Biol Chem* **270**, 6254-60 (1995).
211. Rietveld, A. & Simons, K. The differential miscibility of lipids as the basis for the formation of functional membrane rafts. *Biochim Biophys Acta* **1376**, 467-79 (1998).
212. Brown, D.A. Interactions between GPI-anchored proteins and membrane lipids. *Trends Cell Biol* **2**, 338-43 (1992).
213. Brown, D.A. & Rose, J.K. Sorting of GPI-anchored proteins to glycolipid-enriched membrane subdomains during transport to the apical cell surface. *Cell* **68**, 533-44 (1992).
214. Melkonian, K.A., Chu, T., Tortorella, L.B. & Brown, D.A. Characterization of proteins in detergent-resistant membrane complexes from Madin-Darby canine kidney epithelial cells. *Biochemistry* **34**, 16161-70 (1995).
215. Simons, K. & Toomre, D. Lipid rafts and signal transduction. *Nat Rev Mol Cell Biol* **1**, 31-9 (2000).
216. Guirland, C., Suzuki, S., Kojima, M., Lu, B. & Zheng, J.Q. Lipid rafts mediate chemotropic guidance of nerve growth cones. *Neuron* **42**, 51-62 (2004).
217. Edidin, M. The state of lipid rafts: from model membranes to cells. *Annu Rev Biophys Biomol Struct* **32**, 257-83 (2003).
218. Heerklotz, H. Triton promotes domain formation in lipid raft mixtures. *Biophys J* **83**, 2693-701 (2002).
219. Kabouridis, P.S. Lipid rafts in T cell receptor signalling. *Mol Membr Biol* **23**, 49-57 (2006).
220. Ohtani, Y., Irie, T., Uekama, K., Fukunaga, K. & Pitha, J. Differential effects of alpha-, beta- and gamma-cyclodextrins on human erythrocytes. *Eur J Biochem* **186**, 17-22 (1989).
221. Kilsdonk, E.P., Yancey, P.G., Stoudt, G.W., Bangerter, F.W., Johnson, W.J., Phillips, M.C. & Rothblat, G.H. Cellular cholesterol efflux mediated by cyclodextrins. *J Biol Chem* **270**, 17250-6 (1995).
222. Yancey, P.G., Rodriguez, W.V., Kilsdonk, E.P., Stoudt, G.W., Johnson, W.J., Phillips, M.C. & Rothblat, G.H. Cellular cholesterol efflux mediated by cyclodextrins. Demonstration Of kinetic pools and mechanism of efflux. *J Biol Chem* **271**, 16026-34 (1996).
223. Christian, A.E., Haynes, M.P., Phillips, M.C. & Rothblat, G.H. Use of cyclodextrins for manipulating cellular cholesterol content. *J Lipid Res* **38**, 2264-72 (1997).
224. Szejtli, J. Introduction and General Overview of Cyclodextrin Chemistry. *Chem Rev* **98**, 1743-1754 (1998).
225. Chen, X. & Resh, M.D. Cholesterol depletion from the plasma membrane triggers ligand-independent activation of the epidermal growth factor receptor. *J Biol Chem* **277**, 49631-7 (2002).
226. Subtil, A., Gaidarov, I., Kobylarz, K., Lampson, M.A., Keen, J.H. & McGraw, T.E. Acute cholesterol depletion inhibits clathrin-coated pit budding. *Proc Natl Acad Sci U S A* **96**, 6775-80 (1999).

227. Kwik, J., Boyle, S., Fooksman, D., Margolis, L., Sheetz, M.P. & Edidin, M. Membrane cholesterol, lateral mobility, and the phosphatidylinositol 4,5-bisphosphate-dependent organization of cell actin. *Proc Natl Acad Sci U S A* **100**, 13964-9 (2003).
228. Byfield, F.J., Aranda-Espinoza, H., Romanenko, V.G., Rothblat, G.H. & Levitan, I. Cholesterol depletion increases membrane stiffness of aortic endothelial cells. *Biophys J* **87**, 3336-43 (2004).
229. Manes, S. & Martinez, A.C. Cholesterol domains regulate the actin cytoskeleton at the leading edge of moving cells. *Trends Cell Biol* **14**, 275-8 (2004).
230. Manes, S. & Viola, A. Lipid rafts in lymphocyte activation and migration. *Mol Membr Biol* **23**, 59-69 (2006).
231. Pizzo, P., Giurisato, E., Tassi, M., Benedetti, A., Pozzan, T. & Viola, A. Lipid rafts and T cell receptor signaling: a critical re-evaluation. *Eur J Immunol* **32**, 3082-91 (2002).
232. Rybin, V.O., Xu, X., Lisanti, M.P. & Steinberg, S.F. Differential targeting of beta-adrenergic receptor subtypes and adenylyl cyclase to cardiomyocyte caveolae. A mechanism to functionally regulate the cAMP signaling pathway. *J Biol Chem* **275**, 41447-57 (2000).
233. Crosshwaite, A.J., Seebacher, T., Masada, N., Ciruela, A., Dufraux, K., Schultz, J.E. & Cooper, D.M. The cytosolic domains of Ca²⁺-sensitive adenylyl cyclases dictate their targeting to plasma membrane lipid rafts. *J Biol Chem* **280**, 6380-91 (2005).
234. Fagan, K.A., Smith, K.E. & Cooper, D.M. Regulation of the Ca²⁺-inhibitable adenylyl cyclase type VI by capacitative Ca²⁺ entry requires localization in cholesterol-rich domains. *J Biol Chem* **275**, 26530-7 (2000).
235. Ostrom, R.S., Gregorian, C., Drenan, R.M., Xiang, Y., Regan, J.W. & Insel, P.A. Receptor number and caveolar co-localization determine receptor coupling efficiency to adenylyl cyclase. *J Biol Chem* **276**, 42063-9 (2001).
236. Ostrom, R.S., Liu, X., Head, B.P., Gregorian, C., Seasholtz, T.M. & Insel, P.A. Localization of adenylyl cyclase isoforms and G protein-coupled receptors in vascular smooth muscle cells: expression in caveolin-rich and noncaveolin domains. *Mol Pharmacol* **62**, 983-92 (2002).
237. Ostrom, R.S., Violin, J.D., Coleman, S. & Insel, P.A. Selective enhancement of beta-adrenergic receptor signaling by overexpression of adenylyl cyclase type 6: colocalization of receptor and adenylyl cyclase in caveolae of cardiac myocytes. *Mol Pharmacol* **57**, 1075-9 (2000).
238. Martens, J.R., O'Connell, K. & Tamkun, M. Targeting of ion channels to membrane microdomains: localization of KV channels to lipid rafts. *Trends Pharmacol Sci* **25**, 16-21 (2004).
239. O'Connell, K.M., Martens, J.R. & Tamkun, M.M. Localization of ion channels to lipid Raft domains within the cardiovascular system. *Trends Cardiovasc Med* **14**, 37-42 (2004).
240. Bruses, J.L., Chauvet, N. & Rutishauser, U. Membrane lipid rafts are necessary for the maintenance of the (alpha)7 nicotinic acetylcholine receptor in somatic spines of ciliary neurons. *J Neurosci* **21**, 504-12 (2001).

241. Melkonian, K.A., Ostermeyer, A.G., Chen, J.Z., Roth, M.G. & Brown, D.A. Role of lipid modifications in targeting proteins to detergent-resistant membrane rafts. Many raft proteins are acylated, while few are prenylated. *J Biol Chem* **274**, 3910-7 (1999).
242. Moffett, S., Brown, D.A. & Linder, M.E. Lipid-dependent targeting of G proteins into rafts. *J Biol Chem* **275**, 2191-8 (2000).
243. Okamoto, T., Schlegel, A., Scherer, P.E. & Lisanti, M.P. Caveolins, a family of scaffolding proteins for organizing "preassembled signaling complexes" at the plasma membrane. *J Biol Chem* **273**, 5419-22 (1998).
244. Schreiber, S., Fleischer, J., Breer, H. & Boekhoff, I. A possible role for caveolin as a signaling organizer in olfactory sensory membranes. *J Biol Chem* **275**, 24115-23 (2000).
245. Mahfoud, R., Garmy, N., Maresca, M., Yahi, N., Puigserver, A. & Fantini, J. Identification of a common sphingolipid-binding domain in Alzheimer, prion, and HIV-1 proteins. *J Biol Chem* **277**, 11292-6 (2002).
246. Anderson, R.G. & Jacobson, K. A role for lipid shells in targeting proteins to caveolae, rafts, and other lipid domains. *Science* **296**, 1821-5 (2002).
247. Martens, J.R., Sakamoto, N., Sullivan, S.A., Grobaski, T.D. & Tamkun, M.M. Isoform-specific localization of voltage-gated K⁺ channels to distinct lipid raft populations. Targeting of Kv1.5 to caveolae. *J Biol Chem* **276**, 8409-14 (2001).
248. Romanenko, V.G., Rothblat, G.H. & Levitan, I. Modulation of endothelial inward-rectifier K⁺ current by optical isomers of cholesterol. *Biophys J* **83**, 3211-22 (2002).
249. Romanenko, V.G., Rothblat, G.H. & Levitan, I. Sensitivity of volume-regulated anion current to cholesterol structural analogues. *J Gen Physiol* **123**, 77-87 (2004).
250. Lundbaek, J.A., Birn, P., Hansen, A.J., Sogaard, R., Nielsen, C., Girshman, J., Bruno, M.J., Tape, S.E., Egebjerg, J., Greathouse, D.V., Mattice, G.L., Koeppe, R.E., 2nd & Andersen, O.S. Regulation of sodium channel function by bilayer elasticity: the importance of hydrophobic coupling. Effects of Micelle-forming amphiphiles and cholesterol. *J Gen Physiol* **123**, 599-621 (2004).
251. Brady, J.D., Rich, T.C., Le, X., Stafford, K., Fowler, C.J., Lynch, L., Karpen, J.W., Brown, R.L. & Martens, J.R. Functional role of lipid raft microdomains in cyclic nucleotide-gated channel activation. *Mol Pharmacol* **65**, 503-11 (2004).
252. Brady, J.D., Rich, E.D., Martens, J.R., Karpen, J.W., varnum, M.D. & Brown, R.L. Interplay Between PIP₃ and Calmodulin Regulation of Olfactory Cyclic Nucleotide-Gated Channels. *Proc Natl Acad Sci U S A* **In Press**(2006).
253. Finn, J.T., Grunwald, M.E. & Yau, K.W. Cyclic nucleotide-gated ion channels: an extended family with diverse functions. *Annu Rev Physiol* **58**, 395-426 (1996).
254. Griffith, L.C. Potassium channels: the importance of transport signals. *Curr Biol* **11**, R226-8 (2001).
255. Baylor, D.A., Lamb, T.D. & Yau, K.W. The membrane current of single rod outer segments. *J Physiol* **288**, 589-611 (1979).
256. Seno, K., Kishimoto, M., Abe, M., Higuchi, Y., Mieda, M., Owada, Y., Yoshiyama, W., Liu, H. & Hayashi, F. Light- and guanosine 5'-3-O-(thio)triphosphate-sensitive localization of a G protein and its effector on

- detergent-resistant membrane rafts in rod photoreceptor outer segments. *J Biol Chem* **276**, 20813-6 (2001).
257. Simons, K. & Ikonen, E. Functional rafts in cell membranes. *Nature* **387**, 569-72 (1997).
258. Brown, D.A. & London, E. Structure and origin of ordered lipid domains in biological membranes. *J Membr Biol* **164**, 103-14 (1998).
259. Magee, T., Pirinen, N., Adler, J., Pagakis, S.N. & Parmryd, I. Lipid rafts: cell surface platforms for T cell signaling. *Biol Res* **35**, 127-31 (2002).
260. Anderson, R.G. The caveolae membrane system. *Annu Rev Biochem* **67**, 199-225 (1998).
261. Smart, E.J., Ying, Y.S., Mineo, C. & Anderson, R.G. A detergent-free method for purifying caveolae membrane from tissue culture cells. *Proc Natl Acad Sci U S A* **92**, 10104-8 (1995).
262. Harder, T., Scheiffele, P., Verkade, P. & Simons, K. Lipid domain structure of the plasma membrane revealed by patching of membrane components. *J Cell Biol* **141**, 929-42 (1998).
263. Ostermeyer, A.G., Beckrich, B.T., Ivarson, K.A., Grove, K.E. & Brown, D.A. Glycosphingolipids are not essential for formation of detergent-resistant membrane rafts in melanoma cells. methyl-beta-cyclodextrin does not affect cell surface transport of a GPI-anchored protein. *J Biol Chem* **274**, 34459-66 (1999).
264. Bravo-Zehnder, M., Orio, P., Norambuena, A., Wallner, M., Meera, P., Toro, L., Latorre, R. & Gonzalez, A. Apical sorting of a voltage- and Ca²⁺-activated K⁺ channel alpha -subunit in Madin-Darby canine kidney cells is independent of N-glycosylation. *Proc Natl Acad Sci U S A* **97**, 13114-9 (2000).
265. Benting, J.H., Rietveld, A.G. & Simons, K. N-Glycans mediate the apical sorting of a GPI-anchored, raft-associated protein in Madin-Darby canine kidney cells. *J Cell Biol* **146**, 313-20 (1999).
266. Sowa, G., Pypaert, M. & Sessa, W.C. Distinction between signaling mechanisms in lipid rafts vs. caveolae. *Proc Natl Acad Sci U S A* **98**, 14072-7 (2001).
267. Foster, L.J., De Hoog, C.L. & Mann, M. Unbiased quantitative proteomics of lipid rafts reveals high specificity for signaling factors. *Proc Natl Acad Sci U S A* **100**, 5813-8 (2003).
268. Martinac, B. & Hamill, O.P. Gramicidin A channels switch between stretch activation and stretch inactivation depending on bilayer thickness. *Proc Natl Acad Sci U S A* **99**, 4308-12 (2002).
269. Valiyaveetil, F.I., Zhou, Y. & MacKinnon, R. Lipids in the structure, folding, and function of the KcsA K⁺ channel. *Biochemistry* **41**, 10771-7 (2002).
270. Kramer, R.H. & Molokanova, E. Modulation of cyclic-nucleotide-gated channels and regulation of vertebrate phototransduction. *J Exp Biol* **204**, 2921-31 (2001).
271. Schwencke, C., Yamamoto, M., Okumura, S., Toya, Y., Kim, S.J. & Ishikawa, Y. Compartmentation of cyclic adenosine 3',5'-monophosphate signaling in caveolae. *Mol Endocrinol* **13**, 1061-70 (1999).
272. Lamb, M.E., Zhang, C., Shea, T., Kyle, D.J. & Leeb-Lundberg, L.M. Human B1 and B2 bradykinin receptors and their agonists target caveolae-related lipid rafts to different degrees in HEK293 cells. *Biochemistry* **41**, 14340-7 (2002).

273. Cordeaux, Y. & Hill, S.J. Mechanisms of cross-talk between G-protein-coupled receptors. *Neurosignals* **11**, 45-57 (2002).
274. Smith, K.E., Gu, C., Fagan, K.A., Hu, B. & Cooper, D.M. Residence of adenylyl cyclase type 8 in caveolae is necessary but not sufficient for regulation by capacitative Ca(2+) entry. *J Biol Chem* **277**, 6025-31 (2002).
275. Balasubramanian, S., Lynch, J.W. & Barry, P.H. Calcium-dependent modulation of the agonist affinity of the mammalian olfactory cyclic nucleotide-gated channel by calmodulin and a novel endogenous factor. *J Membr Biol* **152**, 13-23 (1996).
276. Schroeder, F., Jefferson, J.R., Kier, A.B., Knittel, J., Scallen, T.J., Wood, W.G. & Hapala, I. Membrane cholesterol dynamics: cholesterol domains and kinetic pools. *Proc Soc Exp Biol Med* **196**, 235-52 (1991).
277. Rothblat, G.H., Mahlberg, F.H., Johnson, W.J. & Phillips, M.C. Apolipoproteins, membrane cholesterol domains, and the regulation of cholesterol efflux. *J Lipid Res* **33**, 1091-7 (1992).
278. Haynes, M.P., Phillips, M.C. & Rothblat, G.H. Efflux of cholesterol from different cellular pools. *Biochemistry* **39**, 4508-17 (2000).
279. Buck, L. & Axel, R. A novel multigene family may encode odorant receptors: a molecular basis for odor recognition. *Cell* **65**, 175-87 (1991).
280. Ronnett, G.V. & Moon, C. G proteins and olfactory signal transduction. *Annu Rev Physiol* **64**, 189-222 (2002).
281. Ache, B.W. & Young, J.M. Olfaction: diverse species, conserved principles. *Neuron* **48**, 417-30 (2005).
282. Axel, R. Scents and sensibility: a molecular logic of olfactory perception (Nobel lecture). *Angew Chem Int Ed Engl* **44**, 6110-27 (2005).
283. Kleene, S.J. Origin of the chloride current in olfactory transduction. *Neuron* **11**, 123-32 (1993).
284. Kolesnikov, S.S. & Kosolapov, A.V. Cyclic nucleotide-activated channels in carp olfactory receptor cells. *Biochim. Biophys. Acta.* **1150**, 63-72 (1993).
285. Reisert, J., Lai, J., Yau, K.W. & Bradley, J. Mechanism of the excitatory Cl⁻ response in mouse olfactory receptor neurons. *Neuron* **45**, 553-561 (2005).
286. Bradley, J., Reisert, J. & Frings, S. Regulation of cyclic nucleotide-gated channels. *Curr Opin Neurobiol* **15**, 343-9 (2005).
287. Chen, T.Y. & Yau, K.-W. Direct modulation by Ca²⁺-calmodulin of cyclic nucleotide-activated channel of rat olfactory receptor neurons. *Nature* **368**, 545-548 (1994).
288. Liu, M., Chen, T.Y., Ahamed, B., Li, J. & Yau, K.-W. Calcium-calmodulin modulation of the olfactory cyclic nucleotide-gated cation channel. *Science* **266**, 1348-1354 (1994).
289. Varnum, M.D. & Zagotta, W.N. Interdomain interactions underlying activation of cyclic nucleotide-gated channels. *Science* **278**, 110-113 (1997).
290. Trudeau, M.C. & Zagotta, W.N. Calcium/calmodulin modulation of olfactory and rod cyclic nucleotide-gated ion channels. *J. Biol. Chem.* **278**, 18705-18708 (2003).
291. Zheng, J., Varnum, M.D. & Zagotta, W.N. Disruption of an intersubunit interaction underlies Ca²⁺-calmodulin modulation of cyclic nucleotide-gated channels. *J. Neurosci.* **23**, 8167-8175 (2003).

292. Sautter, A., Zong, X., Hofmann, F. & Biel, M. An isoform of the rod photoreceptor cyclic nucleotide-gated channel beta subunit expressed in olfactory neurons. *Proc. Natl. Acad. Sci. U S A* **95**, 4696-4701 (1998).
293. Bonigk, W., Bradley, J., Muller, F., Sesti, F., Boekhoff, I., Ronnett, G.V., Kaupp, U.B. & Frings, S. The native rat olfactory cyclic nucleotide-gated channel is composed of three distinct subunits. *J. Neurosci.* **19**, 5332-5347 (1999).
294. Bradley, J., Bonigk, W., Yau, K.W. & Frings, S. Calmodulin permanently associates with rat olfactory CNG channels under native conditions. *Nat. Neurosci.* **7**, 705-710 (2004).
295. Gordon, S.E., Downing-Park, J., Tam, B. & Zimmerman, A.L. Diacylglycerol analogs inhibit the rod cGMP-gated channel by a phosphorylation-independent mechanism. *Biophys. J.* **69**, 409-417 (1995).
296. Crary, J.I., Dean, D.M., Nguiragool, W., Kurshan, P.T. & Zimmerman, A.L. Mechanism of inhibition of cyclic nucleotide-gated ion channels by diacylglycerol. *J. Gen. Physiol.* **116**, 755-768 (2000).
297. Dean, D.M., Nguiragool, W., Miri, A., McCabe, S.L. & Zimmerman, A.L. All-trans-retinal shuts down rod cyclic nucleotide-gated ion channels: a novel role for photoreceptor retinoids in the response to bright light? *Proc. Natl. Acad. Sci. U S A* **99**, 8372-8377 (2002).
298. Brady, J.D., Rich, T.C., Le, X., Stafford, K., Fowler, C.J., Lynch, L., Karpen, J.W., Brown, R.L. & Martens, J.R. Functional role of lipid raft microdomains in cyclic nucleotide-gated channel activation. *Mol. Pharmacol.* **65**, 503-511 (2004).
299. Grunwald, M.E., Zhong, H., Lai, J. & Yau, K.W. Molecular determinants of the modulation of cyclic nucleotide-activated channels by calmodulin. *Proc. Natl. Acad. Sci. U S A* **96**, 13444-13449 (1999).
300. Bradley, J., Reuter, D. & Frings, S. Facilitation of calmodulin-mediated odor adaptation by cAMP-gated channel subunits. *Science* **294**, 2176-2178 (2001).
301. Munger, S.D., Lane, A.P., Zhong, H., Leinders-Zufall, T., Yau, K.W., Zufall, F. & Reed, R.R. Central role of the CNGA4 channel subunit in Ca²⁺-calmodulin-dependent odor adaptation. *Science* **294**, 2172-2175 (2001).
302. Brown, R.L. & Arsanjani, R. Pseudotoxin binds to the pore turret of cyclic nucleotide-gated ion channels. *Biophys. J.* **82**, 1325a (2002).
303. Logothetis, D.E. & Zhang, H. Gating of G protein-sensitive inwardly rectifying K⁺ channels through phosphatidylinositol 4,5-bisphosphate. *J Physiol* **520 Pt 3**, 630 (1999).
304. Tseng, P.H., Lin, H.P., Hu, H., Wang, C., Zhu, M.X. & Chen, C.S. The canonical transient receptor potential 6 channel as a putative phosphatidylinositol 3,4,5-trisphosphate-sensitive calcium entry system. *Biochemistry* **43**, 11701-8 (2004).
305. Hegg, C.C., Greenwood, D., Huang, W., Han, P. & Lucero, M.T. Activation of purinergic receptor subtypes modulates odor sensitivity. *J Neurosci* **23**, 8291-301 (2003).
306. Wang, M., Kong, Q., Gonzalez, F.A., Sun, G., Erb, L., Seye, C. & Weisman, G.A. P2Y nucleotide receptor interaction with alpha integrin mediates astrocyte migration. *J Neurochem* **95**, 630-40 (2005).
307. Czajkowski, R., Banachewicz, W., Ilnytska, O., Drobot, L.B. & Baranska, J. Differential effects of P2Y1 and P2Y12 nucleotide receptors on ERK1/ERK2 and

- phosphatidylinositol 3-kinase signalling and cell proliferation in serum-deprived and nonstarved glioma C6 cells. *Br J Pharmacol* **141**, 497-507 (2004).
308. Bretscher, M.S. & Munro, S. Cholesterol and the Golgi apparatus. *Science* **261**, 1280-1 (1993).
 309. Skibbens, J.E., Roth, M.G. & Matlin, K.S. Differential extractability of influenza virus hemagglutinin during intracellular transport in polarized epithelial cells and nonpolar fibroblasts. *J Cell Biol* **108**, 821-32 (1989).
 310. Cerneus, D.P., Ueffing, E., Posthuma, G., Strous, G.J. & van der Ende, A. Detergent insolubility of alkaline phosphatase during biosynthetic transport and endocytosis. Role of cholesterol. *J Biol Chem* **268**, 3150-5 (1993).
 311. Milhiet, P.E., Giocondi, M.C., Baghdadi, O., Ronzon, F., Roux, B. & Le Grimmellec, C. Spontaneous insertion and partitioning of alkaline phosphatase into model lipid rafts. *EMBO Rep* **3**, 485-90 (2002).
 312. Molday, R.S. & Molday, L.L. Purification, characterization, and reconstitution of cyclic nucleotide-gated channels. *Methods Enzymol* **294**, 246-60 (1999).
 313. Gaus, K., Zech, T. & Harder, T. Visualizing membrane microdomains by Laurdan 2-photon microscopy. *Mol Membr Biol* **23**, 41-8 (2006).
 314. Kawai, F. & Miyachi, E. Direct suppression by odorants of cyclic nucleotide-gated currents in the newt photoreceptors. *Brain Res* **876**, 180-4 (2000).
 315. Chen, T.Y., Takeuchi, H. & Kurahashi, T. Odorant Inhibition of the Olfactory Cyclic Nucleotide-gated Channel with a Native Molecular Assembly. *J Gen Physiol* **128**, 365-71 (2006).
 316. Pike, L.J. & Casey, L. Cholesterol levels modulate EGF receptor-mediated signaling by altering receptor function and trafficking. *Biochemistry* **41**, 10315-22 (2002).
 317. Huang, C., Hepler, J.R., Chen, L.T., Gilman, A.G., Anderson, R.G. & Mumby, S.M. Organization of G proteins and adenylyl cyclase at the plasma membrane. *Mol Biol Cell* **8**, 2365-78 (1997).
 318. Ostrom, R.S., Bunday, R.A. & Insel, P.A. Nitric oxide inhibition of adenylyl cyclase type 6 activity is dependent upon lipid rafts and caveolin signaling complexes. *J Biol Chem* **279**, 19846-53 (2004).
 319. Brown, R.L., Lynch, L.L., Haley, T.L. & Arsanjani, R. Pseudochetoxin binds to the pore turret of cyclic nucleotide-gated ion channels. *J. Gen. Physiol.* **122**, 749-760 (2003).
 320. Peng, C., Rich, E.D., Thor, C.A. & Varnum, M.D. Functionally important calmodulin-binding sites in both NH₂- and COOH-terminal regions of the cone photoreceptor cyclic nucleotide-gated channel CNGB3 subunit. *J. Biol. Chem.* **278**, 24617-24623 (2003).
 321. Trinder, P. Oxidase determination of plasma cholesterol as cholest-4-en-3-one using iso-octane extraction. *Ann Clin Biochem* **18 (Pt 2)**, 64-70 (1981).